DUAL INHIBITION OF CATHEPSIN G AND CHYMASE AFTER ISCHEMIA REPERFUSION:

THE ROLE OF INFLAMMATORY SERINE PROTEASES IN ISCHEMIA REPERFUSION INJURY

A Dissertation

Submitted to

The Temple University Graduate Board

In Partial Fulfillment

Of the Requirements for the Degree

DOCTOR OF PHILOSOPHY

Ph.D. in Engineering

By

Bahman Hooshdaran

Diploma Date December 2017

Examining Committee Members:

Dr.Abdelkarim Sabri, Thesis advisor, Department of Physiology, Temple University

Dr. Mohammad F Kiani, Thesis Advisory Committee Chair, Department of Bioengineering Temple University

Dr. Nancy Pleshko, Bioengineering, Temple University

Dr. Laurie Kilpatrick, Department of Physiology, Temple University

To my family and my friends

ABSTRACT

Acute myocardial infarction (AMI) is a leading cause of morbidity and mortality in the world (3). Restoration of coronary flow to the ischemic myocardium by interventions such as angioplasty, thrombolytic treatment or coronary bypass surgery is the current standard therapy for AMI (4). However, reperfusion of the ischemic myocardium may result in paradoxical cardiomyocyte dysfunction and worsen tissue damage, in a process known as "reperfusion injury" (5). Ischemic reperfusion (IR) injury may intensify pathological processes that contribute to the generation of oxyradicals, disturbances in cation homeostasis, and depletion of cellular energy stores, which may elicit arrhythmias, contractile dysfunction, and ultrastructural damage of the myocardium. These changes can lead to heart failure and ultimately sudden death. The exact mechanisms of IR injury are not fully known (6). Molecular, cellular, and tissue alterations such as cell death, inflammation, neurohumoral activation, and oxidative stress are considered to be of paramount importance for IR injury development. However, comprehension of the exact pathophysiological mechanisms of IR injury (7) remains a challenge (8).

A large amount of the early cardiac tissue damage that occurs during inflammation post-IR is mediated through early activation of inflammatory cells such as neutrophils and mast cells, which produce reactive oxygen radicals, cytokines/chemokines and release granules containing proteolytic enzymes that are chemoattractant for other leukocyte populations (9). While extensive research has explored the mechanisms responsible for the activation of inflammatory-derived cytokines/chemokines and reactive oxygen species and their roles in the infarcted heart, there is a paucity of information regarding the role of neutrophil- and

mast cell-derived serine proteases on cardiac injury post-IR (7). Inflammatory serine proteases (ISPs) derived from neutrophils, such as cathepsin G (Cat.G), elastase, and proteinase 3, and from mast cells, such as chymase and tryptase, are enzymes known mainly for their function in the intracellular killing of pathogens (10). Their extracellular release upon leukocyte activation is traditionally regarded as the primary reason for tissue damage at the sites of inflammation. However, some evidence indicates that ISPs may also be key regulators of the inflammatory response (11). In the first chapter, we have characterized the kinetic of ISP activation after myocardial IR in mice. Herein we found that neutrophilic-derived serine protease activity (i.e. cathepsin G and elastase) increased rapidly in the injured heart (6-24 h post-IR) and correlated with the infiltration of neutrophils. Increased level of T cell-derived protease granzyme B was also observed in the infarcted heart after IR injury, however, with slow kinetics reaching a maximum around 7 days post-IR. Interestingly, activity of mast-cell derived serine proteases chymase increased early after IR and this increase was sustained for over 7 days post-IR. Collectively, this initial study shows that several inflammatory-cell derived proteases are activated after IR and their action is differentially regulated.

Because human Cat.G and chymase have similar active sites and share some common functions (10, 12), assessing their function in human diseases is complicated by potentially redundant functions and targets. Therefore, any strategy targeting one serine protease will not be successful. In the second chapter, we tested the efficacy of a dual inhibitor of cathepsin G and chymase on the adverse outcome of IR injury. The DCCI used in this study was shown to selectively inhibit Cat.G and chymase *in vitro*, with little effect on several other serine proteases such as thrombin, factor Xa, trypsin, tryptase, proteinase 3, and

elastase (13). We found that Treatment with a DCCI blocked cardiac Cat.G and chymase activity induced after IR, which resulted in decreased immune response in the infarcted heart. Mice treated with DCCI also had less myocardial collagen deposition and showed preserved ventricular function at 1 and 7 days post-IR compared with the vehicle-treated group. DCCI treatment significantly attenuated focal adhesion (FA) complex disruption and myocyte degeneration after IR. From these finding, we concluded that a dual inhibitor targeting Cat.G and chymase is effective in reducing the pathologic severity related to IR injury in association with its ability to limit myocardial proteolytic activity. By attenuating collagen deposition within the myocardium and improving LV function, DCCI may ultimately decrease the progression to heart failure.

To delineate the mechanisms by which DCCI offers cardioprotection against the sequel of Cat.G/chymase-mediated myocyte death and adverse cardiac remodeling and function post-IR, we investigated the effect of DCCI on isolated cardiac myocytes and cardiac fibroblasts, two important cardiac cells that can be targeted by ISPs. We found that treatment of isolated cardiomyocytes with Cat.G or chymase significantly promoted myofibril degeneration and myocyte apoptosis. Conversely, treatment of cardiac fibroblasts with Cat.G or chymase induced migration and differentiation to myofibroblasts. These opposite responses in cardiomyocytes and fibroblasts were blocked by treatment with DCCI. The pleiotropic effects of Cat.G and chymase on cardiac myocytes and fibroblasts raises the intriguing question about the mechanisms by which these extracellular proteases initiate their effects in both cells. We found that DCCI treatment inhibited Cat.G- and chymase-induced MMP2 activation and FA protein degradation in cardiomyocytes. Interestingly, in contrast to cardiomyocytes, Cat.G and chymase led to FA signaling

activation in fibroblasts that culminated to fibroblast migration and differentiation. These data, although are in line with the role of FAK activation in mediating cell survival and growth, suggest a different mechanism of FA signaling regulation between myocytes and fibroblasts.

Systemic inhibition of ISPs may potentially affect immune system functions, including mobilization of cells from the immune system. Therefore, we have investigated a targeted delivery of DCCI specifically to the injured myocardium following IR. In chapter 5 we have adopted an anti-P-selectin conjugated immunoliposomal construct, previously shown to be effective in targeting the injured myocardium (14) and showed that DCCI can be encapsulated with negligible disruption of immunoliposomes structure, and distribution. We investigated next the effects of targeted delivery of DCCI following IR and compared them to systemic delivery of the same (2 mg/kg/d) and high doses of DCCI (10 mg/kg/d). We found that treatment with low doses of targeted DCCI was effective to attenuate the increase in the activity of Cat.G and chymase induced after IR, which resulted in decreased infiltration of neutrophils to the infarcted heart. Systemic treatment with the same doses of DCCI had no effects on Cat.G and chymase activity. Mice treated with targeted DCCI also had less myocardial collagen deposition and showed preserved cardiac function 1 and 7 days post-IR. These results were comparable with systemic treatment of high dose of DCCI. Systemic DCCI treatment attenuated FA complex disruption induced following IR and therefore reduced cardiomyocyte death. We found that targeted delivery of low dose of DCCI was efficient to offer comparable cardioprotective effects.

In conclusion, a dual inhibitor targeting Cat.G and chymase is effective in reducing the pathologic severity related to IR injury in association with its ability to limit myocardial

proteolytic activity. By attenuating collagen deposition within the myocardium and improving LV function, DCCI may ultimately decrease the progression to heart failure. Our study has therefore provided important data to support a previously unknown mechanism implicating Cat.G and chymase in the progression of this disease and the theoretical benefit of using a dual inhibitor targeting Cat.G and chymase in the therapy of acute IR injury.

TABLE OF CONTENT

ABSTRACT ..... **ii**

TABLE OF CONTENT ..... **vii**

LIST OF FIGURES ..... **ix**

LIST OF TABLES ..... **xii**

LIST OF SCHEMES ..... **xiii**

CHAPTER 1 LITERATURE REVIEW PART 1: ISCHEMIA REPERFUSION INJURY **1**

1.1 Introduction 1
1.2 Myocardial Cell Death in Ischemia-Reperfusion Injury 2
1.2.1 Forms of Cell Death Following IR 2
1.3 Sources of Myocardial Ischemia-Reperfusion Injury 4
1.3.1 Reactive Oxygen Species 5
1.3.2 Calcium Overload 6
1.3.3 Signaling Pathways in Cell Death 7
1.3.4 Endothelial Dysfunction 8
1.3.5 Inflammation 9
1.3.6 Initiation of Inflammatory Response 10
1.3.7 Inflammatory Cytokines 12
1.3.8 Leukocyte Chemotaxis in Myocardial Infarction: The Role of Chemokines 14
1.3.9 Leukocyte Infiltration Post IR 15
1.3.10 Cd18 and the Leukocyte Beta 2 Integrin 17
1.3.11 Mechanisms of Leukocyte-Induced Myocardial Injury 18
1.3.12 Role of the Inflammatory Response in Cardiac Repair 24

CHAPTER 2 DUAL INHIBITION OF CATHEPSIN G AND CHYMASE REDUCES MYOCYTE DEATH AND IMPROVES CARDIAC FUNCTION AFTER MYOCARDIAL ISCHEMIA REPERFUSION INJURY **26**

2.1 Abstract 27
2.2 Introduction 29
2.3 Methods 31
2.4 Results 32
2.5 Discussion 39
2.6 Figures and Legends 46

CHAPTER 3 LITERATURE REVIEW PART 2: TARGETED DRUG DELIVERY TO THE MYOCARDIUM **53**

3.1 Delivery Vehicles 54
3.1.1 Liposome Formation: 57
3.1.2 PEGylation 59
3.1.3 Drug Encapsulation 60
3.1.4 Antibody Attachment 61
3.2 Targeted Drug Delivery to the Injured Heart 62

CHAPTER 4 IMMUNOLIPOSOMAL TARGETING OF DUAL CATHEPSIN G AND CHYMASE INHIBITOR IMPROVES CARDIOPROTECTION AFTER MYOCARDIAL ISCHEMIA REPERFUSION INJURY 66
4.1 Abstract 67
4.2 Introduction 68
4.3 Methods 69
4.4 Results 72
4.5 Discussion 77
4.6 Figures and Legends 81
4.7 Supplemental Figures and Tables 87
CHAPTER 5 CONCLUDING REMARKS 92
BIBLIOGRAPHY 99
LIST OF PUBLICATIONS 124

LIST OF FIGURES

Figure 2-1: Inflammatory serine proteases are elevated after ischemia reperfusion (IR). (A-C) The left anterior descending artery was ligated for 30 min to induce ischemia and the heart was subsequently reperfused for 3 h, 6 h, 1 or 7 days. Cathepsin G (Cat.G) (A), elastase (B) and chymase (C) activity levels in the hearts of sham and mice subjected to IR injury were assessed by substrate specific enzymatic activity assay. Results are expressed as relative fluorescence units (RFU)/min/mg protein (n = 6 for each groups). (D) Representative Cat.G and chymase immunostaining of paraffin-embedded heart sections of sham or mice subjected to IR injury. Scale bar: 40μm. (E) Quantification of Cat.G and chymase-positive cells (n = 5 for each groups). Values are presented as mean ± SEM, $^{*}P < 0.05$ vs. WT shams. 46

Figure 2-2: DCCI treatment attenuates inflammation in the reperfused heart. (A-C) Cathepsin G (Cat.G) (A), chymase (B) and myeloperoxidase (MPO) (C) activity in the infarcted LV as determined by enzymatic activity assay (n = 6 for each groups). (D) Representative MPO or toluidine blue (TB) staining of paraffin-embedded heart sections from sham or mice subjected to ischemia reperfusion (IR). Scale bar: 40μm. (E and F) Quantification of MPO- and mast cell-positive cells in mice treated with either vehicle or DCCI (n = 5 for each groups). (G) Left: Immunoblot analysis indicates a decrease in inflammatory signaling in the infarcted region of mice treated with DCCI compared to vehicle post-IR. Right: Quantification of experiments represented as fold change compared to sham animals treated with vehicle (n = 5 for each groups). GAPDH was included as a loading control. Values are presented as mean ± SEM, $*P < 0.05$ vs. shams, $\dagger P < 0.05$ vs. vehicle-treated IR. 47

Figure 2-3: DCCI improves cardiac function post-IR. (A-D) Echocardiography measurement of Left ventricular (LV) ejection fraction (EF) (A), fractional shortening (FS) (B) and LV internal diameter (LVID) in systole (C) and diastole (D). (E and F) Effects of DCCI treatment on IR-induced heart weight (HW) (E) or lung weight (LW) (F) to body weight (BW) ratio (n = 6 shams, n = 8 IR groups). (G and H) Top: Representative images of Evans blue and diphenyl tetrazolium chloride or Masson's trichrome staining on transverse heart sections at day 1 (G) and 7 (H) post-IR, respectively. Bottom: Quantification of the area at risk (AAR) and infarct area (IA) (n = 5 for each groups). Values are presented as mean ± SEM, $^{*}P < 0.05$ vs. sham, $\dagger P < 0.05$ vs. vehicle-treated IR. 48
. 49

Figure 2-4: DCCI deletion offers cardioprotection after acute IR. Ischemia reperfusion (IR) was induced for 24 h. (A) LV tissue sections were assessed for apoptosis using TUNEL assay (green), tropomyosin (red), and DAPI (4′,6-diamidino-2-phenylindole) (blue) staining. Scale bar: 40 μm. (B and C) The number of TUNEL-positive myocytes (B) and non-myocytes (C) in the reperfused area was expressed as a percentage of total nuclei detected by DAPI staining (n = 5 each group). (D) Quantification of caspase-3 activity in the LV using caspase-3 specific fluorogenic substrate (n = 6 each group). (E) Plasma levels of cardiac troponin-I (cTnI) as determined by ELISA assay in samples from vehicle- or DCCI-treated mice 24 h post-IR (n = 6 each group). (F and G) Immunoblot analysis indicates a decrease in pro-apoptotic signaling (F) and focal adhesion signaling (G) in the infarcted region of mice treated with DCCI or vehicle post-IR. Left: Representative immunoblots. Right: Quantification of experiments represented as fold change compared to shams (n = 6 each group). GAPDH was included as a loading control. Values are presented as mean ± SEM, $^{*}P < 0.05$ vs. shams, $\dagger P < 0.05$ vs. vehicle-treated. 49

Figure 2-5: Dual effects of cathepsin G and chymase on focal adhesion signaling and cell detachment. (A-D) Neonatal rat cardiomyocytes (A, B, D) and fibroblasts (A, C, E) were pretreated without or with DCCI (5 μM) prior to treatment with cathepsin G (Cat.G) or chymase for 8 h. (A) Phase-contrast photomicrographs (Bar=100 μm). (B and C) Caspase-3 activity was measured using fluorogenic substrate. (D and E) Left: Representative

immunoblots showing focal adhesion (FA) signaling in cardiomyocytes (D) and fibroblasts (F) treated with Cat.G or chymase for 10 minutes in presence of DCCI or its vehicle. Right: Quantification of experiments expressed as mean ±SEM from 3 separate cultures. * $P < 0.05$ vs. control, †$P < 0.05$ vs. vehicle-treated cells.....50
51

Figure 2-6: DCCI reduces fibrosis and improves cardiac remodeling after IR. Ischemia reperfusion (IR) was induced for 7 days. (A) Picro-sirus red staining and immunohistochemistry against smooth muscle α-actin (SMA) show reduced collagen and myofibroblast deposition in the injured myocardium of mice treated with DCCI compared to those treated with vehicle. (B-C) Semi-quantitative analysis of collagen staining (B) and SMA immunoreactive myofibroblasts (C) expressed as a percentage of total infarct area. (D) Immunoblot analysis indicates a decrease in profibrotic signaling molecules in the infarcted region of mice treated with DCCI vs. the treatment with vehicle post-IR. Left: Representative immunoblots. Right: Quantification of experiments represented as fold change compared to WT animals (n = 6 for each groups). GAPDH was included as a loading control. (E) In-gel zymography (Top) and relative band density quantification (Bottom) indicates a decrease in MMP-2 and -9 activity in the infarcted myocardium of mice treated with DCCI vs. treated with vehicle. (F) Gelatinase activity assay in animals subjected to IR and treated with either vehicle or DCCI (n=5 for each groups). Values are presented as mean ± SEM, *$P < 0.05$ vs. shams, †$P < 0.05$ vs. vehicle-treated IR.....51

Figure 2-7: Cathepsin G and chymase induce cardiac fibroblast migration and differentiation. (A-C) Neonatal rat cardiac fibroblasts were pretreated with DCCI (5μM) or vehicle for 15 minutes and then treated with cathepsin G (Cat.G, 0.02 U/ml) or chymase (100nM) for 36 h and cell lysates were processed for immunoblot analysis. Top: Representative immunoblots. Bottom: Quantification of experiments represented as fold change compared to untreated control (Ctrl). GAPDH was included as a loading control. (D) Migration scratch assay was performed to assess the rate of migration of cardiac fibroblasts untreated or treated with Cat.G or chymase with or without DCCI pretreatment. (E) A significant increase in the migration rate was observed in Cat.G- and chymase-treated fibroblasts compared with controls which was attenuated by DCCI treatment. Scale bar: 200 μm. Results are representative of 3 independent experiments. Data are mean ± SEM; *$P < 0.05$ vs. control; †$P < 0.05$ vs. vehicle-treated fibroblasts.....52

Figure 4-1: DCCI can be encapsulated in long lasting immunoliposomes. (A) ILPs size distribution measured using zeta particle sizer. (B) ILPs zeta potential distribution measured using zeta potential sizer. (C) Fluorogenic intensity of liposomes coated with either anti P-Selectin or IgG antibody and incubated with P-selectin coated 96 well plate and vigorous washing. (D) The inhibitory effect of DCCI encapsulating ILPs was compared by free DCCI to determine the amount of DCCI encapsulated. Results are expressed as relative fluorescence units (RFU)/min (n=3 from 3 different ILPs preparations). (E) The inhibitory effect of ILPs in the presence and absence of Igpal was measured to determine the amount of free and encapsulated drug. Results are expressed as relative fluorescence units (RFU)/min (n= 3 from 3 different ILPs preparations).....81

Figure 4-2: ILP encapsulated DCCI is specifically delivered to the injured myocardium and is effective to inhibit excess ISP activity. (A) Green lipid infused immunoliposomes co-stained with actin in the infarcted LV 6hrs post reperfusion. (B) Cathepsin G (Cat.G), chymase (C) activity in the infarcted LV of animals treated with either 2mg/kg targeted or 10mg/kg/d systemic as determined by enzymatic activity assay (n=6 for each groups). (D) Cat.G (E), chymase (D) activity in the infarcted LV of animals treated with 2mg/kg/d systemically or vehicle as determined by enzymatic activity assay (n=5 for each groups). Values are presented as mean ± SEM, *$P < 0.05$ vs. shams, †$P < 0.05$ vs. vehicle-treated IR.....82

Figure 4-3: DCCI treatment attenuates inflammation in the reperfused heart. (A,B) representative MPO staining and relative quantification of paraffin-embedded heart sections from sham or mice subjected to ischemia reperfusion (IR) Scale bar: 40μm. (C) Activity in the infarcted LV as determined by enzymatic activity assay (n=6 for each groups). Values are presented as mean ± SEM, *P < 0.05 vs. shams, †P < 0.05 vs. vehicle-treated IR. 83

Figure 4-4: DCCI improves cardiac function post-IR. (A-D) Echocardiography measurement of Left ventricular (LV) ejection fraction (EF) (A), fractional shortening (FS) (B) and LV internal diameter (LVID) in systole (C) and diastole (D). (E) Representative images of Tetrazolium staining or Masson's trichrome staining on transverse heart sections at day 1 and 7 days post-IR, respectively. (F) Quantification of the infarcted area at 1 and 7 days post IR (n=5 for each groups). Values are presented as mean ± SEM, *P < 0.05 vs. sham, †P < 0.05 vs. vehicle-treated IR. 84

Figure 4-5: Effective doses of DCCI administration offers cardioprotection after acute IR. Ischemia reperfusion (IR) was induced for 24 h. (A) LV tissue sections were assessed for apoptosis using TUNEL assay (green), tropomyosin (red), and DAPI (4′,6-diamidino-2-phenylindole) (blue) staining. Scale bar: 40 μm. (B) The number of TUNEL-positive myocytes (B) and non-myocytes in the reperfused area was expressed as a percentage of total nuclei detected by DAPI staining (n=5 each group). (C) Quantification of caspase-3 activity in the LV using caspase-3 specific fluorogenic substrate (n=6 each group). (D) Immunoblot analysis indicates a decrease in pro-apoptotic signaling in the infarcted region of mice treated with DCCI or empty ILP or vehicle post-IR. Top: Representative immunoblots. Bottom: Quantification of experiments represented as fold change compared to shams (n=6 each group). GAPDH was included as a loading control. Values are presented as mean ± SEM, *P < 0.05 vs. shams, $_{\dagger}$P < 0.05 vs. vehicle-treated. 85

Figure 4-6: Effective doses of DCCI reduces fibrosis differentiation and improves cardiac remodeling after IR. Ischemia reperfusion (IR) was induced for 7 days. (A) Picro-sirus red staining and immunohistochemistry against smooth muscle α-actin (SMA) show reduced collagen and myofibroblast deposition in the injured myocardium of mice treated with DCCI compared to those treated with either empty ILP or vehicle. (C) Gelatinase activity assay in animals subjected to IR and treated with either vehicle or DCCI (n=5 for each groups). (D) Immunoblot analysis indicates a decrease in profibrotic signaling molecules in the infarcted region of mice treated with DCCI vs. the treatment with either empty ILP or vehicle post-IR. Top: Representative immunoblots. Bottom: Quantification of experiments represented as fold change compared to WT animals (n=6 for each groups). GAPDH was included as a loading control. Values are presented as mean ± SEM, *P < 0.05 vs. shams, $_{\dagger}$P < 0.05 vs. vehicle-treated IR. 86

Figure S1: 2mg/kg/d systemic DCCI offers no improvement in cardiac function post-IR. (A, B) Echocardiography measurement of Left ventricular (LV) ejection fraction (EF) (A), fractional shortening (FS) (B). Values are presented as mean ± SEM, *P < 0.05 vs. sham, $_{\dagger}$P < 0.05 vs. vehicle-treated IR. 91

Figure S2: DCCI administration affects remodeling following IR (A, B) Morphometric measurements of heart weight to body weight (HW/BW) (A), Lung weight to body weight (LW/BW) (B). Values are presented as mean ± SEM, *P < 0.05 vs. sham, $_{\dagger}$P < 0.05 vs. vehicle-treated IR. 91

LIST OF TABLES

Supplemental Table 1: Summary of heart weight, body weight and echocardiographic measurements in 24 h post reperfusion in sham and IR mice treated with either emoty or DCCI encapsualted ILP. 87

Supplemental Table 2: Summary of heart weight, body weight and echocardiographic measurements in 7 days post reperfusion in sham and IR mice treated with empty or DCCI encapsulated ILPs. 88

Supplemental Table 3: Summary of heart weight, body weight and echocardiographic measurements in 24 h post reperfusion in sham and IR mice treated or not with 10mg/kg/d of DCCI. 89

Supplemental Table 4: Summary of heart weight, body weight and echocardiographic measurements in 7 days post reperfusion in sham and IR mice treated or not with 10mg/kg/d of DCCI. 90

LIST OF SCHEMES

Schematic 1-1: Schematics of physiological changes during ischemia and reperfusion resulting in calcium overload. 6
Schematic 1-2. The initiation of inflammatory response following onset of ischemia, through TLRs and NLRP3 containing inflammasomes (3). 11
Schematic 1-3. Schematic demonstrates infiltration of leukocytes, and release of ISPs and their protein targets during IR injury 20
Schematic 3-1: From top to bottom: Schematics of monoclonal antibodies and fragments, synthetic polymer, liposome and quantum Dot. (1) 54
Schematic 3-2. Structure of DOPE DSPC EPC and a phospholipid (2) 57
Schematic 3-3. Structure of a PEGylated liposome (2) 59

CHAPTER 1

LITERATURE REVIEW

PART 1: ISCHEMIA REPERFUSION INJURY

1.1 Introduction

Despite all medical and technological advances, coronary heart disease is still number one cause of death in all industrial countries (15). In 2017, the world health organization (WHO) reported that more than 17 million die every year from different types of coronary heart disease (16). A number that compared to 7 million in 2008 has increased more than 200% (16). The most common cause of deaths amongst these pathological conditions is attributed to detrimental outcomes of acute myocardial ischemia and ischemia reperfusion (IR) (17).

Myocardial Ischemia, or insufficient blood flow, is a result of abrupt occlusion of a coronary artery. Unrelieved ischemia causes permanent damage to the myocardium previously supplied by the occluded artery. Therefore, timely reperfusion is the primary treatment in this stage. Although necessary to prevent the expansion of damage and infarct a large body of experimental and clinical evidence supports the notion that reperfusion by itself induces additional damage to the myocardium, known as IR injury (18). It has been

shown that IR injury can be the source of up to 50% of the whole infarct size (19, 20). In dogs undergoing 40 minutes of coronary occlusion followed by 20mins of reperfusion caused more damage that 60 minutes of just ischemia with no reperfusion (21).

the most detrimental outcome of IR incident is the loss of functional cardiomyocytes which is then replaced by fibrotic scar tissue (22). Scar tissue cannot contribute to the myocardium contractile function, which therefore results in worsening of cardiac function and can ultimately lead to cell death (23). Therefore, the most therapeutic approaches aim at reducing cardiomyocyte death following IR injury.

1.2 Myocardial Cell Death in Ischemia-Reperfusion Injury

The number of functioning cardiac cells post-IR can significantly predict the following remodeling, and progression to heart failure (17). Therefore, in an attempt to minimize myocyte death and injury it is important to recognize the mechanisms and corresponding sources that lead to cell death following IR. Apoptosis and necrosis are two major forms of cell death occurring following IR (24). Whether necrosis or apoptosis is the most frequent form of cell death after IR has been an issue of debate (25). Below, we briefly describe each form of cell death and their mechanism following IR.

1.2.1 Forms of Cell Death Following IR

Cell death is a common incident in living organisms. But, in 1972 Kerr et al. adapted the term “apoptosis” to the programmed cell death (26). Apoptosis is highly dependent on energy and is controlled genetically by a sequence of events. Apoptosis is crucial in normal physiological conditions for example in removal of specific cells during development or

during cell turnover in mature tissue (27). Morphologically, apoptosis is characterized by membrane budding, cell contraction and chromatin condensation, which generates a horseshoe shape nucleus and leads to rupture of cell into fragments (28). Fragmentation of cells into membrane bound parts, restricts the release of cellular content and consequent inflammatory reaction (29). Apoptosis is chemically characterized by the activation of caspases, DNA fragmentation by cleavage, and preservation of ATP levels (30). The availability of ATP is highly important as chromatin shrinkage and nuclei fragmentation, two crucial steps of apoptosis require ATP (31). Necrosis however, is characterized by an increase in membrane permeability, cell swelling and release of cellular content. The release of cellular components leads to discharge of proinflammatory molecules, a process which can initiates the inflammatory response (20).

Although the mechanism of apoptosis and necrosis differ significantly, they may happen at the single time point of one pathological condition. Various factors like severity and characteristics of the pathological condition, can dictate the dominant form of cell death (32). One of the most important factors dictating which type of cell death occurs is ATP availability (33). Reperfusion is associated with the reintroduction of ATP which points at higher occurrence of apoptosis compared to necrosis. It is probable, however, that throughout IR process, some cells get exposed to severe trauma and experience necrosis, while others which are in the adjacent area progress to apoptosis (34).

Although necrosis and apoptosis are the most common forms of cell death following IR, other less frequent types of cell death, such as autophagy and necroptosis may also occur following IR (35). Autophagy is known as a beneficial process which occurs at basal levels in normal conditions. However, during IR, autophagy is hyper-activated in response to

energy crisis, oxidative stress, and altered autophagosomes concentration in cardiomyocytes (36). Several pathways have been studied to inhibit autophagy after reperfusion. However, none of them has reached clinical trials as the underlying mechanism is not well understood (37). Also, any therapeutic approach aiming at blocking autophagy needs to inhibit excessive autophagy related to IR process without affecting the basal necessary levels. Another form of cell death which has recently been discovered is Necroptosis. Necroptosis is a term that bears the idea of programmed necrosis (38). This process is mediated through a caspase-independent signaling pathway which has both characteristics of necrosis and apoptosis. Necroptosis is most significant under severe inflammatory conditions where inflammatory cytokines and chemokines such as tumor necrosis factor (TNF-α) present at high concentrations (39). It was shown that Necrostatin-1 (Nec-1) which can block TNF-α mediated necroptosis significantly reduced infarct size in a porcine model of IR injury (40).

In conclusion, it appears that although necrosis is a common phenomenon in ischemic condition the majority of cell death following reperfusion is contributed to apoptosis. Therefore, therapeutics aiming at decreasing cell death following IR are often aimed at reducing apoptotic pathways.

1.3 Sources of Myocardial Ischemia-Reperfusion Injury

The mechanisms responsible for myocardial IR injury have not yet been elucidated in detail, increasing evidence points at various major culprits of biochemical and pathophysiological changes during this event such as reactive oxygen species (ROS), calcium overload and inflammatory response (41). Although these factors can collaborate

to induce injury, the extent each one promotes cell death and cardiac damage post-IR needs further clarification.

1.3.1 Reactive Oxygen Species

Reactive oxygen species (ROS) are free radicals with very short half-lives. They are key signaling molecules at low concentrations. However, at high concentrations of ROS can affect cell function through lipid peroxidation and oxidation of proteins in cardiac cells (42, 43). During IR, ROS concentration may increase up to 100 times compared to normal conditions. This is mainly due to increased production of ROS from xanthine oxidase, mitochondria and NADPH oxidases. Also, following IR, the conversion of reactive oxidants to reactive species is significantly amplified.

ROS can affect membrane proteins responsible in cation transport and lipid peroxidation which results in altered cation homeostasis. A good example of this broad function is the effect of oxidative stress on neonatal cardiac myocytes. Siwik et al. showed that high concentrations of oxidative stress can lead to cardiac cell death. However, at low concentrations, oxidative stress promotes cell growth (44). Therapeutic approaches like administration of antioxidant have shown enhanced recovery of cardiac function and reduced infarct size following IR.

1.3.2 Calcium Overload

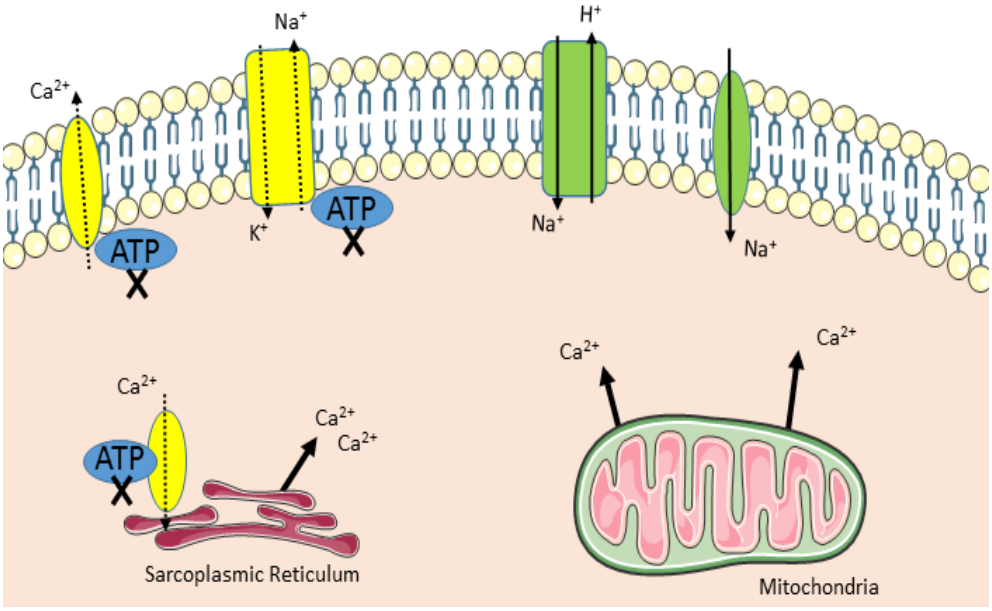

Schematic 1-1: Schematics of physiological changes during ischemia and reperfusion resulting in calcium overload.

During ischemia, hypoxic cells become dependent on anaerobic metabolism, which results in buildup of lactate, NAD+ and ultimately acidosis. To restore the PH, H^+ ions are exchanged by Na^{2+} ions. Na^{2+} ions, are then exchanged by Ca^{2+} via Na/Ca exchangers (45). This results in a significant increase in Ca^{2+} levels (46). Furthermore, throughout IR, both endo/sarcoplasmic reticulum Ca^{2+} storage and membrane Ca^{2+} handling change (47). Ca^{2+} reuptake is weakened, while Ca^{2+} release by ryanodine receptors is elevated, therefore, amplifying intercellular Ca^{2+} levels (48). These changes in Ca^{2+} concentration lead to activation of various pathways, which can lead to cell death (49). For example, cells store the excessive Ca^{2+} ions in the mitochondria through Ca^{2+} uniporters. If this influx exceeds certain levels, it can trigger activation of mitochondrial permeability transition

pores (MPTP) (50). Calpains which are proteases activated by Ca^{2+} are also targets of IR induced calcium overload (51). Calpains can degrade intercellular proteins, such as cytoskeletal and mitochondrial proteins (52). Increased Ca^{2+} concentration also results in the production of pyrophosphate complexes and the formation of uric acid, which in turn can attach to infalmmasomes. This process leads to elevated production of cytokines like TNFα and IL-1β (53). Therefore, changes in Ca^{2+} concentration has significant effects on cardiovascular physiology and remodeling following IR.

1.3.3 Signaling Pathways in Cell Death

Cytochrome c is attached to phospholipids, in the inner membrane of mitochondria (54, 55). Ca^{2+} overload can induce permeability transition pore (PTP) opening which results in mitochondria rapture and release of cytochrome c to the cytosol. Also apoptotic initiating proteins such as proteins of Bcl-2 family, like Bax initiate cytochrome c release even without opening of PTP pores, (56) leading to the release of cytochrome c. The released cytochrome c can initiate apoptosis however, alone, it is not sufficient to complete the process. Gabriel showed that Bcl-2 overexpression can inhibit apoptosis even after cytochrome c is released to the cytosol (57). Various proteins especially those from the Bcl-2 family are known to modulate PTP opening (58). These proteins are primarily expressed on the surface of the endoplasmic reticulum, as well as the mitochondrial and nuclei membrane. They are either anti-apoptotic such as Bcl-xL or pro-apoptotic such as Bad and Bax. Pro-apoptotic proteins initiate cytochrome c release and can lead to apoptosis (58). For example, Bax and Bad, can directly induce permeability of the mitochondrial outer membrane, and therefore the release of cytochrome c to the cytosol (59). Bax however can interact with the outer membrane of mitochondria independent of PTP

opening (60) and lead to cytochrome c release. This suggested pathway may explain how cytochrome c is secreted from mitochondria even without PTP formation and swelling. Anti-apoptotic proteins of this family can protect the mitochondrial membrane integrity, restricting release of cytochrome c (61). They can also attenuate oxidative stress after IR, which can in turn inhibit PTP opening (62). Overall this balance between anti and pro apoptotic proteins, determines the cell survival after stresses such as IR.

1.3.4 Endothelial Dysfunction

IR is associated with vascular endothelial dysfunction through multiple mechanisms resulting from overproduction of reactive oxygen species (ROS), Ca^{2+} imbalance and reduction of nitric oxide (NO) levels. (63, 64). Following reperfusion, the NO levels decrease within 3-5 minutes (65). Various pathways have been suggested resulting in reduced NO levels such as NO destruction by ROS (64, 66). NO is known to be involved in the neural controlling of heart rate, and neuronal transmission in cardiac ganglia, in addition to its vascular dilatory properties (67). Also, NO can preserve myocardial reperfusion by inhibiting platelet aggregation and leukocyte adherence to the vascular endothelium.

Normally endothelial cells (ECs) form a barrier against inflammation by preventing neutrophil and platelet activation. However, following IR, the increase in ROS results in upregulation of adhesion molecules such as E-selectin, P-selectin and ICAMs on the surface of the endothelial cells which facilitate activation and infiltration of inflammatory cells (68-70). Also, elevated ROS increases the permeability of the endothelial barrier

which further accelerates the infiltration of inflammatory cells. The role of inflammatory response in IR mediated injury is detailed in the following section.

1.3.5 Inflammation

Almost a century ago, scientists suggested that myocardial infarction and subsequent reperfusion can initiate intense inflammatory response which is associated by the invasion of leukocytes to the infarcted myocardium (71). Later, leukocytes were associated with cardiomyocyte detachment that could extend the IR injury (72). The first experimental evidence verifying this theory came after the protective effect of anti-inflammatory drugs were observed in animal models of myocardial ischemia and ischemia reperfusion (73). Therefore, extensive research was conducted on approaches limiting the inflammatory response after ischemia either by reducing the production of chemotactic factors (74, 75) or by injection of lipoxygenase inhibitors (76, 77), all of which were successful in limiting infarct size and in improving cardiac function after IR. Furthermore, those approaches that reduced infiltration of neutrophils for example by neutrophil depletion were also effective in decreasing ischemia related injury in some animal models (78).

Although these results were overwhelmingly positive, transition of all anti-inflammatory approaches to clinical settings failed. For example, Phase II trial of anti-CD18 therapy which had shown significant cardioprotective effects in animal models, (79, 80) resulted in no beneficiary effects in patients (81). Although these differences in results from animal studies and clinical trials may point at the inherent dangers of using animal models to simulate human diseases, the more important lesson is the need for a deeper and more detailed understanding of the inflammatory process and its components in order to design

a better and more effective and specific therapeutic approach. The inflammatory response following ischemia has a complex and multifaceted network of biochemical steps modulated by various molecules. In the next sections, different components of the inflammatory cascade are briefly reviewed with a bigger focus on the inflammatory serine proteases.

1.3.6 Initiation of Inflammatory Response

During onset of ischemia, necrosis of cardiac cells leads to the release of the subcellular membrane as an alarm signal (damage associated molecular pattern or DAMP) (82). These molecules then activate the toll-like receptors (TLRs) and interleukin-1 (IL-1) signaling cascade which subsequently activates the nuclear factor-κB (NF-κB) system and results in the production of inflammatory cytokines, chemokines and adhesion molecules (83).

TLRs are key regulators of the inflammatory response (84). Amongst 13 different TLRs that have been recognized in mammalians, TLR4 is known as the most important receptor in regulation of the inflammatory response in the infarcted heart (85). TLR4 can act as a sensing receptor for DAMPs in sterile tissue injuries. Mice deficient in TLR4 had smaller infarction and also less

leukocyte infiltration following infarction (86). Furthermore, these mice had significantly less amounts of TNF-α and IL-β expression following onset of ischemia (87). Another inflammatory triggering pathway following infarction is mediated through inflammasomes, cytoplasmic protein complexes which can activate caspase-1 and release IL-1β. Inflammasomes typically contain at least one of the NLR protein family. Amongst different inflammasomes, NLRP3 containing inflammasomes are known mostly for

recognizing DAMPs and therefore contributing to the sterile inflammatory conditions such as ischemia and ischemia reperfusion (88, 89). Following activation, NLRP3 containing inflammasomes can interact with the ASC adaptor which in turn activates caspase-1. Caspase-1 can switch IL1-β to its active form (90). Inhibition of NLRP3 showed to preserve myocardium integrity and function and also to reduce the infarct size following ischemia (91).

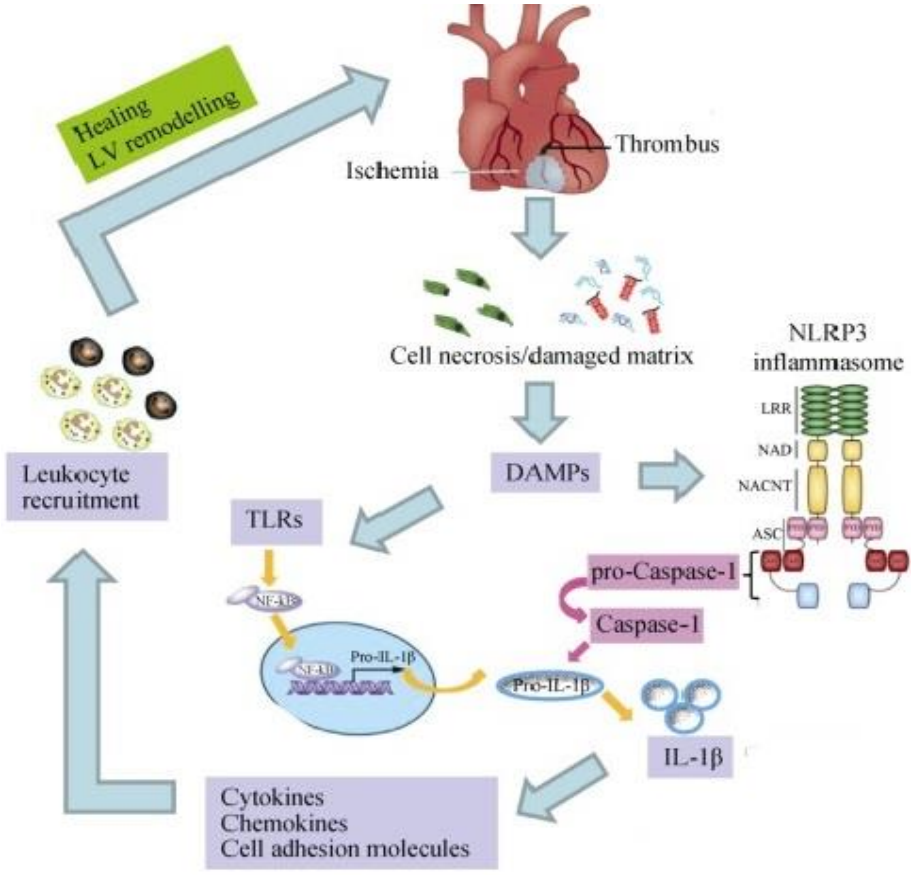

Schematic 1-2. The initiation of inflammatory response following onset of ischemia, through TLRs and NLRP3 containing inflammasomes (3).

1.3.7 Inflammatory Cytokines

A series of cytokines, chemokines and adhesion molecules are activated as a result of ischemia and ischemia reperfusion. Although IL1-β is the gatekeeper of inflammatory response, other cytokines such as IL-6, IL-8, and TNF-α, are also released following activation of NF-κβ by TLR mediators and play a role in initiation and resolution of inflammations.

TNF-α is the most important cytokine in the post ischemia myocardium physiology. TNF-α is produced by various cell types such as lymphocytes, macrophages, cardiomyocytes and vascular smooth muscle cells (92). TNF-α is an initiator of other cytokines such as IL-1 and IL-8 (93) and therefore can significantly modulate the inflammatory response. Besides its role in inflammation, TNF-α is considered to induce heart injury through changes in Ca^{2+} handling. In a hamster model of IR TNF-α directly decreased contractile function (94).

IL-1 is another important mediator of the inflammatory response following IR. IL-1 has two forms IL-1α and IL-1β (95). The latter is easier to detect in the blood and therefore has been the focus of most investigations (96). Beside inflammasomes and caspase-1 mediated IL-1 activation, neutrophil proteases such as cathepsin G can also process the IL-1β precursor to its active form (97). Following activation, IL-1β induces upregulation of ICAM-1 and VCAM-1 adhesion molecules on the surface of smooth muscle cells, facilitating adhesion of leukocytes (98). It has been shown that TNF-α, IL-1 can induce cardiomyocyte apoptosis through the release of cytochrome c and activation of caspase-3 (99).

Initially IL-6 was introduced as a T-cell only derived cytokine. However, later it was shown that other cell types such as monocytes and macrophages can also release IL-6 (100). IL-6 has a key role in the resolution of inflammation and clearance of apoptotic neutrophils which is crucial in initiation of the healing process. Also, IL-6 can regulate the neutrophil trafficking through STAT-3 mediated pathway.

Like other types of cytokines, high levels of IL-8 is expressed in the myocardium following IR injury (101). Also, IL-8 is considered a potent participant in granular enzymatic release and oxidative burst in neutrophils, which in turn leads to further damage in the ischemic heart. Whether IL-8 is a pro or anti-inflammatory cytokine is controversial. Some studies showed an inhibitory effect of IL-8 on leukocyte-endothelial binding by inhibition of L-selectin and LECAM-1 expression (102). In other studies, IL-8 has shown to be pro-inflammatory by inducing endothelium swelling (103). Beside the conflicting role of IL-8 on regulation of inflammation, IL-8 is reported to have negligible effect on myocardial contractility following IR. Therefore IL-8 may be just a minor effector of inflammatory response following IR (104).

Overall the initiation and resolution of inflammation is affected by various cytokines, and therefore these molecules can affect the remodeling and fate of injured myocardium post-IR. Although cytokines appear to be perfect therapeutic targets, recent failure of TNF-α inhibitors in the treatment of ischemic patients emphasizes on the complexities of affecting these pleiotropic mechanisms in the heart. Therefore, any targeted cytokine should be defined for its timing and quantity before further investigation.

1.3.8 Leukocyte Chemotaxis in Myocardial Infarction: The Role of Chemokines

Recently, chemoattractants or as called, chemokines, have been shown to promote quick induction of leukocyte migration (105). Certain chemokines have further effects on leukocyte adhesion, activation and apoptosis. Chemokines, can bind to one or several types of G-protein-coupled receptors (106) which can be divided into two main groups, CXC and CC. The naming comes from the placement of the first two cysteine groups (107). In mammalians, chemokine upregulation is an important effector of inflammatory response following IR (108). Depending on their function, chemokines can be divided into two major categories. First homeostatic chemokines which are consistently expressed and are important for basal levels of leukocyte locomotion . The second group of chemokines are upregulated following inflammatory response and participate in the intense recruitment of leukocytes (109). So far, ROS, activation of NF-κB and TNF-α are the main known sources of the chemokine upregulation and synthesize following IR (110).

GRP-a/KC, one of the CXC chemokines which can act as neutrophil attractant is reported to be induced in a rat model IR (111). GRP-a/KC have effects beyond those in trafficking of leukocytes and can modulate angiogenesis in the infarcted heart (112). Stromal cell derived factor1 (SDF-1), another chemokine of CXC family plays a key role in vasculature development and angiogenesis (113). SDF-1can induce chemotaxis of $CD34^{+}$ s progenitor cells and modulates various stem cell functions (114). However, the role of SDF-1 on the inflammatory response following IR is unknown.

The most well-studied CC chemokine is monocyte chemoattractant prteoin1 (MCP-1) which is a strong chemoattractant of monocytes and T cells (115). MCP-1 also plays an important role on non-hematopoietic cell functions. It can induce angiogenesis and affect

fibroblasts phenotype by increasing collagen expression and regulating MMP production (116). It has been shown that following IR, MCP-1 is upregulated in mouse and rat models of IR. MCP-1 deficient mice had lower infiltration of macrophages, reduced myofibroblasts accumulation but had similar infarct size following IR (106). Another well-studied CC chemokine, MIP-1 is also a mononuclear cell chemoattractant. MIP-1 was significantly upregulated in a murine model of MI (117, 118). However, the exact role of MIP-1 on cardiac injury and repair is still unknown. In conclusion chemokines are key players of the inflammatory response especially in recruitment of leukocytes. Also, chemokines can directly affect cardiac repair and remodeling independent of their function on leukocyte infiltration.

1.3.9 Leukocyte Infiltration Post IR

One of the primary links from the chain of events leading to the infiltration of leukocytes includes leukocyte entrapment in the microvasculature (119). Entrapment process can be affected by multiple factors such as the phenotype of the leukocytes, and vasculature conditions. Chemotactics can change neutrophils shape, rigidity and deformability (120). Also, neutrophil released autacoids can induce platelet aggregation and vasoconstriction and therefore can affect neutrophil entrapment (121).

Although these changes in shape and rigidity of neutrophils are important in leukocyte aggregation and infiltration to the ischemic myocardium (122), leukocyte-endothelium interaction is by far the most influential effector of infiltration process. This interaction can occur through adhesion molecules which ultimately leads to margination and ultimately

adhesion of leukocytes to the endothelium. Findings on neutrophil-endothelium interaction has led to a harmonic model for leukocyte recruitment to the injured myocardium (123).

There is a bulk of evidence suggesting that leukocyte-endothelial interaction is heavily modulated by a chain of molecular events which are the characteristics of biochemical and morphological changes associated with the adhesion process (124). In normal conditions, leukocytes rarely interact with the endothelium. However, following proper inflammatory stimuli, leukocytes roll along the post-capillary venous at speeds significantly lower than normal conditions. Some of these rolling cells bind firmly to the endothelium and then in the presence of proper chemotactic stimuli, change shape and finally extravasate to the extracellular space. Each of these steps require the presence of specific sets of adhesion molecules (125).

Selectins are the initiators of capturing leukocytes from rapid blood flow by initiation of rolling (126). Selectins consist of three major cell-surface molecules, L,E, and P-selectins. L-selectin is expressed solely in hematopoietic cells, while almost all types of leukocytes express L-selectin throughout their differentiation (127-129). Following activation, expressed L-selectins are quickly removed by shedding (130). The wide-ranging expression of L-selectin is associated by its role in trafficking of almost every type of leukocytes. E-selectin is expressed only 4-6 hours after endothelial cell activation in response to cytokines such as TNF-α or IL-1β (131). Those circulating leukocytes which express the correct ligands can bind with low affinity to expressed E-selectins. P-selectin is mostly expressed on Weibel Palade bodies of the endothelial cells as well as in the α granules of platelets (132, 133). Unlike E-selectin, within minutes of inflammatory stimuli, P-selectin is transported to the surface of the cells. This process excludes the need of new

protein synthesis (117) and can be initiated by variety of molecules such as histamines, free radicals, and cytokines (134, 135).

All selectins are important in migration and infiltration of leukocyte to the infarcted tissue (136). Transgenic mice have produced substantial information about the role of selectins. L-selectin KO mice, showed a significant decrease of leukocyte infiltration to the inflamed site (137). P-selectin KO mice showed almost no rolling and thus a delayed neutrophil infiltration to the site of injury (138). On the other hand, E-selectin KO mice showed normal leukocyte recruitment in response to inflammatory stimuli (139). Administration of monoclonal antibodies against L- and P-selectin reduced endothelial activation and therefore attenuated infiltration of neutrophils to infarcted myocardium (140, 141). These observations collectively show the significant role of selectins in leukocytes migration after IR.

1.3.10 Cd18 and the Leukocyte Beta 2 Integrin

Even though rolling is necessary for adherence of leukocytes to the endothelium, selectin based adhesion is not firm, and infiltration will not occur unless other adhesion molecules complete the process (142). Integrins are a family of heterodimeric glycoproteins which include α and β subunits. Integrins are transferred to the surface of the cell as a complex, in response to proper stimuli (143). Integrin based therapeutic approaches have been used to moderate the inflammatory response and reduce injury (144, 145). In a canine model of IR, antibodies against integrins (CD18) decreased cell necrosis 6 hours post reperfusion (146) and resulted in reduced infarct size and improved cardiac function (144). CD18 knock out mice showed reduce neutrophil infiltration and cardiomyocyte necrosis post-IR

compared to wild type (147), suggesting the important role of integrins in inflammatory response.

1.3.11 Mechanisms of Leukocyte-Induced Myocardial Injury

Infiltrated leukocytes can induce significant injury to the delicate structure of myocardium (83). leukocytes can secrete toxic products such as proteolytic enzymes and ROS after infiltration in the infarcted region that may lead to increased cardiac injury (148, 149). Below we will review the mechanisms of leukocyte mediated injury following IR.

Adhesion-Dependent Cytotoxicity

ICAM-1 is one the ligands of the CD18 integrin family (150). ICAM-1 is expressed by various cell types (151). It has been shown that neutrophil-cardiomyocytes adhesion happens only if the cardiomyocytes were stimulated to express ICAM-1 and the neutrophils to express Mac-1 (72). Cardiomyocytes can express ICAM-1 in response to various stimuli such as IL-1, TNF-α and IL-6 (152). Neutrophil activation on the other hand, can be affected by C5a and IL-8 (153). Neutrophil-cardiomyocytes binding was observed to be specific to Mac1-ICAM1 interaction as it was blocked by ICAM-1 blocking antibodies and was unaffected by antibodies against CD11a (which can block neutrophil adhesion to endothelial cells) (154). Neutrophils appear to be cytotoxic following this adhesion as they induce permeant contraction in cardiomyocytes (153).

Inflammatory Proteases

Although direct binding of neutrophils to cardiomyocytes can be the source of significant cell death and injury (72), most leukocyte-mediated injury originates from the factors

which are released by infiltrating leukocytes. Activated leukocytes secrete reactive oxygen species (ROS), different cytokine and chemokines and a variety of other enzymes such as inflammatory proteases (155). The role of ROS and cytokines/chemokines on IR mediated injury is mentioned in previous sections. Inflammatory serine proteases play significant role in body's defense mechanism. Also, they have an impact on vascular homeostasis and tissue remodeling. sequencing human genome revealed that almost 2% of all human genes are either protease or protease inhibitor related, suggesting the importance of proteases (156). At least 561 proteases and homologs were found in human degradome (157). Moreover, multiple studies have shown that beyond their proteolytic characteristics, proteases have diverse regulatory functions. They can induce their effects through intercellular signaling pathways, caspase activity and modulating specific receptors and cytokines (158-160). Inflammatory proteases play crucial role in cardiovascular pathophysiology following IR. In this study we have focused on inflammatory serine proteases (ISPs). ISPs are a subfamily of proteases which can cleave peptide bonds of proteins, where serine serves as the nucleophilic amino acid at the enzyme's active site.

ISPs can modulate several cellular functions through protease activated receptors (PARs) (161). PARs are transmembrane G-protein coupled receptors (GPCRs) that have significant roles in coagulation, inflammation, thrombosis, cardiac hypertrophy and fibrosis (162). All types of PARs can be found in vasculature and some inflammatory cells (163). PARs have a distinct mechanism of activation which separates them from other G protein coupled receptors (GPCRs) that are modulated and activated reversibly by small molecules (164). PARs except for PAR3, can also be activated by small synthetic peptides. It's noteworthy that proteases can negatively regulate pathways by cleaving PARs (165).

PAR1 and PAR2 can modulate multiple cellular functions such as proliferation, hypertrophy and angiogenesis. As proteases are usually activated during

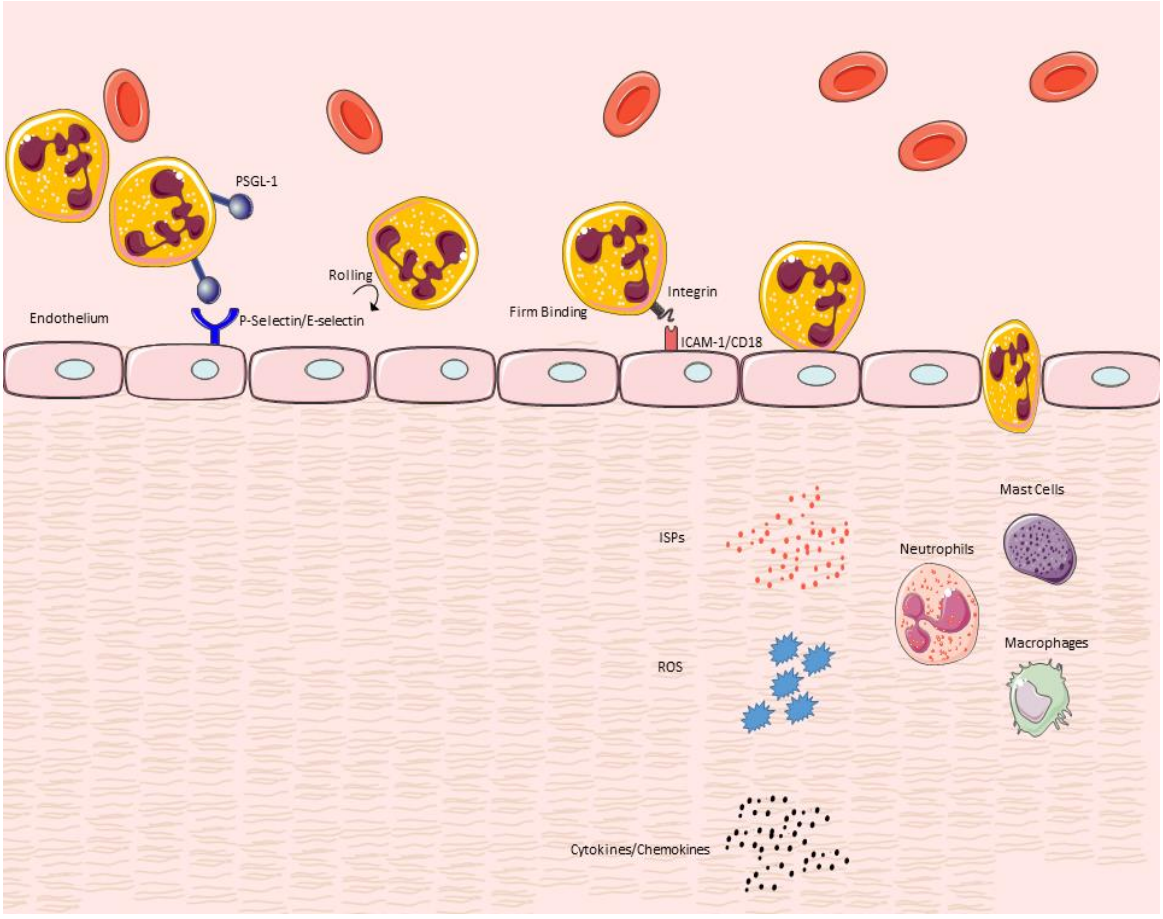

Schematic 1-3. Schematic demonstrates infiltration of leukocytes, and release of ISPs and their protein targets during IR injury

pathological conditions such as inflammation, PARs are considered to play crucial role in alteration of vasculature homeostasis following IR (166). Although PARs are key players of cardiovascular function following IR, ISPs can assert their function through PAR-independent pathways. Below we will briefly discuss each protease and its mechanism of action.

Neutrophil Serine Proteases

Elastase: Elastase is one the major proteases secreted by neutrophils (167). Following activation, elastase directly affects degradation of extracellular matrix (ECM) components such as collagen, fibronectin and elastin (168). Elastase also has a pro-inflammatory effect. It can degrade E-cadherin and VE-cadherin and therefore increase permeability of endothelial and epithelial cells (169). Elastase can also degrade IL-1β, IL-1, IL-2 and at the same time promote secretion of IL-6 and IL-8 which result in increased leukocyte migration, infiltration and ultimately propagation of inflammation (170, 171). During IR, elastase mediates tissue injury by degrading collagen structures, thus damaging endothelium and therefore promoting infiltration of neutrophils that are already adherent to the endothelium (172). Elastase inhibition, also reduced reperfusion mediated neutrophil accumulation in the infarcted region post-IR (173). Additional studies in in a rat model of myocardial ischemia showed that inhibition of elastase improved cardiac function and suggested that this cardio protective effect was observed due to reduced neutrophil infiltration. These evidences suggest that inhibition of elastase have cardio protective effects following onset of IR. However, whether these results are due to reduced neutrophil infiltration or due to inhibition of direct elastase effects on cardiac cells is not unveiled.

Cathepsin G: Cathepsin G (Cath.G) is another major ISP released by neutrophils. Cath.G can hydrolyze different types of proteins including inflammatory cytokines and chemokines (174), and can work as a chemoattractant for other types of leukocytes, such as T cells (175-177). Cath.G is known to be elastolytic and therefore important in the process tissue remodeling (178). Cath.G can activate MMPs like MMP2 and MT1-MMP in fibroblasts, endothelial cells and cardiomyocytes (179-181).

Cath.G can directly induce cardiomyocyte apoptosis and death. Previous studies from our group shows that Cat.G induces MMP2 cleavage through activation of MT1-MMP, leading to shedding of HB-EGF and transactivation of EGFR. Cat.G mediated activation of EGFR and subsequent dephosphorylation of focal adhesion kinases (FAK) may explain the anoikis and apoptosis observed following Cat.G treatment. (181)

Furthermore, proteolytic activity of Cath.G can lead to production of angiotensin II and therefore increase in expression of MCP-1 (182). Pintucci et al showed that Cath.G can attenuate plasminogen activator of endothelial cells which is mediated via secretion of its natural inhibitor from the endothelium's ECM (183). Same experiments revealed that Cath.G can activate the release of its inhibitor (PAI-1) from the platelet, leading to increased thrombogenic function. Cath.G deficient mice showed increased survival in renal ischemia model. (184). Also, wild type mice had severe cell death in shape of apoptosis and necrosis whilst Cath.G KO mice had 70% reduction in apoptotic cells. Also, Cath.G triggers TGF-β1 activity which promotes fibrosis. Cath.G KO mice have shown to have normal neutrophil development (185). These mice however had impaired wound healing abilities (186) and reduced tissue injury in renal models of IR (187). However, the role of cathepsin G in myocardial IR has never been delineated.

Proteinase 3: proteinase 3 (PR3) is also released by activated neutrophils and endothelial cells (188, 189). Beside degrading ECM, PR3 has other deleterious effects such as endothelial cell apoptosis through caspase mediated pathways (190). PR3 can activate TNF-α from its membrane bound form (191), activate IL1-β, and generate angiotensin I and II (192). Recently PR3 has been suggested as a mortality and heart failure prognosis marker following ischemia and ischemia reperfusion (193).

Mast cell serine proteases

Although Mast cells are primarily known for their specific function during allergic episodes, they are a major player of inflammatory response (194). In a canine model of IR, Number of mast cells was elevated in the infarcted myocardium during healing period (195). Mast cells are the initial sources of premature TNF-α (196). They generate cytokines and growth factors such as VEGF and bFGF, which can modulate fibroblast growth, ECM synthesis and angiogenesis (197). Also, mast cells can affect the healing and remodeling of the infarcted tissue via expressing gelatinase A and B, which have pivotal roles in angiogenesis and ECM degradation (198). Beside cytokines and growth factors, mast cells are major sources of inflammatory serine proteases (199). Although Cath.G can be expressed by mast cell, major mast cell proteases include chymase and tryptase which are stored in their granules (200). It has been shown that the density of cardiac mast cells is remarkably increased in patient with ischemic condition (201).

Although tryptase and chymase can activate PAR2 (202), their enzymatic activity can affect other proteins especially those implicated in cardiovascular pathophysiology (203). Tryptase for example, can convert and activate pro-urokinase (204). Chymase can affect endothelial ECM and induce secretion of TGF-β, an initiator of fibrosis and angiogenesis (205). Chymase also has a role in conversion of angiotensin type I to type II, functioning as a vasoconstrictor and an important player of remodeling after IR injury (206). Furthermore, chymase is known to promote MMP-9 activation by cleaving specific sites

of the catalytic domain of MMP-9, which has been shown to increase infarct size and fibrosis following IR (207). Oral administration of chymase inhibitor, significantly attenuated the increase in plasma cardiac troponin I in dog model of IR (208). Same study showed significant degradation of endoplasmic reticulum (ER) and mitochondria in adult myocytes treated with chymase. In another study perforemd in rats, oral administration of a chymase inhibitor increased survival rate compared to non-treated animals following IR (209). In hamsters, oral administration of a chymase inhibitor resulted in better cardiac function following IR. In pig model of IR, administration of a chymase inhibitor significantly reduced infarct size, attenuated serum cardiac troponin-I levels and inhibited activation of MMP-9 in the infarcted myocardium (210). On the other hand, in a study on dog model of MI, treatment with chymase inhibitor had only antiarrhythmic effects and showed no effects on infarct size (211). In conclusion, it seems that, chymase inhibition can be a potential target to reduce cardiac injury after ischemia and ischemia reperfusion. The exact mechanism underlying this cardio-protective effect cannot be understood from these studies.

1.3.12 Role of the Inflammatory Response in Cardiac Repair

Although inflammation and its components have been recognized extensively as possible sources of cell death and injury (212). There is bulk evidence suggesting healing properties of the inflammatory response.

Mononuclear Cell Infiltration

Monocytes infiltrate the infarcted myocardium and modulate the inflammatory cascade. Following dynamic changes in cytokines and growth factors in the injured heart, infiltrated

monocytes maturate to macrophages (213). Macrophage can play various roles in the remodeling and healing of the injured myocardium. They clear the infarct from dead cardiomyocytes and apoptotic neutrophils by phagocytosis (214). Also macrophages can serve as major sources of cytokine and growth factor production which in turn can induce fibroblast activation and new vessel formation (215, 216). Macrophages can affect ECM remodeling through synthesis of both MMPs and MMP inhibitors (217).

Persistent presence of neutrophils following the onset of ischemia or IR results in excessive release of their toxic, tissue injuring intercellular contents (218). Therefore removal of apoptotic neutrophils is vital for proper healing of the injured myocardium (219). Apoptotic neutrophils produce signals which initiate macrophage mediated clearance. At the initial steps of apoptosis, the "find me" flags are upregulated by apoptotic neutrophils. Then the "eat me" signals are upregulated on the surface of the dying neutrophils (220). Macrophages express variety of receptors that can bind to "eat me" signals. Also, following digestion of apoptotic neutrophils, macrophages switch to an anti-inflammatory phenotype, releasing anti-inflammatory cytokines such as TGF-β and IL-10 (221) . Interestingly macrophage digestion of apoptotic neutrophils results in release of growth factors such as VEGF and HGF which are associated with tissue healing and repair following IR (222).

CHAPTER 2

DUAL INHIBITION OF CATHEPSIN G AND CHYMASE REDUCES MYOCYTE DEATH AND IMPROVES CARDIAC FUNCTION AFTER MYOCARDIAL ISCHEMIA REPERFUSION INJURY

Hooshdaran, Dual inhibition of cathepsin G and chymase is cardioprotective

BAHMAN HOOSHDARAN, MS[1], MIKHAIL A KOLPAKOV, MD, PHD[1], XINJI GUO, PHD[1], SONNI A MILLER, PHD[1], TAO WANG, MD, PHD,[1] DOUGLAS G TILLEY, PHD[2], KHADIJA RAFIQ, PHD[3], ABDELKARIM SABRI, PHD[1,4]

[1]Cardiovascular Research Center and [2] Center of Translational Medicine, Lewis Katz School of Medicine, Temple University, Philadelphia, PA. [3]Center of Translational Medicine, Thomas Jefferson University, Philadelphia, PA.

[4]**Address correspondence to**: Abdelkarim Sabri, Ph.D.

Cardiovascular Research Center, Temple University

MERB 1045, 3500 N. Broad Street, Philadelphia, PA 19140, USA

Tel. 215-707-4915; Fax. 215-707-5737

E-mail. sabri@temple.edu

Subject Codes: Heart failure, Ischemia, Inflammation, Basic Science Research, Cell signaling/signal transduction**.**

2.1 Abstract

Background: Early reperfusion of ischemic cardiac tissue - ischemia/reperfusion (IR) - increases inflammatory cell infiltration which contributes to cardiomyocyte death and loss of cardiac function. Neutrophil- and mast cell-derived proteases, cathepsin G (Cat.G) and chymase, are released early after IR, but their function is complicated by potentially redundant actions and targets. This study investigated whether a dual inhibition of Cat.G and chymase influences cardiomyocyte injury and wound healing after experimental IR in mice.

Methods and Results: Treatment with a dual Cat.G and chymase inhibitor (DCCI) blocked cardiac Cat.G and chymase activity induced after IR, which resulted in decreased immune response in the infarcted heart. Mice treated with DCCI also had less myocardial collagen deposition and showed preserved ventricular function at 1 and 7 days post-IR compared with the vehicle-treated group. DCCI treatment significantly attenuated focal adhesion (FA) complex disruption and myocyte degeneration after IR. Treatment of isolated cardiomyocytes with Cat.G or chymase significantly promoted FA signaling downregulation, myofibril degeneration and myocyte apoptosis. Conversely, treatment of cardiac fibroblasts with Cat.G or chymase induced FA signaling activation along with an increase in migration and differentiation to myofibroblasts. These responses in cardiomyocytes and fibroblasts were blocked by treatment with DCCI.

Conclusions Cat.G and chymase are key mediators of myocyte apoptosis and fibroblast migration and differentiation that play a role in adverse cardiac remodeling and function post-IR. Thus, dual targeting of neutrophil- and mast cell-derived proteases could be used

as novel therapeutic strategy to reduce post-IR inflammation and improve cardiac remodeling.

2.2 Introduction

Restoration of blood flow after acute myocardial infarction limits infarct size and reduces mortality. However, reestablishing blood flow is often followed by a second set of stresses, a phenomenon referred to as ischemia-reperfusion (IR) injury, which can result in additional myocardial damage and account for up to half of total infarct size.(223, 224) factors contributing to IR injury are complex and include microvascular obstruction, inflammation, release of reactive oxygen species, radicals, myocardial stunning, and activation of cardiac cells apoptosis and necrosis.(18, 223, 224) A large amount of the early cardiac tissue damage that occurs during inflammation post-IR is mediated through early activation of neutrophils and mast cells, which produce reactive oxygen radicals and release granules containing proteolytic enzymes that are chemoattractants for other leukocyte populations.(225, 226) While extensive research has explored the mechanisms responsible for the activation of inflammatory-derived cytokines/chemokines and reactive oxygen species and their roles in the infarcted heart, there is a paucity of information regarding the role of neutrophil- and mast cell-derived serine proteases on cardiac injury post-IR.(227)

Inflammatory serine proteases (ISPs) derived from neutrophils, such as cathepsin G (Cat.G), elastase, and proteinase 3, and from mast cells, such as chymase and tryptase, are enzymes known mainly for their function in the intracellular killing of pathogens.(228, 229) Their extracellular release upon leukocyte activation is traditionally regarded as the primary reason for tissue damage at the sites of inflammation. However, some evidence indicates that ISPs may also be key regulators of the inflammatory response.(228, 229) ISPs cleave and functionally modulate a number of protein substrates, including clotting

factors, neutrophil chemoattractants, and extracellular (ECM) components (*e.g.* proteoglycans, collagen, elastin, fibronectin).(10, 12) The adverse effects of Cat.G and chymase go beyond the breakdown of matrix proteins or the generation of cytokines and chemokines, which stimulate the infiltration of inflammatory cells. Recent studies from our lab and others identified cardiac myocytes and fibroblasts as additional cell targets for Cat.G and chymase.(230-232) Both Cat.G and chymase induce morphological changes in cardiomyocytes that disrupt intercellular contacts and focal adhesion (FA) signaling.(232, 233) Chymase can also trigger signaling in cardiac fibroblasts that leads either to proliferation at low dose or death by autophagy at high dose.(234, 235) However, the molecular mechanisms by which Cat.G and chymase modulate cardiac myocyte and fibroblast function are still largely unknown.

Because human Cat.G and chymase have similar active sites and share some common functions,(10, 12) assessing their function in human diseases is complicated by potentially redundant functions and targets. One strategy has been to develop dual Cat.G-chymase inhibitors (DCCI).(13) The DCCI used in this study was shown to selectively inhibit Cat.G and chymase *in vitro* (IC50= 53nM for Cat.G and 90nM for chymase), with little effect on several other serine proteases such as thrombin, factor Xa, trypsin, tryptase, proteinase 3, and elastase (IC_{50} > 100 μM).(13) DCCI has been shown to markedly reduce neutrophil influx and nitric oxide levels associated with LPS-induced lung inflammation.(236) In the present study, we describe how DCCI administration to mice subjected to IR injury resulted in reduced myocardial Cat.G and chymase activity and pathologic remodeling associated with IR. We show that it also reduced collagen deposition within the myocardium and prevented left ventricular (LV) dysfunction. Our findings provide evidence that a dual

inhibitor targeting Cat.G and chymase may be of therapeutic benefit in protecting the heart from IR injury.

2.3 Methods

Experimental protocol: All mice were maintained in accordance with protocols approved by the Animal Care and Use Committee of Temple University. Ten-week-old C57BL6 male mice were anesthetized with a mixture of ketamine (100 mg/kg) and xylazine (10 mg/kg) and left thoracotomy was performed under mechanical ventilation. Body temperature was maintained by a heated surgical platform and was monitored throughout surgery using a rectal sensor. A 6-0 suture with a slipknot was tied around the left anterior descending (LAD) coronary artery to produce ischemia. Consistent elevation of the ST segment was observed in lead II tracings following occlusion of the LAD coronary vessel. Regional ischemia was confirmed by visual inspection under a dissecting microscope (Nikon) by discoloration of the occluded distal myocardium. The ligation was released after 30 minutes of ischemia and the tissue was allowed to reperfuse as confirmed by visual inspection. The chest wall was closed with 8-0 silk and then the animal was removed from the ventilator and kept warm in the cage maintained at 37°C overnight. A sham procedure constituted the surgical incision without LAD ligation. Hearts were harvested after 1 or 7 days of reperfusion.

To investigate the role of Cat.G and chymase, mice were randomly divided into 4 major groups, consisting of: (1) sham mice receiving DCCI (EMD Millipore, 219372) (10 mg/kg body weight; n = 8); (2) sham mice receiving vehicle (0.1% DMSO in NaCl 0.9%; n = 8); (3) IR mice receiving 10 mg/kg DCCI (n = 8); and (4) IR mice receiving vehicle (0.1%

DMSO in NaCl 0.9%, n = 8). DCCI or its vehicle were administered by means of single intravenous bolus injection immediately after reperfusion of the ischemic myocardium (for mice subjected to IR for 24 h) and treated daily via intrapertonial injection (for mice subjected to IR injury for 7 days).

Data Analysis: Summary data are presented as mean ± SEM. For comparisons of >2 groups, one way ANOVA or, more generally, the generalized linear regression approach was employed for normal distributions and the Kruskal Wallis test for non-normal or small sample situations. Two group comparisons were analyzed by the two-sample *t* test or nonparametric Wilcoxon rank test, whenever appropriate (e.g., when the sample size was small and/or the distribution was not normal). All *in vitro* experiments were performed at least three times from three different cultures and the data values were scaled to controls. A value of $p<0.05$ was considered statistically significant.

An Expanded Methods section is provided in the Supplemental material.

2.4 Results

DCCI treatment attenuates the severity of the acute inflammatory response after IR. Initially, we determined the time course of the increase in myocardial neutrophil and mast cell-derived protease activity after induction of IR injury, wherein myocardial Cat.G, elastase and chymase activity were measured at 3 h, 6 h, 1 and 7 days after IR. While the activity of each protease increased after IR, Cat.G and elastase protease activity underwent early transient increases, returning to baseline at 7 days post-IR (Figures 1A and 1B), while chymase activity increased early and was sustained for over 7 days post-IR (Figure 1C). Immunohistochemistry results further corroborate the changes observed in protease

activity, as Cat.G-positive cells in the heart were markedly increased at 1 day post-IR, but decreased to baseline at 7 days post-IR (Figures 1D and 1E). In contrast, chymase-positive cells were elevated at both 1 and 7 days post-IR (Figures 1D and 1F). These data highlight the differential kinetics of Cat.G and chymase activity following acute cardiac injury, and suggest that targeting both could have more impact on preventing the deleterious effects of sustained protease activity over time.

To evaluate the efficacy of inhibiting both Cat.G and chymase in preventing the sequelae of IR injury, we treated mice with DCCI for 1 and 7 days. DCCI was given during reperfusion at 10 mg/kg intravenously and thereafter injected every day intraperitoneally for 6 days. This dose was based on the biological half-life of DCCI and on *in vivo* experiments in which the compound's effectiveness was evaluated in an acute lung injury model.(236) The mice were sacrificed at 1 day after IR (a time point coinciding with peak inflammatory cell infiltration and myocyte loss) and at 7 days post-IR, coinciding with peak scar formation and repair.(225) At 1 and 7 days post-IR, myocardial Cat.G and chymase proteolytic activity were significantly reduced in DCCI-treated mice compared with vehicle-treated mice (Figures 2A and 2B), while Cat.G and chymase activity were not significantly altered in DCCI- and vehicle-treated sham-operated mice. Myocardial myeloperoxidase (MPO) activity was measured to determine the impact of DCCI on the infiltration of inflammatory cells after IR. In DCCI-treated mice, MPO activity was markedly reduced compared with that in vehicle- treated mice (Figure 2C). Post-IR immunohistological examination of DCCI- and vehicle-treated mouse hearts further corroborated these data (Figure 2D), as the number of MPO-positive neutrophils were markedly reduced in the infarcted regions of DCCI- versus vehicle-treated mouse hearts

(Figures 2D and 2E). DCCI-treated mice also show less infiltration of mast cells (Figures 2D and 2F), Mac-3-positive macrophages and CD3-positive T-cells (Supplemental Figure S1) in the infarcted area compared to vehicle-treated group. Moreover, activation of pro-inflammatory signaling pathways, STAT3 and NF-kB, and accumulation of pro-inflammatory cytokines that mediate early infiltration of leukocytes in the infarcted myocardium, tumor necrosis factor- (TNF)α and interleukin- (IL)-1β,(237, 238) were markedly reduced in the infarcted regions of DCCI- versus vehicle-treated mouse hearts (Figure 2G). Collectively, these data show that dual inhibition of Cat.G and chymase activity reduces early inflammatory responses following IR injury.

Dual inhibition of Cat.G and chymase improves cardiac function.

We next explored the impact of Cat.G and chymase inhibition on cardiac function at 1 and 7 days post-IR. DCCI-treatment did not alter baseline heart weight-to-body weight ratio, heart rate, or LV dilatation in sham-operated animals (Figure 3 and Supplemental Tables 1 and 2). However, DCCI-treated mice displayed a significant preservation in post-IR cardiac function versus vehicle-treated mice, including LV ejection fraction and fractional shortening (Figures 3A and 3B). LV end-systolic and diastolic dimensions (Figures 3C and 3D) were also shown to undergo better preservation post-IR in DCCI- versus vehicle-treated mice. Morphometric analysis indicates the presence of cardiac hypertrophy and concomitant signs of cardiac failure, such as an increase in lung weight, in vehicle-treated mice, whereas only the latter pathological response was reduced in the DCCI-treated mice at 7 days post-IR (Figures 3E and 3F and Supplemental Table 2). Infarct size measurements as percentage of area at risk or LV circumference indicated 34 ±2% and 38 ±4% of the LV to be affected by the infarct at 1 and 7 days in vehicle-treated mice, respectively, whereas

the infarct accounted for 24 ±3% and 26 ±2% of the LV in DCCI-treated mice (Figures 3G and 3H). Thus, the integrity of the infarcted area was maintained after IR in DCCI-treated mice with reduced LV dilatation compared to vehicle-treated mice, which results in a better cardiac function post-IR.

Dual inhibition of Cat.G and chymase is cardioprotective.

The extent of myocardial infarct and impairment in cardiac performance depends on the levels of cardiomyocyte loss post-IR, which we measured in vehicle- and DCCI-treated mice 1 day post-IR via terminal deoxynucleotidyl transferase dUTP nick end labeling (TUNEL). Consistent with a protective effect of protease inhibition at time of IR, mice that were treated with DCCI had a reduced number of TUNEL-positive myocytes 1 day following reperfusion compared to vehicle-treated mice (Figures 4A-4C). Cardiac caspase-3 activity (Figure 4D) and circulating plasma levels of cardiac troponin-I (cTnI, Figure 4E) were also reduced in DCCI- versus vehicle-treated mice 1 day post-IR. DCCI-treated mice also showed reduced expression of pro-apoptotic molecule Bcl2 and enhanced accumulation of signaling molecules known to inhibit cell apoptosis such as Bax and XIAP compared to vehicle-treated mice (Figure 4F), confirming the cytoprotective effect of dual inhibition of Cat.G and chymase at the time of injury.

DCCI protects IR-induced FA signaling alteration.

Both Cat.G and chymase have been shown to induce myocyte apoptosis via downregulation of FA signaling *in vitro*.(231, 232) Thus, we explored whether DCCI treatment alters IR-induced FA signaling in the heart. Vehicle-treated mice showed decreased FAK and paxillin protein accumulation that correlated with a decrease in cTNI

expression (Figures 4G). In contrast, DCCI-treated mice showed less IR-induced FAK, paxillin and cTnI degradation compared to vehicle-treated mice. Collectively, these data show that dual Cat.G and chymase inhibition protects FA signaling and induces cardio protective signaling events to promote myocyte survival in the heart following IR.

To directly demonstrate that the cardioprotective effects of DCCI after IR may result from direct actions of Cat.G and chymase on cardiomyocytes, we investigated the effect of DCCI on cardiomyocyte apoptosis induced by these proteases. Treatment of neonatal rat cardiomyocytes (NRCMs) with Cat.G or chymase for 8 h markedly induced myocyte detachment and increased caspase-3 activity (Figures 5A and 5B). In contrast, treatment with DCCI blunted both myocyte detachment and cell death induced by Cat.G and chymase treatment. Conversely, treatment of neonatal rat cardiac fibroblasts (NRCFs) with Cat.G or chymase for 8 h did not induce detachment or caspase-3 activity (Figures 5A and 5C), demonstrating a differential response between myocytes and fibroblasts after Cat.G or chymase treatment.

To delineate the mechanisms involved in the differential response between cardiac myocytes and fibroblasts, we assessed the impact of DCCI on Cat.G- and chymase-induced FA signaling, which we have shown previously to play an important role in Cat.G- and chymase-induced myocyte detachment and apoptosis.(231, 232) Myocytes treated with Cat.G or chymase showed markedly reduced FAK and paxillin tyrosine phosphorylation after treatment for 10 min (Figure 5D), which were markedly reduced by DCCI. DCCI treatment also inhibited FAK, paxillin and cardiac troponin I degradation induced by Cat.G treatment for 4 h (Supplemental Figure S2). Conversely, Cat.G or chymase treatment induced FAK and paxillin tyrosine phosphorylation in fibroblasts, demonstrating activation of FA signaling

(Figure 5E). These data highlight a major molecular mechanism by which Cat.G and chymase signaling induces distinct outcomes in cardiomyocytes versus fibroblasts.

Mice treated with DCCI are protected against profibrotic remodeling induced after IR injury.

Based on our findings that Cat.G and chymase do not induce fibroblast detachment and death, we next explored the potential role of DCCI on cardiac fibrosis and remodeling responses post-IR. Collagen fractional area in the non-infarcted region of the heart was not different between DCCI- and vehicle-treated groups (Figures 6A and 6B). However, DCCI-treated mice had significantly less collagen accumulation in the infarcted region compared with vehicle-treated mice at day 7 post-IR. To determine the mechanisms of decreased collagen accumulation after DCCI treatment, we evaluated accumulation of myofibroblasts, which are a primary source of extracellular matrix (ECM) protein synthesis in the infarcted myocardium.(239) Analysis of smooth muscle α-actin (SMA) staining showed minimal accumulation of myofibroblasts in sham-operated hearts (not shown) which progressively increased in vehicle-treated mice infarcts (Figures 6A and 6C). DCCI-treated mice showed reduced myofibroblast density and decreased accumulation of profibrotic CTGF and TGFβ gene expression in the infarcted heart (Figures 6C and 6D). We also investigated whether DCCI treatment affects ECM degradation after IR. Both pro- and active-MMP2/9 levels, as well as gelatinase activity, were significantly reduced in the infarcts of DCCI- versus vehicle-treated mice 7 days post-IR (Figure 6E and 6F). Levels of pro-MMP2/9 were similar in DCCI-treated shams compared to vehicle-treated mice. Thus, inhibition of Cat.G and chymase activity results in fibroblast differentiation and

activity following IR that is associated with diminished ECM accumulation and preserved cardiac contractile dysfunction.

Cat.G and chymase induces fibroblast migration and differentiation.

Because fibroblasts are important components of fibrosis, we determined whether Cat.G or chymase directly influenced fibroblast migration and ECM protein accumulation in isolated neonatal rat cardiac fibroblasts. In control experiments, we established that treatment with Cat.G or chymase increased SM α-actin expression, indicating fibroblast differentiation to myofibroblasts (Figure 7A). Cat.G or chymase treatment also increased TGF-β1 and collagen I expression, indicative of enhanced secretory phenotype. Conversely, concurrent treatment with DCCI blocked Cat.G- or chymase-induced responses in cardiac fibroblasts.

We next determined whether Cat.G- or chymase-induced fibroblast differentiation modulates activation of NF-κB and STAT3 activation, important mediators of cardiac inflammation and fibrosis following injury.(225) Cat.G or chymase treatment was sufficient to activate endogenous NF-κB and STAT3, responses that were abolished by treatment with DCCI (Figure 7B). The proinflammatory effect of Cat.G and chymase was further corroborated by changes in the expression of the NF-κB/STAT3-responsive genes such as TNF-α and IL-1β, which were upregulated in Cat.G- or chymase-treated fibroblasts compared with control cells, and treatment with DCCI blocked these responses (Figure 7C).

Given these findings with respect to cell differentiation, we also sought to determine whether fibroblast migration and differentiation are sensitive to DCCI. Figure 7D shows

representative phase-contrast micrographs of scratch assays of confluent fibroblast cell monolayers. Both Cat.G and chymase increased fibroblast migration compared with vehicle (Figure 7E). Importantly, the degree of cell migration observed with Cat.G was not significantly different from that of chymase-treated cells. Fibroblast migration induced by Cat.G or chymase was significantly diminished after treatment with DCCI compared with vehicle-treated cultures. Collectively, these data demonstrate that Cat.G and chymase can directly trigger fibroblast migration and differentiation to myofibroblasts.

2.5 Discussion

The current study provides new insights into the mechanisms of pathological remodeling during early induction of IR injury. We demonstrate that dual inhibition of Cat.G and chymase activity is associated with a decrease in the pathologic severity of the cardiac inflammatory response, myocyte apoptosis and fibrosis post-IR. The reduced adverse remodeling in the DCCI-treated mice was associated with improved myocardial function when compared with that in the vehicle-treated mice. Interestingly, we found that Cat.G and chymase activate signaling pathways that culminate to detachment and apoptosis of myocytes, while they promote migration and differentiation of fibroblasts. This dichotomic outcome between cardiac myocytes and fibroblasts is likely related to differential regulation of FA signaling by Cat.G and chymase. These novel findings show that one of the earliest events in mediating cardiac dysfunction after IR injury involves an increased activation of Cat.G and chymase and points to DCCI as a therapeutic benefit.

The major effect underlying the absence of severe tissue injury after cardiac IR in DCCI-treated mice is the inability to sustain the presence of inflammatory cells in the heart after

reperfusion. The decreased Cat.G and chymase activity observed after reperfusion in ischemic hearts from DCCI-treated mice was accompanied by a decrease in infiltration of neutrophils and mast cells. These cells have been reported to infiltrate early after myocardial injury and produce chemokines, which may amplify and sustain the intensity of leukocyte migration to the site of myocardial injury.(240, 241) Accordingly, we show that DCCI-treated mice hearts have reduced production of inflammatory cytokines, IL-1β and TNF-α, and decreased accumulation of macrophages and T cells in the infarcted heart at day 1 and 7 post-IR compared to vehicle-treated mice. data extend previous studies showing the role of Cat.G and chymase in mediating monocytes, neutrophils or T cells migration *in vitro* and in the processing and maturation of several cytokines and chemokines including IL-1α, IL-6, and TNF-α.(228) In addition to these direct actions of Cat.G and chymase on inflammatory cells, DCCI-treated mice also show limited tissue exposure to myeloperoxidase, which is a major mediator of tissue damage after injury through generation of hypochlorous acid and reactive oxygen species.(242) The short term of myeloperoxidase activity observed in the heart from DCCI-treated animals argues that the initial burst of myeloperoxidase does not induce or sustain substantial injury in the absence of Cat.G or chymase. Collectively, these data emphasize the importance of Cat.G and chymase in mediating early cardiac immune response post-IR.

The limited exposure of the ischemic heart to Cat.G- and chymase-mediated events during reperfusion in DCCI-treated mice resulted in clear reductions in tissue injury and improvement in cardiac contractile function. One important consequence was a substantial decrease in cardiomyocyte apoptosis in the ischemic hearts. Several studies have demonstrated cardiomyocyte apoptosis after reperfusion of ischemic hearts and the

correlation between the number of apoptotic cells and the severity of cardiac dysfunction.(243) Whether the absence of Cat.G/chymase or the resultant limited exposure to myeloperoxidase or other inflammatory cell-derived cytokines/chemokines underlie this decrease in apoptosis cannot be defined from this study. However, both Cat.G and chymase have been shown to act directly on cardiomyocytes and promote apoptosis.(231, 232) In this study, we found that treatment with DCCI prevented FA protein degradation, myofibril degeneration and myocyte apoptosis induced after 24 h of IR injury and after treatment of isolated cardiomyocytes with Cat.G or chymase. The fact that the kinetics of FA signaling downregulation coincide with myocyte apoptosis post-IR strongly suggest that one of the earliest events leading to myocyte apoptosis after IR injury may involve a loss of ECM network surrounding myocytes and a lack of survival signaling emanating from ECM receptors, integrins, in response to elevated levels of Cat.G and chymase. The suppression of FA signaling downregulation by DCCI further supports the active role of Cat.G and chymase on cardiomyocyte stress during acute IR.

The induction of myocyte death has been proposed to be a principal factor leading to the tissue fibrosis that develops after IR injury.(244) Consistent with the lack of sustained Cat.G/chymase activity and decreased apoptosis of myocytes, there was a clear decrease in collagen deposition observed in hearts from DCCI-treated mice post-IR when compared with vehicle-treated mice. We also found that DCCI-treated mice present less myofibroblast accumulation at day 7 post-IR. This latter has been shown to be a primary source of ECM protein synthesis and pro-inflammatory cytokines in the infarcted myocardium.(239) Moreover, DCCI may have more direct antifibrotic effects as Cat.G and chymase may liberate TGF-β from the ECM, thereby stimulating fibroblast

differentiation and ECM synthesis,(223, 245-247) In this study, we show that DCCI treatment blocked both TGF-β and CTGF accumulation in the infarcted heart at day 7 post-IR and in isolated fibroblasts treated with Cat.G or chymase, which resulted in a decrease in ECM accumulation, fibroblast migration and differentiation to myofibroblasts. Cat.G and chymase can also affect ECM accumulation through activation of MMP-2 and -9(181, 207) which could degrade cardiac interstitial matrix, expand the healing infarct(248) and promote cardiac dilatation.(249) We show that DCCI treatment attenuated MMP-2/9 activation after IR *in vivo* and in isolated cardiac fibroblasts exposed to Cat.G or chymase (Supplemental Figure S3), suggesting that Cat.G and chymase-dependent activation of MMPs is also important in post-IR infarct remodeling and function.

The pleiotropic effects of Cat.G and chymase on cardiac myocytes and fibroblasts raises the intriguing question about the mechanisms by which these extracellular proteases initiate their effects in both cells. We have previously documented the role of MMP activation as a mechanism by which Cat.G induces FA signaling downregulation and myocyte apoptosis.(181) Consistent with these findings, DCCI treatment inhibited Cat.G- and chymase-induced MMP2 activation and FA protein degradation in cardiomyocytes (Supplemental Figure S3). Interestingly, in contrast to cardiomyocytes, Cat.G and chymase led to FA signaling activation in fibroblasts that culminated to fibroblast migration and differentiation. These data, although are in line with the role of FAK activation in mediating cell survival and growth, suggest a different mechanism of FA signaling regulation between myocytes and fibroblasts. Previous studies from our group in myocytes showed the role of protein tyrosine phosphatase SHP2 in mediating Cat.G-induced FA signaling downregulation and myocyte apoptosis.(181, 231) Whether SHP2 activation is

differentially regulated in cardiac fibroblasts versus cardiomyocytes in response to Cat.G or chymase needs further investigation. These data collectively show the pleiotropic actions of these proteases to trigger cardiomyocyte death and fibroblast migration/differentiation and the beneficial effect of DCCI treatment in preventing these effects.

The current study provides evidence that targeting neutrophil- and mast cell-derived proteases was efficient in protecting the heart from early myocyte death and excessive fibroblast migration and ECM accumulation, that contribute to adverse cardiac remodeling and contractile dysfunction. Moreover, DCCI can modulate cardiac remodeling and function indirectly by inhibiting Cat.G and chymase actions to convert angiotensin I to angiotensin II,(250, 251) a known humoral factor that promote cardiac hypertrophy, fibrosis, and remodeling.(22) Based on evidence that Cat.G and chymase have similar active sites, share some common targets and have potentially redundant functions, our strategy has been to use a dual inhibitor that selectively targets both Cat.G and chymase, without affecting other serine proteases.(13) There has been considerable interest to develop inhibitors of neutrophil- and mast cell-derived proteases, which contribute to cardiac injury and inflammation. Previous studies have shown the beneficial effect of inhibiting chymase on IR injury in dogs and pigs.(210, 252) However, in these studies there was no assessment of chymase inhibition on a more prolonged reperfusion on myocardial function and infarct extension. In rodents, the use of chymase inhibitor monotherapy provided mixed results with studies showing improved survival and reduced post-myocardial infarction cardiac hypertrophy and dysfunction with chymase inhibitor monotherapy,(253, 254) while others were negative.(255) This discrepancy using chymase

inhibitor monotherapy could be related to the fact that other inflammatory proteases such as Cat.G may play a redundant role in the pathophysiology of IR injury. Therefore, our results with DCCI suggest that inhibition of more than one crucial inflammatory protease might afford effective pharmacotherapy and show that restoration of a "protease-antiprotease balance" by the administration of exogenous inhibitors reduce excessive accumulation of inflammatory cells and their secreted proteases and could have therapeutic utility after myocardial IR injury.

In conclusion, a dual inhibitor targeting Cat.G and chymase is effective in reducing the pathologic severity related to IR injury in association with its ability to limit myocardial proteolytic activity. By attenuating collagen deposition within the myocardium and improving LV function, DCCI may ultimately decrease the progression to heart failure. Our study has therefore provided important data to support a previously unknown mechanism implicating Cat.G and chymase in the progression of this disease and the theoretical benefit of using a dual inhibitor targeting Cat.G and chymase in the therapy of acute IR injury.

ACKNOWLEDGEMENTS

None

SOURCE OF FUNDING

This work was supported by the National Institute of Health (HL360338 and HL 360343) and American Heart Association (14PRE20380518).

DISCLOSURES

None

2.6 Figures and Legends

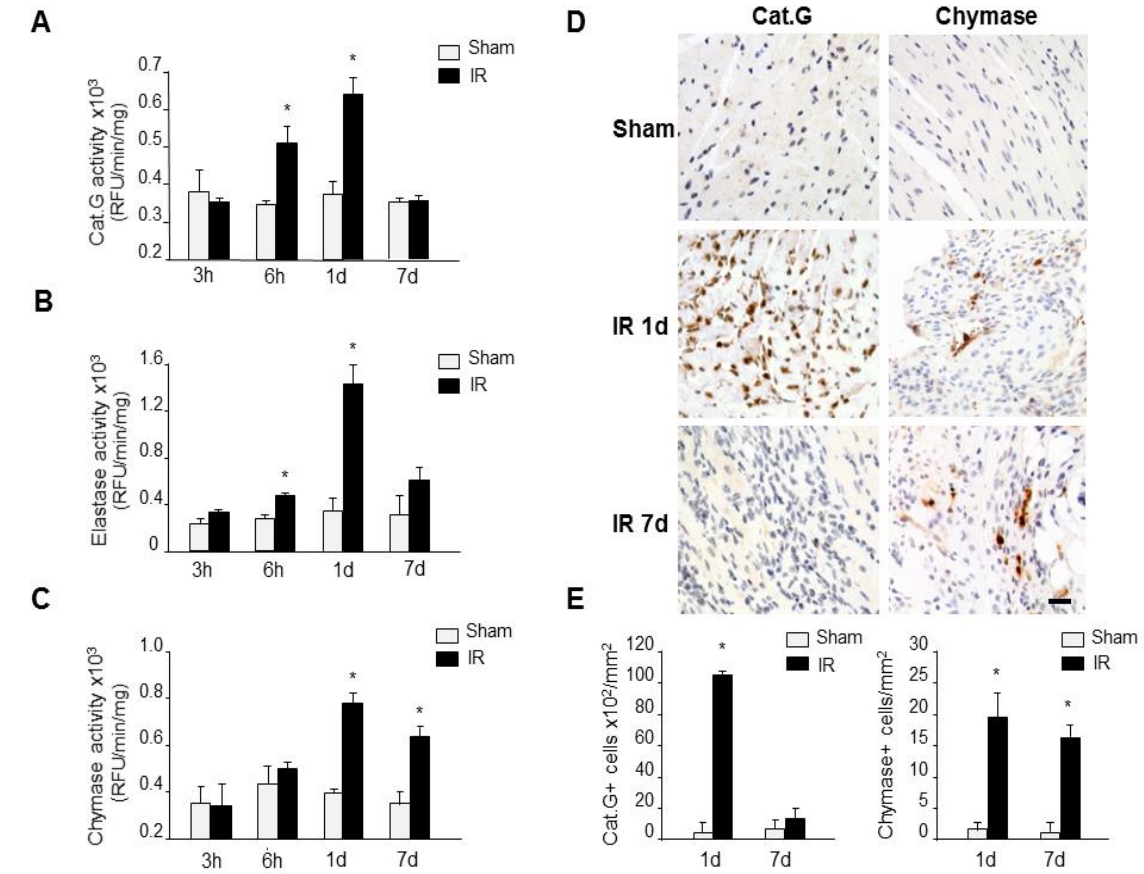

Fig 1

Figure 2-1: Inflammatory serine proteases are elevated after ischemia reperfusion (IR). (A-C) The left anterior descending artery was ligated for 30 min to induce ischemia and the heart was subsequently reperfused for 3 h, 6 h, 1 or 7 days. Cathepsin G (Cat.G) (A), elastase (B) and chymase (C) activity levels in the hearts of sham and mice subjected to IR injury were assessed by substrate specific enzymatic activity assay. Results are expressed as relative fluorescence units (RFU)/min/mg protein (n = 6 for each groups). (D) Representative Cat.G and chymase immunostaining of paraffin-embedded heart sections of sham or mice subjected to IR injury. Scale bar: 40µm. (E) Quantification of Cat.G and chymase-positive cells (n = 5 for each groups). Values are presented as mean ± SEM, $^{*}P < 0.05$ vs. WT shams.

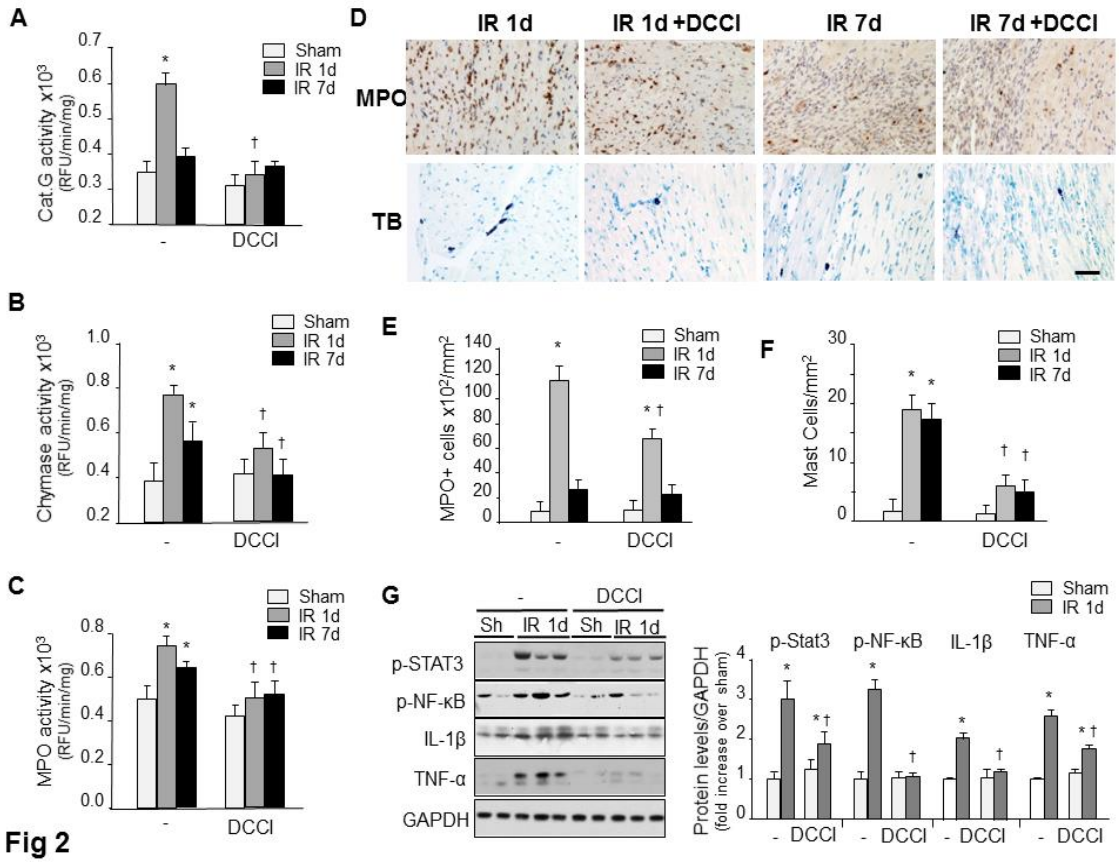

Fig 2

Figure 2-2: DCCI treatment attenuates inflammation in the reperfused heart. (A-C) Cathepsin G (Cat.G) (A), chymase (B) and myeloperoxidase (MPO) (C) activity in the infarcted LV as determined by enzymatic activity assay (n = 6 for each groups). (D) Representative MPO or toluidine blue (TB) staining of paraffin-embedded heart sections from sham or mice subjected to ischemia reperfusion (IR). Scale bar: 40μm. (E and F) Quantification of MPO- and mast cell-positive cells in mice treated with either vehicle or DCCI (n = 5 for each groups). (G) Left: Immunoblot analysis indicates a decrease in inflammatory signaling in the infarcted region of mice treated with DCCI compared to vehicle post-IR. Right: Quantification of experiments represented as fold change compared to sham animals treated with vehicle (n = 5 for each groups). GAPDH was included as a loading control. Values are presented as mean ± SEM, *P < 0.05 vs. shams, †P < 0.05 vs. vehicle-treated IR.

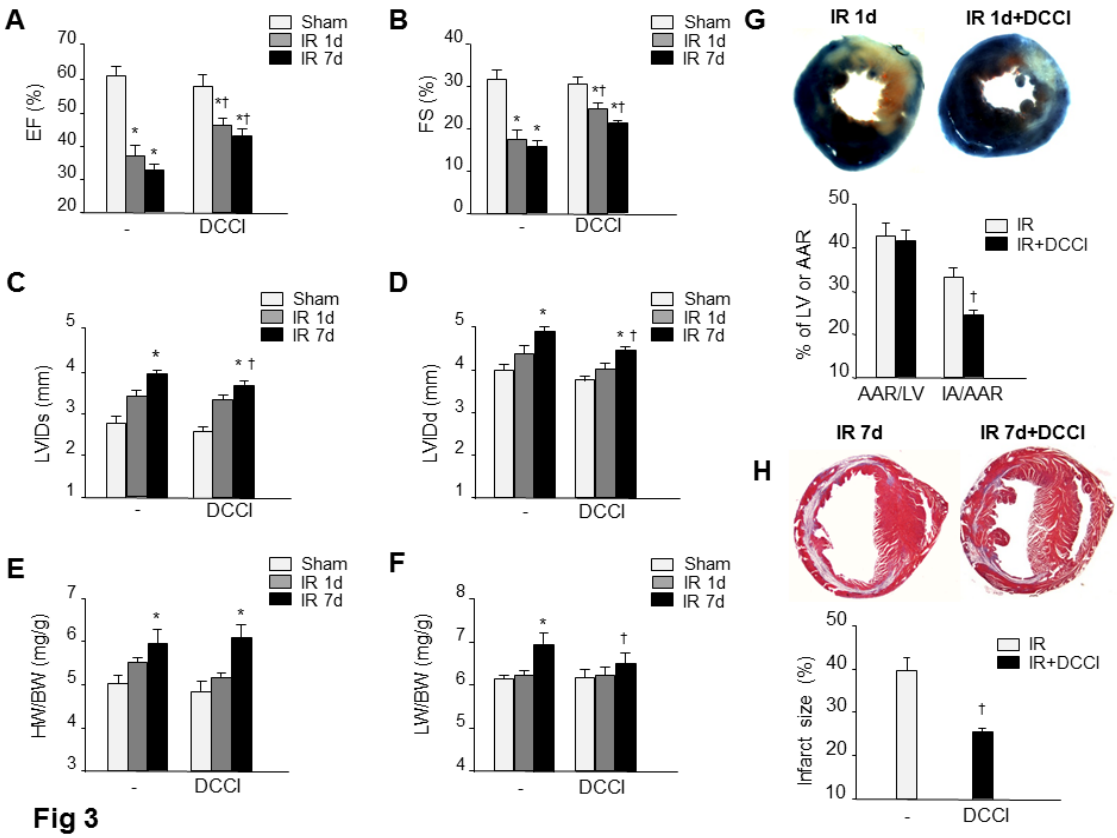

Fig 3

Figure 2-3: DCCI improves cardiac function post-IR. (A-D) Echocardiography measurement of Left ventricular (LV) ejection fraction (EF) (A), fractional shortening (FS) (B) and LV internal diameter (LVID) in systole (C) and diastole (D). (E and F) Effects of DCCI treatment on IR-induced heart weight (HW) (E) or lung weight (LW) (F) to body weight (BW) ratio (n = 6 shams, n = 8 IR groups). (G and H) Top: Representative images of Evans blue and diphenyl tetrazolium chloride or Masson's trichrome staining on transverse heart sections at day 1 (G) and 7 (H) post-IR, respectively. Bottom: Quantification of the area at risk (AAR) and infarct area (IA) (n = 5 for each groups). Values are presented as mean ± SEM, $^{*}P < 0.05$ vs. sham, †$P < 0.05$ vs. vehicle-treated IR.

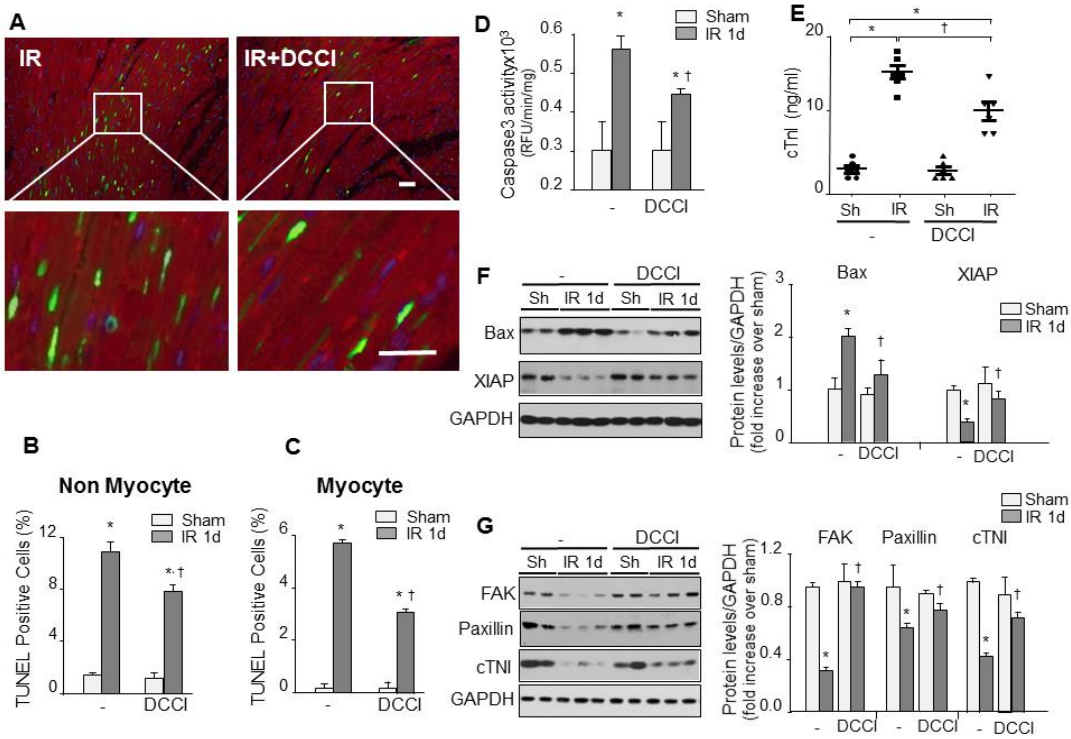

Fig 4

.

Figure 2-4: DCCI deletion offers cardioprotection after acute IR. Ischemia reperfusion (IR) was induced for 24 h. (A) LV tissue sections were assessed for apoptosis using TUNEL assay (green), tropomyosin (red), and DAPI (4′,6-diamidino-2-phenylindole) (blue) staining. Scale bar: 40 μm. (B and C) The number of TUNEL-positive myocytes (B) and non-myocytes (C) in the reperfused area was expressed as a percentage of total nuclei detected by DAPI staining (n = 5 each group). (D) Quantification of caspase-3 activity in the LV using caspase-3 specific fluorogenic substrate (n = 6 each group). (E) Plasma levels of cardiac troponin-I (cTnI) as determined by ELISA assay in samples from vehicle- or DCCI-treated mice 24 h post-IR (n = 6 each group). (F and G) Immunoblot analysis indicates a decrease in pro-apoptotic signaling (F) and focal adhesion signaling (G) in the infarcted region of mice treated with DCCI or vehicle post-IR. Left: Representative immunoblots. Right: Quantification of experiments represented as fold change compared to shams (n = 6 each group). GAPDH was included as a loading control. Values are presented as mean ± SEM, $^{*}P < 0.05$ vs. shams, †$P < 0.05$ vs. vehicle-treated

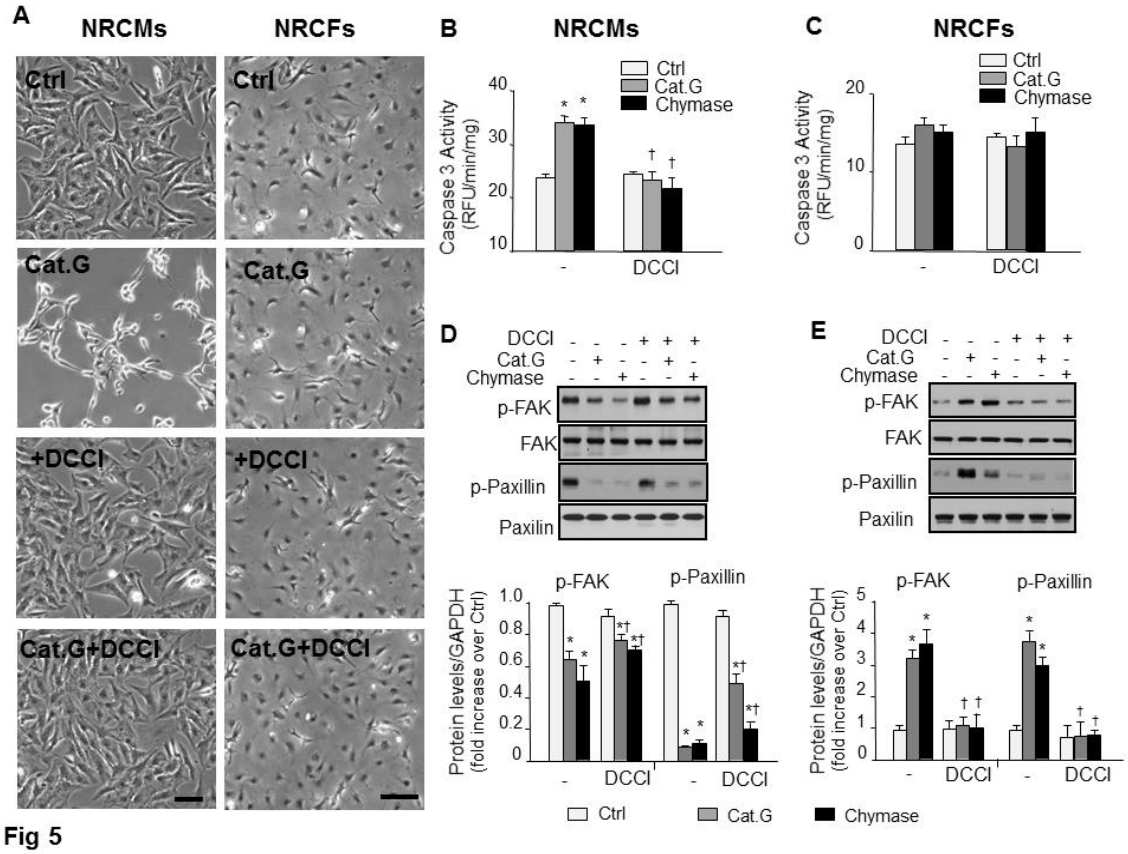

Fig 5

Figure 2-5: Dual effects of cathepsin G and chymase on focal adhesion signaling and cell detachment. (A-D) Neonatal rat cardiomyocytes (A, B, D) and fibroblasts (A, C, E) were pretreated without or with DCCI (5 μM) prior to treatment with cathepsin G (Cat.G) or chymase for 8 h. (A) Phase-contrast photomicrographs (Bar=100 μm). (B and C) Caspase-3 activity was measured using fluorogenic substrate. (D and E) Left: Representative immunoblots showing focal adhesion (FA) signaling in cardiomyocytes (D) and fibroblasts (F) treated with Cat.G or chymase for 10 minutes in presence of DCCI or its vehicle. Right: Quantification of experiments expressed as mean ±SEM from 3 separate cultures. * $P < 0.05$ vs. control, †$P < 0.05$ vs. vehicle-treated cells.

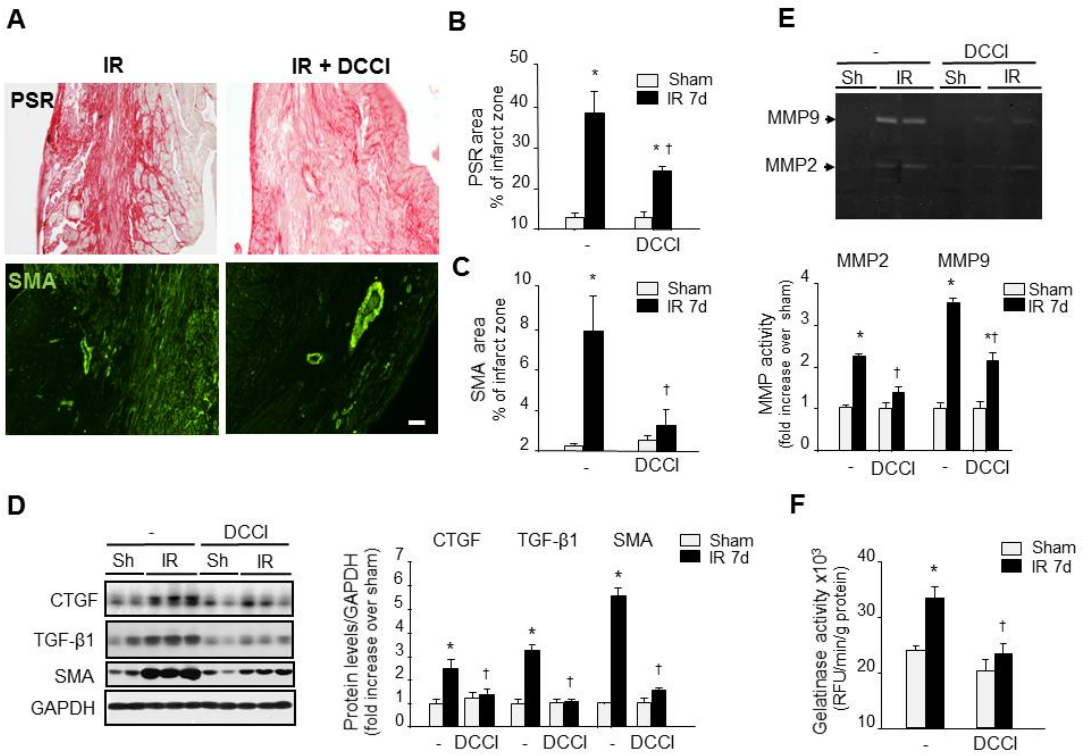

Fig 6

Figure 2-6: DCCI reduces fibrosis and improves cardiac remodeling after IR. Ischemia reperfusion (IR) was induced for 7 days. (A) Picro-sirus red staining and immunohistochemistry against smooth muscle α-actin (SMA) show reduced collagen and myofibroblast deposition in the injured myocardium of mice treated with DCCI compared to those treated with vehicle. (B-C) Semi-quantitative analysis of collagen staining (B) and SMA immunoreactive myofibroblasts (C) expressed as a percentage of total infarct area. (D) Immunoblot analysis indicates a decrease in profibrotic signaling molecules in the infarcted region of mice treated with DCCI vs. the treatment with vehicle post-IR. Left: Representative immunoblots. Right: Quantification of experiments represented as fold change compared to WT animals (n = 6 for each groups). GAPDH was included as a loading control. (E) In-gel zymography (Top) and relative band density quantification (Bottom) indicates a decrease in MMP-2 and -9 activity in the infarcted myocardium of mice treated with DCCI vs. treated with vehicle. (F) Gelatinase activity assay in animals subjected to IR and treated with either vehicle or DCCI (n=5 for each groups). Values are presented as mean ± SEM, $^{*}P < 0.05$ vs. shams, †$P < 0.05$ vs. vehicle-treated IR.

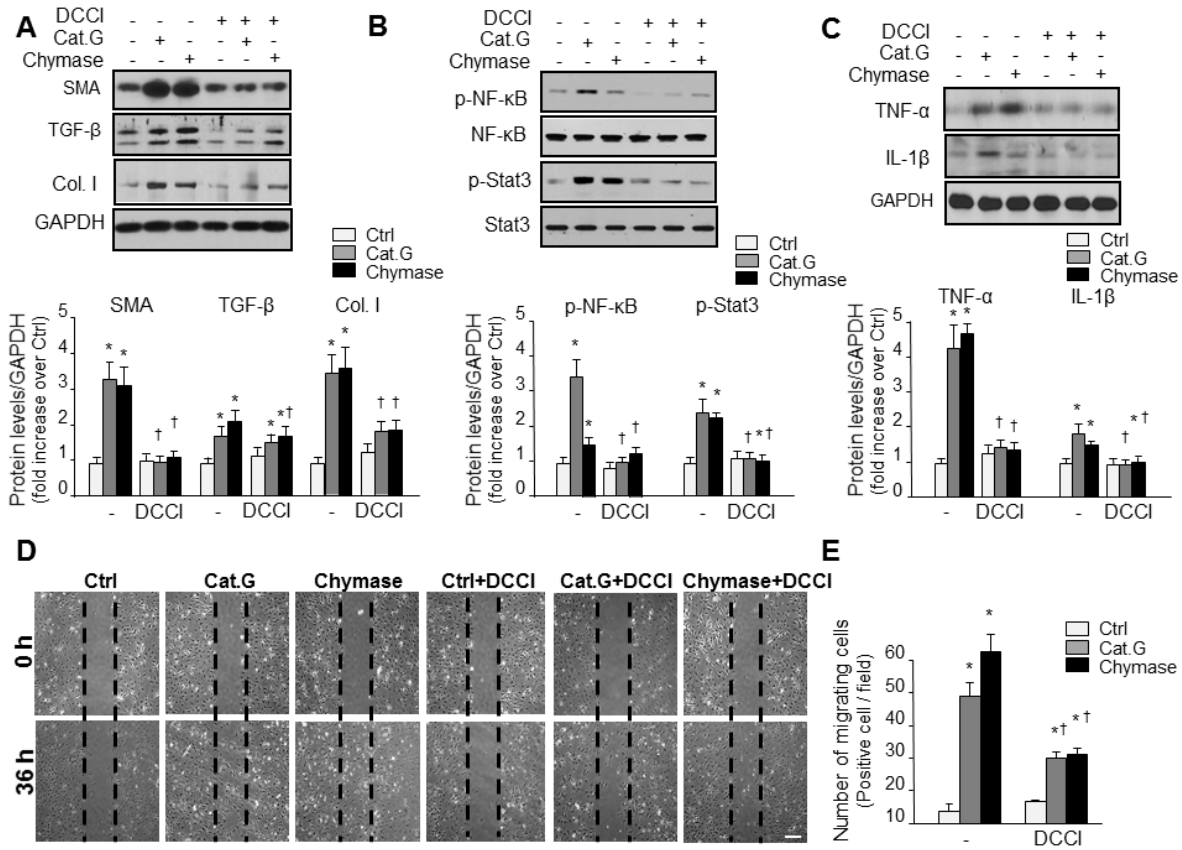

Fig 7

Figure 2-7: Cathepsin G and chymase induce cardiac fibroblast migration and differentiation. (A-C) Neonatal rat cardiac fibroblasts were pretreated with DCCI (5μM) or vehicle for 15 minutes and then treated with cathepsin G (Cat.G, 0.02 U/ml) or chymase (100nM) for 36 h and cell lysates were processed for immunoblot analysis. Top: Representative immunoblots. Bottom: Quantification of experiments represented as fold change compared to untreated control (Ctrl). GAPDH was included as a loading control. (D) Migration scratch assay was performed to assess the rate of migration of cardiac fibroblasts untreated or treated with Cat.G or chymase with or without DCCI pretreatment. (E) A significant increase in the migration rate was observed in Cat.G- and chymase-treated fibroblasts compared with controls which was attenuated by DCCI treatment. Scale bar: 200 μm. Results are representative of 3 independent experiments. Data are mean ± SEM; $^{*}P < 0.05$ vs. control; †$P < 0.05$ vs. vehicle-treated fibroblasts.

CHAPTER 3

LITERATURE REVIEW PART 2: TARGETED DRUG DELIVERY TO THE MYOCARDIUM

Difficulties in the treatment of severe diseases like cancer have motivated scientists to adopt multidisciplinary methods to deliver agents and drugs in a target specific manner (256). These developing approaches mostly aim at minimizing the side effects and at the same time increasing the bioavailability and therapeutic index of the desired drugs at the specific site of the disease.

In 1906, Ehrlich introduced the idea of targeted delivery in the form of magic bullets (257). He believed that someday chemists will be able to generate substances that can specifically target agents, responsible for each disease. Nowadays the term "targeted drug delivery" is defined as the buildup of active drugs or reagents in the desired target whilst minimizing their accumulation in other organs. Ideally the concentration of delivered agents should be above effective in the targeted regions and below toxic in non-targeted ones.

Recent advancements in the field of nanotechnology has led to development of different carriers. These carriers known as drug vehicles have different characteristics, and therefore each suits specific delivery needs. To design and choose the best vehicle for any delivery need, a multifaceted decision-making process is necessary: First, the vehicle should be recognized only by the desired diseased cells and no other healthy ones to achieve a selective and specific delivery. Second, the vehicle must stay stable in the plasma for long circulating times. Other important criteria are the carrier-drug complex toxicity,

immunogenicity and biodegradability. Lastly, following selective binding to the desired site, the drug should be easily released from the complex to affect the targeted cells or tissue.

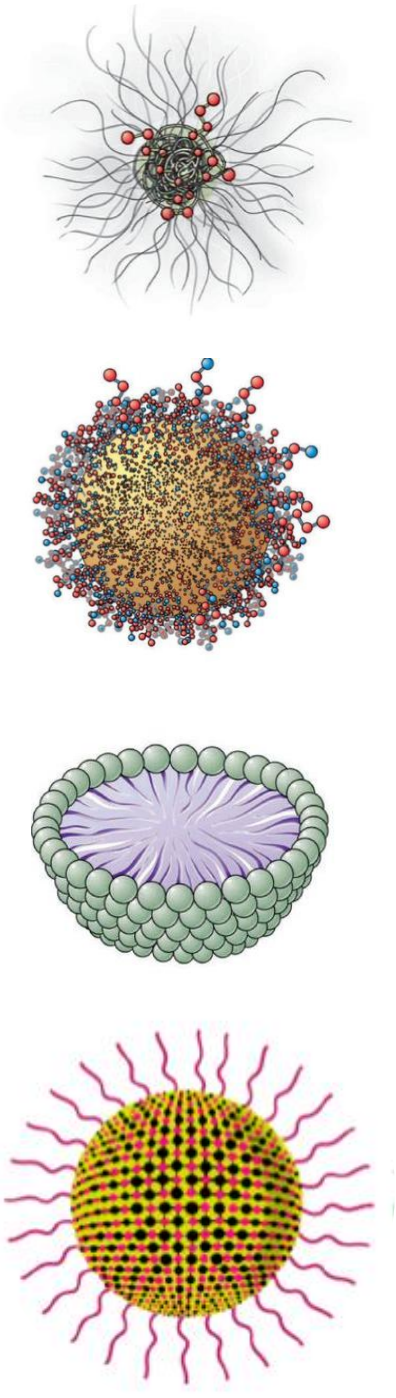

Schematic 3-1: From top to bottom: Schematics of monoclonal antibodies and fragments, synthetic polymer, liposome and quantum Dot. (1)

3.1 Delivery Vehicles

Drug delivery vehicles, or as they are called drug vectors, are the backbone of successful targeted delivery. A proper vehicle transports and delivers its payload to the desired site while protecting it from degradation and clearance in plasma and other organs (258). Currently used vehicles can be divided into particulate, soluble and cellular carriers. Next, we will introduce some of the most commonly used carriers.

Monoclonal antibodies and fragments. Most antibody-based delivery methods have been developed to meet the needs of anti-cancer therapies. These approaches are mostly designed based on the presence or upregulation of specific antigens on the surface of the tumor cells. The drug is released from the antibody-drug conjugate following enzymatic cleavage of the linker molecule, which

is present only at the tumor site. Mylotarg is a FDA-approved example of antibody conjugated drug that has been used for leukemia treatment (259).

Modified (plasma) proteins. Small proteins can encapsulate and deliver therapeutics based on their size and solubility properties. Different targeting moieties such as sugars and other ligands can be coupled to these proteins for a more specific delivery. However, this process needs complicated pre-modifications of proteins. Liver cells have been successfully targeted with heavily modified albumin proteins (260).

Soluble synthetic polymers. Advancements in polymeric chemistry have enabled scientists to design novel synthetic polymers for drug delivery purposes. Innovative chemical approaches are used for tailoring conjugates and encapsulating drugs and agents. N(-2-hydroxypropyl) methacrylamide (HMPA) polymers have been extensively studied for anti-cancer therapy as they provide a solution for selective and targeted chemotherapy (261).

Microspheres and nanoparticles. Nanoparticles range from 0.2 to 0.5μm and microspheres range from 30 to 200μm. Desired drugs and therapeutics can be either attached to the surface or encapsulated inside the carrier's core based on their physiochemical characteristics. The site of encapsulation can significantly affect the pharmacokinetics of the drug release. After accumulation at the targeted site, these particles quickly become internalized through phagocytosis by the targeted cells. Some examples of these newly developed microspheres include micelles, carbon nanoparticles and silica nanoparticles. Due to their chemical and mechanical stability, silica nanoparticles are perfect candidates for drug delivery purposes. Surface modification methods are used to

accurately tune surface zeta potential values (262). The negative charge on the surface of silica particles prevents quick clearance from the circulation (263).

Lipoproteins Lipid particles are natural lipid bilayers that can be used for targeted delivery purposes. Low density lipoproteins (LDL) and high density lipoproteins (HDL) can be modified to integrate lipophilic drugs. Other glycolipids can be fused with the lipoproteins' backbone, as a targeting moiety. LDL and HDL have been used extensively for delivery of the drugs to the liver (264).

Quantum dots are semiconductor nanoparticles that range between 10-500nm in size. The size of quantum dots can be accurately tuned. Also, surface markers can be attached to the surface to achieve better targeting properties. Quantum dots have been extensively used as imaging moieties (265).

Liposomes are self-assembled, spherical bilipid particles. Size-wise, liposome constructs can range from 20nm to several micrometers depending on the application. Amphiphilic lipids are the backbone of any liposomal construct. The most significant characteristic of amphiphiles is their self-assembly properties which are due to their special preference to hydrophobic and hydrophilic solvents (266).

Usually amphiphiles have a polar hydrophilic head and a non-polar hydrophobic tail. Amphiphiles in an aqueous medium form aggregates to reduce the hydrophobic hydrophilic interactions. This phenomenon is called self-assembly, and it reduces the total energy of the system and increases the total entropy. Following self-assembly, amphiphilic lipids form bilayers. Usually lipid bilayers consist of two hydrocarbon tails attached to a hydrophilic head group, which can be positively, negatively or neutrally charged (267-

269). Phospholipids are the most common form of lipid bilayers which are found in most cell membranes. Phospholipids have two acyl tails attached to a head by a glycerol backbone. Below is a schematic of a phospholipid, R1 and R2 represent saturated and unsaturated acyl tails and R3 is the hydrophobic head. If the concentration of phospholipids exceeds critical values, they form lamellar constructs. It is worth mentioning that this

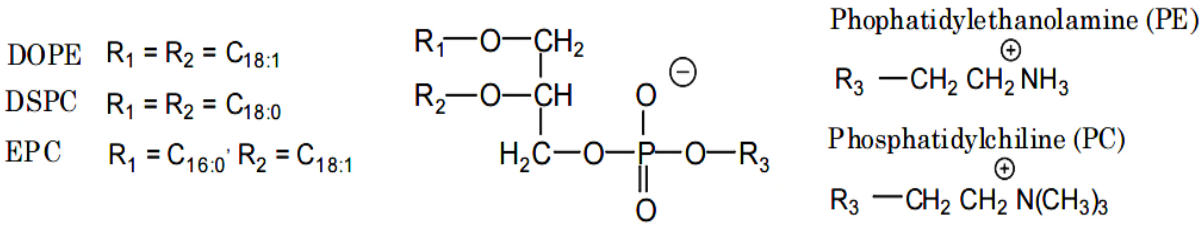

Schematic 3-2. Structure of DOPE DSPC EPC and a phospholipid (2)

lamellar phase can change with the temperature. For example, at low temperatures a phospholipid may obtain a solid conformation with high packing of hydrocarbon tails. The same phospholipid construct at higher temperatures or addition of an unsaturated acyl tail may obtain a more liquid crystalline status (glass transition temperature) (270). At this point the tails are highly disordered and have higher motility. This phenomenon is especially important as phospholipid-based nanocarriers can be resized at this high temperature to yield a size homogenous preparation.

3.1.1 Liposome Formation:

Liposome formation can be described as a competition between two forces. One is the curvature energy, and the other is the edge energy of the lamellar layer. A lamellar fragment, when in an aqueous solution, has high surface tension at the rim of the layer. Curvature reduces this energy, and finally the lowest energy is achieved at a spherical form

(271, 272). On the other hand, this process increases the curvature energy, which reaches its peak in the spherical form. This excess free energy is independent of the liposome radius. Therefore, for a liposome preparation, bigger liposomes are energetically favored.

General method of liposome preparation: All methods developed to prepare liposomes involve four basic stages: First, lipids are dried from their solvent medium. Second, the lipids are dispersed in the media. Resulting liposome are purified, and finally products are analyzed to confirm the construct integrity and homogeneity. Amongst various techniques, thin-film hydration method is the most versatile and commonly used approach. In this method, lipids at desired concentrations are dissolved and mixed in excess amount of organic solvent to guarantee a homogenous mixture. Chloroform or chloroform/methanol mixture is the most commonly used solvent. Typically, lipids are mixed at 10-20mM concentration. Although it is possible to make higher concentrations, other steps may limit the highest workable concentration. After all lipids are completely solved, the solvent is removed either by passing nitrogen gas or by freeze-drying or a mixture of these two methods. This step yields a thin lipid film. It is important to mention that the residual solvent can significantly reduce the quality of the liposome preparation. The lipid film is then hydrated by the addition of an aqueous solution, producing multi-lamellar vehicles at different sizes. To achieve a size-homogenous preparation, liposomes at their glass transition temperature are passed through filters with desired sizes. Using light scattering methods, the size is confirmed for next steps.

3.1.2 PEGylation

Any liposome preparation should be stable. The stability of liposomes is highly dependent on the liposome-liposome interactions and the balance between attractive and repulsive forces. If repulsive forces overcome the attractive forces, the formation stays stable. It has been shown that a polymeric coating significantly increases liposome stability. Polymers are either grafted or adsorbed to liposome surfaces (273, 274). In the grafting method, polyethylene glycol (PEG) lipids are typically used. The hydrophilic chain of PEG lipids covers the surface of the liposomes. These chains are a source of repulsive forces when two liposomes are near each other. As two liposome get closer these polymer chains are compressed, which results in an unfavorable increase in the entropy of the system (275).

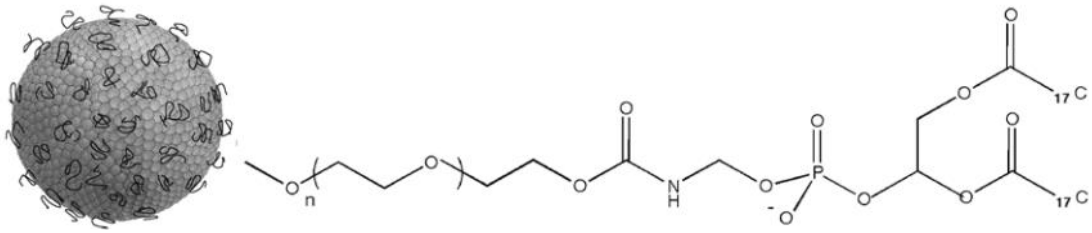

Schematic 3-3. Structure of a PEGylated liposome (2)

The process of coating liposome with PEG lipids is called PEGylation. PEGylation not only increases the colloidal stability in a solution, but also promotes the biological stability, which is crucial to achieve longer circulation times (276).

When in circulation, lipoproteins and opsonins interact with liposomes. Lipoprotein interactions include lipid exchange, which ultimately leads to liposomes destruction (277). Opsonisation is a process in which macromolecules like immunoglobulins are marked and later cleared as part of the body's defense mechanism. After being marked, targeted

molecules are engulfed by special macrophages from reticuloendothelial system. Thus, most of the typical liposomes are cleared from the circulation within a few minutes (278). PEGylated liposomes can prevent the marking process as the PEG lipid long chains work as a barrier against surface interaction with marker molecules. This modification can change the circulation time from minutes to days (276, 278). A long circulating formation is crucial for effective and organ-specific delivery of desired drugs and agents.

3.1.3 Drug Encapsulation

Drug molecules can interact with liposomes in several different ways depending on the drug's solubility and polarity. Water soluble drugs are easily encapsulated in the core compartment whilst water insoluble drugs can be encapsulated in the hydrophobic membrane. Encapsulation process can be either either passive or by active (remote loading). In the passive method, hydrophilic drugs are entrapped automatically upon hydration into the hydrophilic core of the liposomes. The encapsulating efficiency of this method is low due to the small volumetric ratio of liposome core to surrounding medium (279). Therefore, improved approaches such as remote loading have been developed to increase the entrapment efficiency (280). In these methods, neutral drugs can move from outside to the inside of the liposomes because of PH difference, and become charged once they are inside (281). Therefore, they are not able to pass back outside of the liposomes. The outside-inside concentration difference stays high and derives the outside drug to pass through the membrane and deposit in the aqueous core of the liposomes.

Hydrophobic drug encapsulation however, should be approached by different methods. One of the simplest methods that have been exploited for encapsulation of the hydrophobic

drugs is to incorporate them with the lipids in the organic solvent before rehydration (282). When encapsulated, they stay in the liposomal membrane as they have very low potency to move to aqueous surrounding. There are limitation facing this approach for example encapsulated molecules can undergo physiochemical changes, reducing their effectiveness and activity during the process of liposome formation and extrusion (283).

3.1.4 Antibody Attachment

Over the past few years, different approaches have been developed to attach antibodies to liposomal constructs (284, 285). This is achieved either by direct attachment of antibodies to the lipid head group of non-PEGylated liposomes or by direct conjugation to PEGylated liposomes (286). Although first method results in liposomes with effective targeting ability, the constructed immunoliposomes are quickly cleared following administration to the bloodstream. The second method however, yields longer lasting liposomes, but with much lower targeting ability (287). Recently it is suggested to attach the targeting moieties to the free terminus of PEG chains. Immunoliposomes constructed using this method were effective in targeting desired cells. However, circulation time was inversely proportional to antibody density (287). Anti-HER2 coated immunoliposomes, had better site-specific delivery when the antibody was attached to the PEG chain compared to those in which the antibody was attached to membrane surface (288, 289). Nowadays, targeting moieties are usually attached to liposomes thorough PEG chains.

In order to attach a targeting moiety, PEG chains should be activated and functionalized. Various forms of PEG-X are now commercially available in which X is a reactive functionalized group to facilitate binding process. Most of these functionalized PEGs, use

hetero bifunctional PEG derivatives, which contain hydroxyl and carboxyl or even amine groups. Typically, the hydroxyl end-group of PEG lipids are modified to procedure a urethane attachment to the hydrophobic lipid chain of the phospholipids. In another method, which has been used in this project, PEG lipids are activated with maleimide groups. Maleimide then attaches to thiol group which is functionalized on the desired antibody. This method yields strong antibody-liposome binding, which facilitates the targeting process.

3.2 Targeted Drug Delivery to the Injured Heart

The demand to deliver growth factors needed to revascularize injured myocardium and the potential side effects of using systemic delivery methods have initiated the interest to develop heart specific delivery approaches (290). Various methods and techniques have been developed for this purpose. Here we briefly review these approaches and their advantages and disadvantages.

Direct injection of drugs and agents to the myocardium has been suggested to deliver drugs with low half-lives as quickly as possible to the infarcted region (291-294). This approach has been used to deliver VEGF, which had significant improvements in cardiac remodeling (295). Intra-cardiac injection of adeno-cyclin has shown to have beneficial effects and improve cardiac function (296). Koch et al. showed that direct injection of adenovirus containing calcium S100A1 gene into the infarcted myocardium promoted the expression of S100A1, resulting in better handling of calcium in sarcoplasmic reticulum and ultimately improved contractile function and left ventricular remodeling (297). In another study, direct intra-myocardial injection of VEGF encoding plasmids to the

infarcted myocardium of pigs, showed to promote cardiomyocyte mitosis (298). Despite these promising results, direct delivery of agents has difficulties due to nonstop pumping and vigorous shear forces in the heart which in turn quickly clear and reduce the bioavailability of the drug at the site of injury.

High frequency heart focused ultrasound beams can be used to achieve heart specific delivery. Ultrasound energy can be used to disturb the vehicle integrity and unload encapsulated drugs only at the site of the injury (299). The disruption of the vehicles can at the same time induce disruption in endothelium which helps with the uptake of the released drug. High frequency ultrasound delivery has been used to deliver VEGF encoding gene to the infarcted myocardium in a rat MI model and showed that the expression of VEGF in the ischemic myocardium was higher in ultrasound treated animals compared to control (300). Although effective, this approach faces complexities as it is difficult to focus the energy beam directly to desired site. Focusing the ultrasound beam, directly to the infarcted region is very complicated. Also, during its passing through the chest cavity the energy beam can lose its energy and effectives.

Nanocarriers can accumulate in the infarcted myocardium due to high permeability of the endothelium post-IR (301). For example, polymeric micelles passively accumulate the infarcted tissue based on their small size (7-20 nm in diameter) (302). Although effective, a more efficient delivery can be achieved by actively targeting vehicles to specific upregulated ligands in the injured site. Following IR, cardiac cells which are going through apoptosis and necrosis lose their membrane integrity. Cytoskeletal proteins are therefore revealed which can in turn be targeted for site specific delivery purposes (303). Torchilin et al. have developed liposomes tagged with anti-myosin antibodies and showed that not

only these liposomes accumulate in the infarcted myocardium but also, they can save cardiomyocyte from death by fusing and sealing the membrane. Following this treatment, the infarct size was significantly reduced compared to non-treated animals (303).

Another sets of molecules which have recently been exploited as targeting ligands are the adhesion molecules (304). Following IR, there is a significant increase of adhesion molecules such as P-selectin and ICAM-1 on the surface of endothelium in the infarct and border zone. A process that is necessary for infiltration of inflammatory cells (305). Upregulation of P-selectin has been detected 4 h after infarction which is remained elevated than normal up to 48 hours after the acute phase of infarction. Immunoliposomes labeled with anti-P-selectin have been used to target VEGF following myocardial infarction (290). This treatment increased cardiac function, detected 4 weeks post treatment (306).

In our study we have adopted the P-selectin coated liposomal based targeted delivery method, and developed a DCCI encapsulating myocardium specific delivery construct. We then investigated whether targeted administration of DCCI is effective in reducing excessive ISP activity following IR and compared its efficacy to the same and higher doses of systemic DCCI administration. Further we evaluated the effects of targeted DCCI administration on infiltration of inflammatory cells. Also, we investigated the effects of targeted DCCI administration on cardiac function, and compared it to systemic delivery to evaluate whether targeted delivery method enhances cardio protective effects of DCCI. The ability to save in-danger cardiomyocyte is the pillar of our therapeutic approach. Therefore, we evaluated the effects of targeted delivery of DCCI on cardiomyocyte death and subsequent infarct size following IR. Finally, we evaluated the effects of targeted

delivery of DCCI on fibrosis and remodeling in animals treated with DCCI encapsulated immunoliposomes and compared it to systemic delivery method.

These results can be found in the next chapter in the form of a paper, which is being prepared for submission to Circulation Journal.

CHAPTER 4

IMMUNOLIPOSOMAL TARGETING OF DUAL CATHEPSIN G AND CHYMASE INHIBITOR IMPROVES CARDIOPROTECTION AFTER MYOCARDIAL ISCHEMIA REPERFUSION INJURY

BAHMAN HOOSHDARAN, MS[1], MIKHAIL A KOLPAKOV, MD, PHD[1], XINJI GUO, PHD[1], SONNI A MILLER, PHD[1], TAO WANG, MD, PHD,[1] DOUGLAS G TILLEY, PHD[2], KHADIJA RAFIQ, PHD[3], YUAN TANG, PHD[5] , MOHAMMD F.KIANI, PHD[5] ,ABDELKARIM SABRI, PHD[1,4]

[1]Cardiovascular Research Center and [2] Center of Translational Medicine, Lewis Katz School of Medicine, Temple University, Philadelphia, PA. [3]Center of Translational Medicine, Thomas Jefferson University, Philadelphia, PA. [5]Department of Engineering, Temple University, Philadelphia, PA

[4]**Address correspondence to**: Abdelkarim Sabri, Ph.D.

Cardiovascular Research Center, Temple University

MERB 1045, 3500 N. Broad Street, Philadelphia, PA 19140, USA

Tel. 215-707-4915; Fax. 215-707-5737 E-mail. sabri@temple.edu

Subject Codes: Targeted Drug Delivery, Immunoliposomes, Ischemia Reperfusion, Inflammation, Basic Science Research.

4.1 Abstract

Introduction: Neutrophil- and mast-cell-mediated inflammation accounts for substantial fraction of the myocardial injury occurring after ischemia reperfusion (IR). However, no standard anti-inflammatory therapy has been developed for clinical myocardial IR injury. Here, we designed and tested a novel immunoliposomal drug delivery vehicle targeting neutrophil- and mast cell-derived serine proteases, cathepsin G and chymase, to enhance specific delivery of drug carriers to the infarct region.

Methods and Results: C57BL/6 mice were subjected to myocardial ischemia for 30 minutes followed by reperfusion for 1 and 7 days and the effect of a potent non-peptide dual inhibitor of cathepsin G and chymase (DCCI) on inflammation and cardioprotection were characterized. DCCI was delivered just after reperfusion either systemically (2 or 10 mg/kg, i.v.) or encapsulated in anti-P-selectin conjugated immunoliposomes (ILPs) (2 mg/kg, i.v.). Targeted delivery of DCCI-loaded ILPs reduced cardiac levels of cathepsin G and chymase activity induced at day 1 and 7 post-IR and attenuated neutrophil infiltration in the infarct region compared to mice treated with empty ILPs. ILP targeted delivery of DCCI also reduced myocyte apoptosis (-35% in TUNEL+ myocytes, $p<0.05$), limited infarct size (-45%, $p<0.05$) and improved cardiac function (+10% in ejection fraction, $P<0.05$) post-IR compared to empty ILP-treated mice. Interestingly, DCCI-loaded ILPs significantly reduced fibroblast proliferation and differentiation to myofibroblasts, which resulted in less collagen accumulation. Equivalent doses of DCCI (2 mg/kg/d) administered systemically were not efficacious. However, structural and functional improvements similar to those obtained with targeted delivery of DCCI were obtained with systemic delivery of higher dose of DCCI (10 mg/kg/d).

Conclusions: These findings reveal the role of neutrophil- and mast-cell-derived proteases as key mediators of myocyte apoptosis and cardiac dysfunction post-IR and show that immunoliposomal targeted inhibition of inflammatory proteases could be used as future therapy to enhance cardiac remodeling and function post-IR.

4.2 Introduction

Restoration of blood flow after acute myocardial infarction limits infarct size and reduces mortality. However, reestablishing blood flow is often followed by a second set of stresses, a phenomenon referred to as ischemia-reperfusion (IR) injury, which can result in additional myocardial damage and may account for up to half of total infarct size (223, 224).

A large amount of the early cardiac tissue damage that occurs during inflammation post-IR is mediated through early activation of neutrophils and mast cells, which produce reactive oxygen radicals and release granules containing proteolytic enzymes (307). Inflammatory serine proteases (ISPs) are enzymes derived from neutrophils, such as cathepsin G (Cat.G), elastase, and proteinase 3, and from mast cells, such as chymase and tryptase (158). ISPs are known mainly for their function in the intracellular killing of pathogens (228, 229). Their extracellular release upon leukocyte activation is traditionally regarded as the primary reason for tissue damage at the sites of inflammation (308).

We have previously shown that excessive activity of cathepsin G and chymase following IR stimulates cardiomyocyte apoptosis and induces cardiac injury and dysfunction. At the same time, ISPs induce fibroblast proliferation, migration and subsequent fibrosis of myocardium (309). Administration of a potent dual inhibitor of cathepsin G and chymase

following IR can attenuate these adverse outcomes. Despite the cardioprotective effects observed by administration of DCCI, systemic delivery of effective doses of DCCI may be associated with complexities due to non-specific inhibition of ISPs enzymatic function in other organs and cells.

Targeted delivery approaches may enable us to dodge these adverse side effects by increasing organ specificity of administrated DCCI. Various approaches have been developed over the past few years for a heart specific delivery of agents and therapeutics (310). One of the most frequently used delivery systems are the nano-particulate drug carriers that often passively accumulate in regions of high vascular permeability such as those present in the infarct tissue at a rate several times higher than that observed in the adjacent normal myocardium (14). The upregulation of a number of endothelial cell adhesion molecules, including intercellular adhesion molecule-1 (ICAM-1) and platelet selectin (P-selectin) within the injured tissue was used recently as targets for treatment or selective delivery of therapeutic agents to the infarct region (304, 306).

In the present study, we describe how immunoliposome (ILP) encapsulated DCCI is effective in targeting injured myocardium of mice subjected to IR and that targeted DCCI administration is efficient in reducing cathepsin G and chymase activity and pathological remodeling associated after IR. We Also show that it reduces collagen deposition within the myocardium and prevents left ventricular dysfunction. Our findings provide evidence that dual targeted inhibition of cathepsin G and chymase may be of therapeutic benefit in protecting the heart from IR injury.

4.3 Methods

Experimental protocol: All animals were kept in accordance with protocols approved by the Animal Care and Use Committee of Temple University. Ten weeks-old C57BL6 male mice were anesthetized with a mixture of ketamine (100 mg/kg) and xylazine (10 mg/kg) and left thoracotomy was performed under mechanical ventilation. Body temperature was maintained by a heated surgical platform and was monitored throughout surgery using a rectal sensor. A 6-0 suture with a slipknot was tied around the left anterior descending (LAD) coronary artery to produce ischemia. Consistent elevation of the ST segment was observed in lead II tracings following occlusion of the LAD coronary vessel. Regional ischemia was confirmed by visual inspection under a dissecting microscope (Nikon) by discoloration of the occluded distal myocardium. The ligation was released after 30 minutes of ischemia and the tissue was allowed to reperfuse as confirmed by visual inspection. The chest wall was closed with 8-0 silk and then the animal was removed from the ventilator and kept warm in the cage maintained at 37°C overnight. A sham procedure constituted the surgical incision without LAD ligation. Hearts were harvested after 1 or 7 days of reperfusion.

To investigate the role of Cat.G and chymase inhibition, mice were randomly divided into 8 major groups, consisting of: (1) sham mice receiving systemic or ILP encapsulated DCCI (EMD Millipore, 219372) (10 or 2 mg/kg and 2mg/kg of body weight respectively; n=8); (2) sham mice receiving either vehicle (0.1% DMSO in NaCl 0.9%; n=8) or empty ILPs (n=8); (3) IR mice receiving 10 mg/kg DCCI (n=8); and (4) IR mice receiving vehicle (0.1% DMSO in NaCl 0.9%, n=8). DCCI or its vehicle were administered by means of single intravenous bolus injection immediately after reperfusion of the ischemic myocardium (for mice subjected to IR for 24 h and 7 days targeted delivery) and treated

daily via intraperitoneal injection (for mice subjected to IR injury and systemic 7 days treatment).

Preparation of DCCI Immunoliposomes Conjugated to Anti-P-Selectin:

Liposomes are composed of 44% molar ratio of hydrogenated soy L-α-phosphatidylcholine (HSPC), 44% molar ratio of cholesterol, 2% molar ratio of 1,2-distearoyl-sn-glycero-3-phosphoethanolamine-N-[(polyethylene glycol)2000] (DSPE-PEG2000), 2% molar ratio of DSPE-PEG-maleimide (Avanti,Alabaster, AL), 1% molar ratio of fluorescence lipid 1,2-dioleoyl-sn-glycero-3-phosphoethanolamine-N-(Cyanine 5) (Avanti), and 8% molar ratio of DCCI. After mixing in excess amount of chloroform. Solvent was removed under vacuum overnight and then lipid film was rehydrated with PH 7.4 phosphate buffered saline. The lipids were then extruded at 60°C (Lipex, Canada) 10 times with a 0.2-μm filter and then 10 times with 0.1-μm filter (Nucleopore; General Electric Co., Pleasanton, CA, USA), yielding liposomes with 100nm±10 nm diameter, as was measured by optical scattering using a particle sizer (Zetasizer 1000 HAS; Malvern Instruments, Malvern, UK). Non-capsulated DCCI was then removed by a hand filtering system (X1-500S-100-20N, Spectrum Labs, CA, USA).

Stealth liposomes were conjugated to either IgG anti-mouse or IgG_{2a} mAb RMP-1 to mouse P-selectin. The anti-P-selectin storage buffer was separated using a centrifuge filter system (Microcon YM-30, Millipore, MA, USA). The immunoliposomes were resuspended in a 60-μM triethanolamine (TEA), 100 mM NaCl, and 1 mM EDTA buffer (pH 8.0). Anti P-selectin antibody was thiolated using iminothiolane and then resuspended in Tris-saline buffer (PH 6.0) using the Microcon centrifuge filter system. To attach the

antibody, liposomes were incubated with thiolated anti P-selectin for 24 hours at 4°C. Free antibodies were then separated using the Spectrum hand filtration system. A similar process with the exception of DCCI addition was used to prepare empty anti-P-selectin conjugated immunoliposomes.

Data Analysis*:* Summary data are presented as mean ± SEM. For comparisons of >2 groups, two way ANOVA was employed followed by Tukey's post hoc test. Two group comparisons were analyzed by the two-sample *t* test,. A value of $p<0.05$ was considered statistically significant.

4.4 Results

DCCI can be encapsulated passively by self-assembled anti-P-Selectin coated immunoliposomes.

We have used self-assembly method to encapsulate DCCI in 100 nm diameter anti-P-Selectin tagged immunoliposomes (ILPs). Encapsulation of DCCI did not significantly change size and zeta potential distribution of ILPs (Figures 1A and 1B). To confirm the attachment of antibody to DCCI encapsulating ILPs, we performed binding assay test. We observed that ILPs coated with anti-P-Selectin had significantly higher binding to P-selectin coated surface, compared to those coated with IgG (Figure 1C). The encapsulated efficiency of DCCI was measured using enzymatic activity assay. Using DCCI as standard, encapsulated DCCI is measured at 0.2 mg/ml of ILPs preparation (Figure 1D). To verify that the measured DCCI activity is from encapsulated and not free DCCI, we measured the ability of inhibiting Cath.G activity with or without the presence of Igpal, an organic solvent able to break ILPs and free the encapsulated DCCI. We observed that ILPs not

incubated with Igpal had insignificant Cath.G inhibition compared to those incubated with Igpal (Figure 1E).

Targeted DCCI treatment attenuates the severity of the acute inflammatory response after IR

To evaluate the efficacy of targeted inhibition of Cat.G and chymase in attenuating IR mediated inflammation, we treated mice with DCCI, either systemically or targeted via ILP encapsulation. For targeted delivery of DCCI, 2mg/kg of ILP encapsulated DCCI was administrated intravenously at the reperfusion time at of mice body weight. For systemic delivery, DCCI was administrated at the time of reperfusion at either 2mg/kg/d or 10mg/kg/d intravenously for the first day and after that repetitive intraperitoneal injection till 7 days post reperfusion. Mice were sacrificed either at 1day (a time point coinciding with peak inflammatory cell infiltration and myocyte loss) and at 7 days post-IR, coinciding with peak scar formation and repair.

First, we investigated whether DCCI is effectively delivered to the injured myocardium. We integrated fluorogenic lipids into the DCCI encapsulated ILPs noticed high amount of ILP accumulation in the infarcted myocardium 1 day post IR (Figure 2A).

Consistent with this result, we observed that at 1 and 7 days post-IR Cat.G and chymase enzymatic activities were attenuated in both 10 mg/kg/d systemic and 2 mg/kg targeted DCCI delivery compared to either vehicle or empty ILP treated mice. No significant reduction in these proteases was observed with systemic delivery of 2 mg/kg/d of DCCI (Figure 2D, 2E). Also, we measured the off-target effects of administration of effective doses of systemic and targeted DCCI administration and observed that those animals

treated with 10 mg/kg/d of systemic DCCI had significantly lower ISP activity in the spleen whilst no reduction of activity was observed in animals treated DCCI encapsulated ILPs.

Myocardial myeloperoxidase (MPO) activity was measured to determine the impact of DCCI on the infiltration of inflammatory cells after IR. In both systemic 10 mg/kg/d and targeted 2 mg/kg DCCI-treated mice, MPO activity was markedly reduced compared to those treated either with vehicle or empty ILPs treated mice (Fig. 3C). Post-IR immunohistological examination of hearts confirmed these data (Fig. 3A and 3B), as the number of MPO-positive neutrophils were markedly reduced in the infarcted regions of administration effective method of DCCI groups compared to either vehicle or empty ILP-treated animals.

Targeted inhibition of Cat.G and chymase improves cardiac function.

We next explored and compared the effect of Cat.G and chymase inhibition on cardiac function at 1 and 7 days post-IR and compared it to systemic inhibition. Neither targeted nor systemic delivery of DCCI did alter baseline heart weight-to-body weight ratio, heart rate, or LV dilatation in sham-operated animals (tables 1-4). However, systemic delivery of 10 mg/kg/d and targeted delivery of 2 mg/kg of DCCI displayed a significant preservation in post-IR cardiac function versus either vehicle or empty ILPs treated mice, including LV ejection fraction and fractional shortening (Figures 4A and 4B). LV end-systolic and diastolic dimensions (Figures 4C and 4D) were also shown to undergo better preservation post-IR in this two DCCI-treated groups- versus either vehicle or empty ILPs-treated mice. No improvement was observed in animals treated with systemic administration of 2 mg/kg/d compared to vehicle treated mice (Supplemental Figure S1).

Morphometric analysis indicates the presence of cardiac hypertrophy and concomitant signs of cardiac failure, such as an increase in lung weight, in vehicle-treated mice and mice treated with empty ILPs, whereas only the latter pathological response was reduced in the DCCI-treated mice at 7 days post-IR (Supplemental Figure S2).

Infarct size measurements as percentage of area at risk or LV circumference indicated 27 ±2% and 35 ±4% of the LV to be affected by the infarct at 1day for empty ILP and vehicle treated mice, and 37±6% and 36±5% 7 after IR in ILP and vehicle treated mice respectively, whereas the infarct accounted for 17 ±3% and 26 ±2% of the LV in 10 mg/kg systemic and 2 mg/kg targeted DCCI administrated mice at 1 day and 20 ±3% and 23 ±5% for 10 mg/kg systemic and 2 mg/kg targeted DCCI administrated mice at 7 days post-IR. (Figures 4E and 4F). Thus, the integrity of the infarcted area was maintained after IR in targeted DCCI-treated mice with reduced LV dilatation compared to either vehicle or empty ILP treated mice, which results in a better cardiac function post-IR.

Targeted dual inhibition of Cat.G and chymase is cardioprotective.

The main factor contributing to infarct size and cardiac dysfunction developed after IR is the level of cardiomyocyte loss. We measured cardiomyocyte apoptosis in vehicle, empty ILP, systemic DCCI and targeted DCCI via terminal deoxynucleotidyl transferase dUTP nick end labeling (TUNEL). As expected from the effect of ISP inhibition, mice which were treated with either 10 mg/kg of systemic DCCI or 2 mg/kg of targeted DCCI had a reduced number of TUNEL-positive myocytes 1 day following reperfusion compared to those treated with either vehicle- or empty ILPs. (Figures 5A, 5B). Cardiac caspase-3 activity (Figure 5C) was also reduced in these two DCCI-treated groups versus vehicle or empty ILP treated mice 1 day post-IR. These data collectively show cardioprotective effects of targeted administration of DCCI following IR.

Targeted delivery of DCCI attenuates profibrotic remodeling induced after IR injury.

We have previously shown that Cat.G and chymase have distinct effects on cardiomyocytes and fibroblasts. Although lethal when treated on cardiomyocytes, we have previously shown that ISPs induce migration and differentiation of fibroblasts. Here we explored the potential effect of targeted delivery of DCCI on cardiac fibrosis and remodeling responses post-IR and compared it to systemic delivery of higher doses of systemic delivery of DCCI. Collagen fractional area in the non-infarcted region of the heart was not different between DCCI- and vehicle-treated groups (Figs. 6A and 6B). However, both systemic delivery of 10mg/kg/d and targeted delivery of 2 mg/kg DCCI-treated mice had significantly less collagen accumulation in the infarcted region compared with vehicle-treated mice at day 7 post-IR. To determine the mechanisms of decreased collagen accumulation after DCCI treatment, we evaluated accumulation of myofibroblasts, which are a primary source of extracellular matrix (ECM) protein synthesis in the infarcted myocardium (239). Analysis of smooth muscle α-actin (SMA) staining showed minimal accumulation of myofibroblasts in sham-operated hearts (not shown) which progressively increased in vehicle-treated mice and mice treated with empty ILPs infarcts (Figs. 6A and 6C). DCCI-treated mice showed reduced myofibroblasts density a decreased accumulation of profibrotic CTGF and TGF-β protein expression in the infarcted heart (Figs. 6D). We also investigated whether DCCI treatment affects ECM degradation after IR as gelatinase activity, was significantly reduced in the infarcts of DCCI- versus vehicle-treated mice 7 days post-IR (Fig. 6E). Thus, inhibition of Cat.G and chymase activity results in fibroblast differentiation and activity following IR that is associated with diminished ECM accumulation and preserved cardiac contractile dysfunction.

4.5 Discussion

Excessive enzymatic activity of ISPs is a major source of myocyte death and cardiac dysfunction as well as excessive fibrosis and adverse remodeling following onset of IR (311). In our previous study, we have shown that prolonged inhibition of cathepsin G and chymase, two major ISPs known to be potent in affecting cellular function, can minimize these effects. However, this approach may face difficulties due to non-specific attenuation of ISPs activity in remote organs or potential side effects such as impaired mobilization of leukocytes, which are beneficial in cardiac healing and repair. Therefore, in this study, we evaluated the potentials of targeted delivery of DCCI using an anti-P-selectin tagged immunoliposomal delivery system which has previously shown to effectively target the injured myocardium.

We were able to encapsulate DCCI with minimum disturbance to the ILPs structure and functionality. Using this targeted platform, low administrated doses were effective to inhibit excessive ISP activities following IR, when the systemic administration of the same doses of DCCI was inefficient to do so. This may be point at high myocardium specific biodistribution of DCCI encapsulated ILPs. The decrease in cathepsin G and chymase activity in animals treated with DCCI encapsulating ILPs, attenuated pathological severity of the cardiac inflammatory response such as myocardium exposure to the infiltration of neutrophils and correlated MPO activity, which is known as a contributor to myocardial tissue injury.

Although the elevated activities of most ISPs such as neutrophil released cathepsin G and elastase are transient and attenuate after the first 24 hours post IR, other types of ISPs such as mast cell released chymase have shown persistent elevated activities even at 7 days post

IR. Therefore, to keep the DCCI therapeutic index above effective values, repetitive administration of high doses is required, which can significantly increase the risk of toxicity and side effects. Also, systemic inhibition of ISPs in late stages post IR can affect infiltration of beneficial leukocytes such as macrophages which are responsible to initiate healing process.

This may affect ISPs functions in remote organs as well as other inflammatory cells that are important in the healing process, such as macrophages. The myocyte loss following IR is the primary source of cardiac dysfunction and following pathological deterioration of myocardium integrity. We observed a substantial decrease in cardiomyocyte apoptosis in the ischemic hearts of mice treated with DCCI encapsulated ILPs, which was comparable to cardioprotective effects observed in mice treated with significantly higher doses of systemic DCCI. This reduction in number of apoptotic cells, observed in mice treated with targeted DCCI, correlated with the significant reduction of the infarct size both 1 and 7 days post IR in these mice. These results may be due to the absence of Cat.G/chymase or the resultant limited exposure to myeloperoxidase or other inflammatory cell-derived cytokines/chemokines underlie this decrease in apoptosis.

Several studies have demonstrated cardiomyocyte apoptosis after reperfusion of ischemic hearts and the correlation between the number of apoptotic cells and the severity of cardiac dysfunction (243). Expectedly, cardiac function was significantly improved in targeted DCCI-treated mice which was comparable to the improvement observed in mice treated with high doses of systemic DCCI.

Tissue fibrosis that develops after IR is contributed to apoptosis of myocytes, and at the same time myofibroblasts accumulation. Here we observed that consistent with reduced apoptosis and tissue infarct, mice treated with either low doses of targeted DCCI or high doses of systemic DCCI had attenuated ECM deposition compared to those treated with either vehicle or empty ILPs. Furthermore, these treatments reduced accumulation of myofibroblasts and expression of both TGF-β and CTGF accumulation in the infarcted heart at day 7 post IR.

The current study provides evidence that targeting neutrophil- and mast cell-derived proteases was efficient in protecting the heart from the early myocyte death, excessive fibroblast migration and ECM accumulation that contribute to adverse cardiac remodeling and contractile dysfunction. We previously have shown that systemic inhibition of Cath.G and chymase is beneficial as they share same active sites and targets. Although to inhibit the prolonged activity of chymase after onset of IR, everyday injection of DCCI is required which may intensify the adverse effects of ISP inhibition in remote organs. However, taking advantage of slow and tissue specific delivery of ILPs, can address this issue. In conclusion, a myocardium specific dual inhibition of Cat.G and chymase is effective in reducing the pathologic severity related to IR injury in association with its ability to limit myocardial proteolytic activity and at the same time preventing non-specific ISP inhibition in other organs. Thus, this platform can potentially be considered as a future therapeutic intervention for IR injury.

Promising results from our study suggest the potential of using this immunoliposomal delivery platform for delivering anti-inflammatory agents. Slow and myocardium specific delivery characteristics of the ILP based delivery method can address the issues facing

traditional anti-inflammatory approaches and therefore, may open a new avenue to revisit those failed clinical trials aiming at inhibiting inflammatory response.

4.6 Figures and Legends

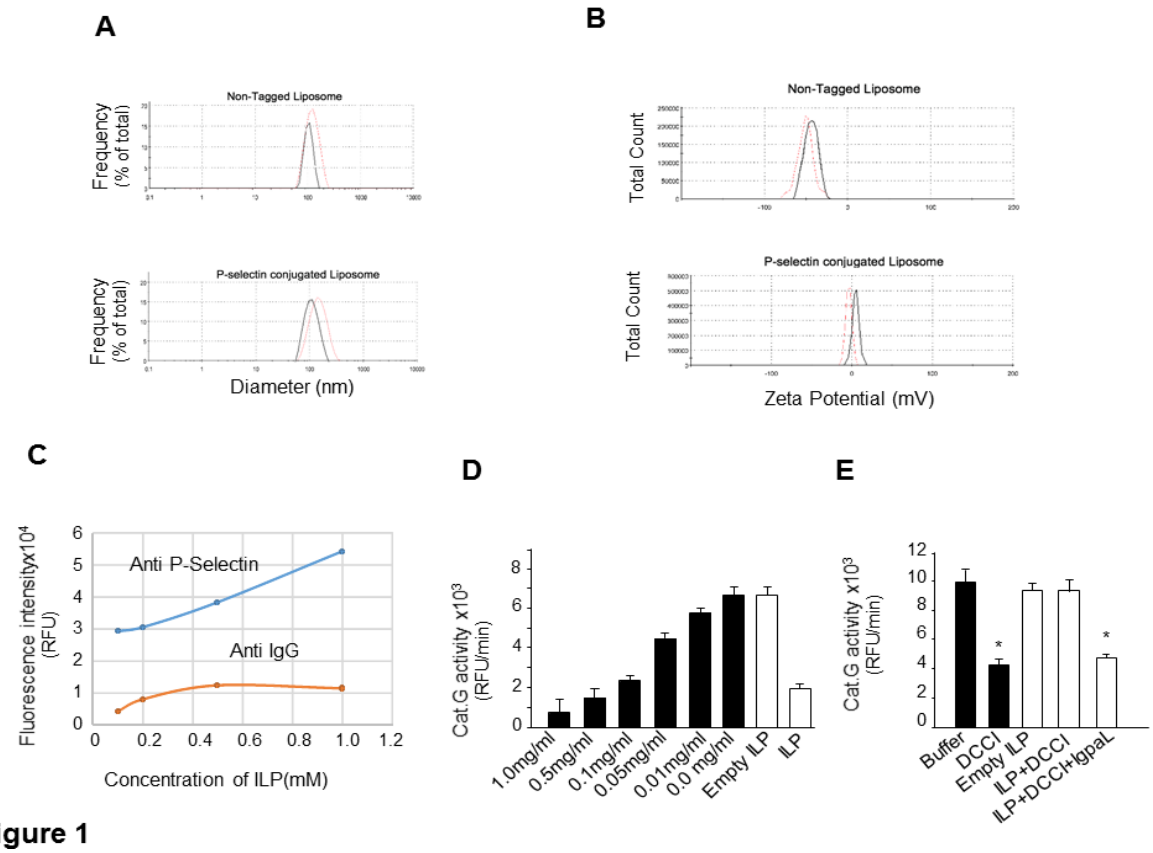

Figure 1

Figure 4-1: DCCI can be encapsulated in long lasting immunoliposomes. (A) ILPs size distribution measured using zeta particle sizer. (B) ILPs zeta potential distribution measured using zeta potential sizer. (C) Fluorogenic intensity of liposomes coated with either anti P-Selectin or IgG antibody and incubated with P-selectin coated 96 well plate and vigorous washing. (D) The inhibitory effect of DCCI encapsulating ILPs was compared by free DCCI to determine the amount of DCCI encapsulated. Results are expressed as relative fluorescence units (RFU)/min (n=3 from 3 different ILPs preparations). (E) The inhibitory effect of ILPs in the presence and absence of Igpal was measured to determine the amount of free and encapsulated drug. Results are expressed as relative fluorescence units (RFU)/min (n= 3 from 3 different ILPs preparations).

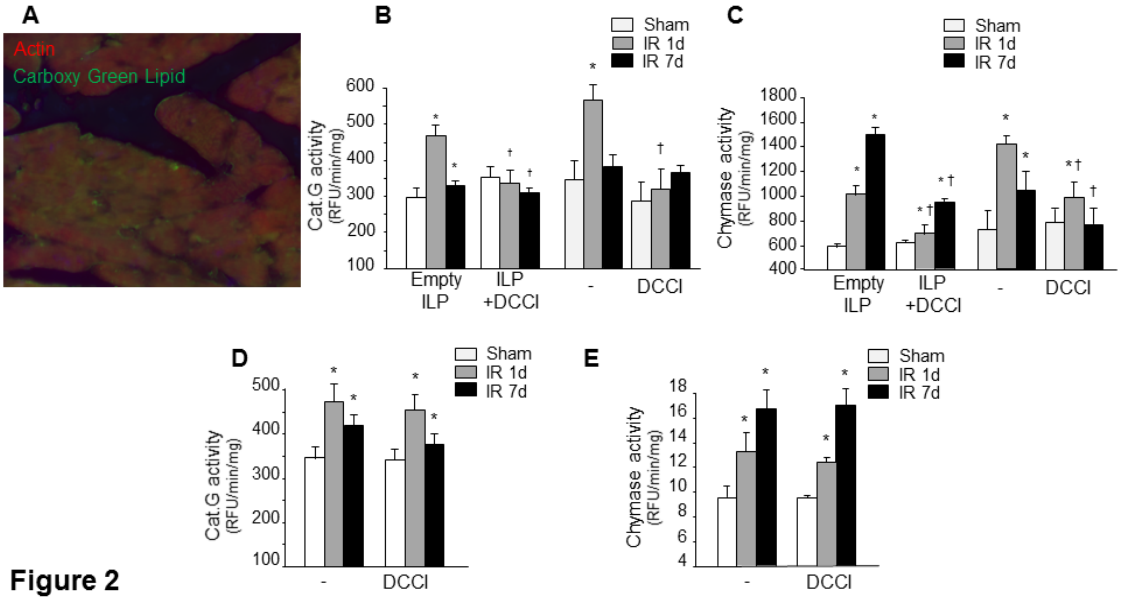

Figure 2

Figure 4-2: ILP encapsulated DCCI is specifically delivered to the injured myocardium and is effective to inhibit excess ISP activity. (A) Green lipid infused immunoliposomes co-stained with actin in the infarcted LV 6hrs post reperfusion. (B) Cathepsin G (Cat.G), chymase (C) activity in the infarcted LV of animals treated with either 2mg/kg targeted or 10mg/kg/d systemic as determined by enzymatic activity assay (n=6 for each groups). (D) Cat.G (E), chymase (D) activity in the infarcted LV of animals treated with 2mg/kg/d systemically or vehicle as determined by enzymatic activity assay (n=5 for each groups). Values are presented as mean ± SEM, $^{*}P < 0.05$ vs. shams, $_{\dagger}P < 0.05$ vs. vehicle-treated IR.

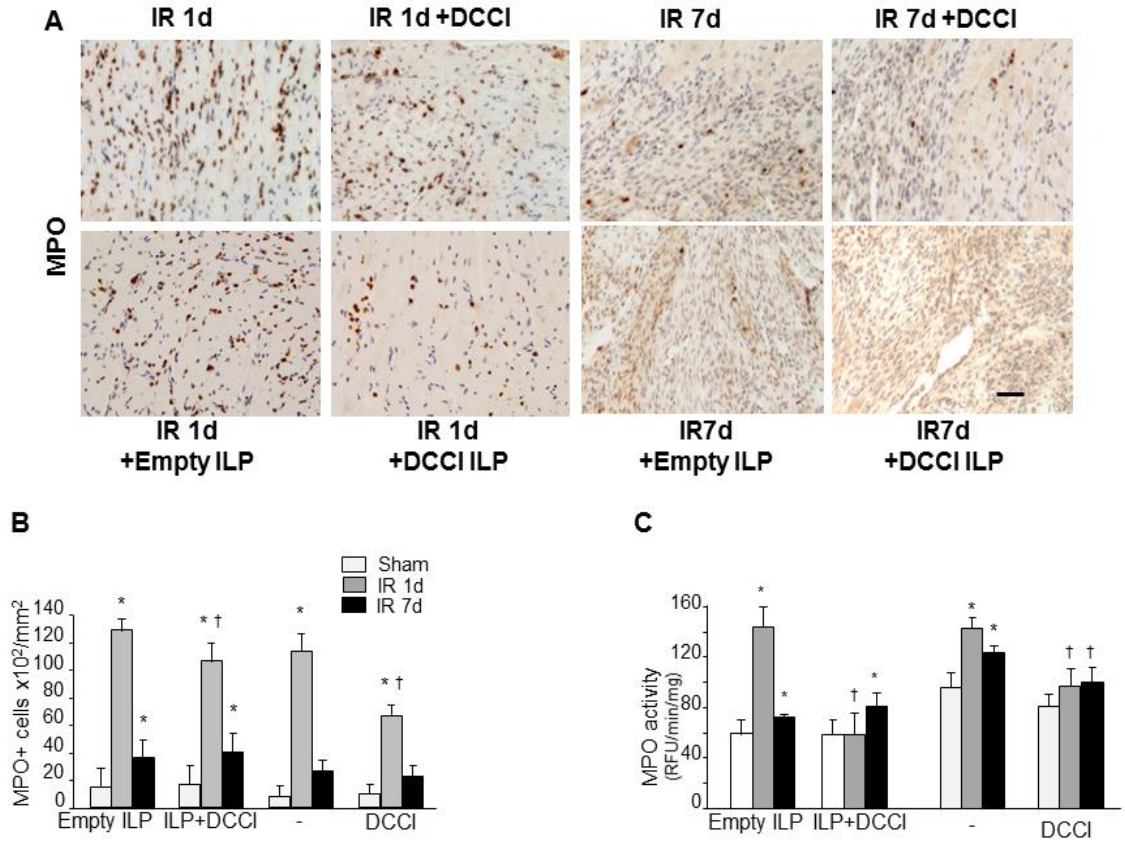

Figure 3

Figure 4-3: DCCI treatment attenuates inflammation in the reperfused heart. (A,B) representative MPO staining and relative quantification of paraffin-embedded heart sections from sham or mice subjected to ischemia reperfusion (IR) Scale bar: 40μm. (C) Activity in the infarcted LV as determined by enzymatic activity assay (n=6 for each groups). Values are presented as mean ± SEM, *P < 0.05 vs. shams, †P < 0.05 vs. vehicle-treated IR.

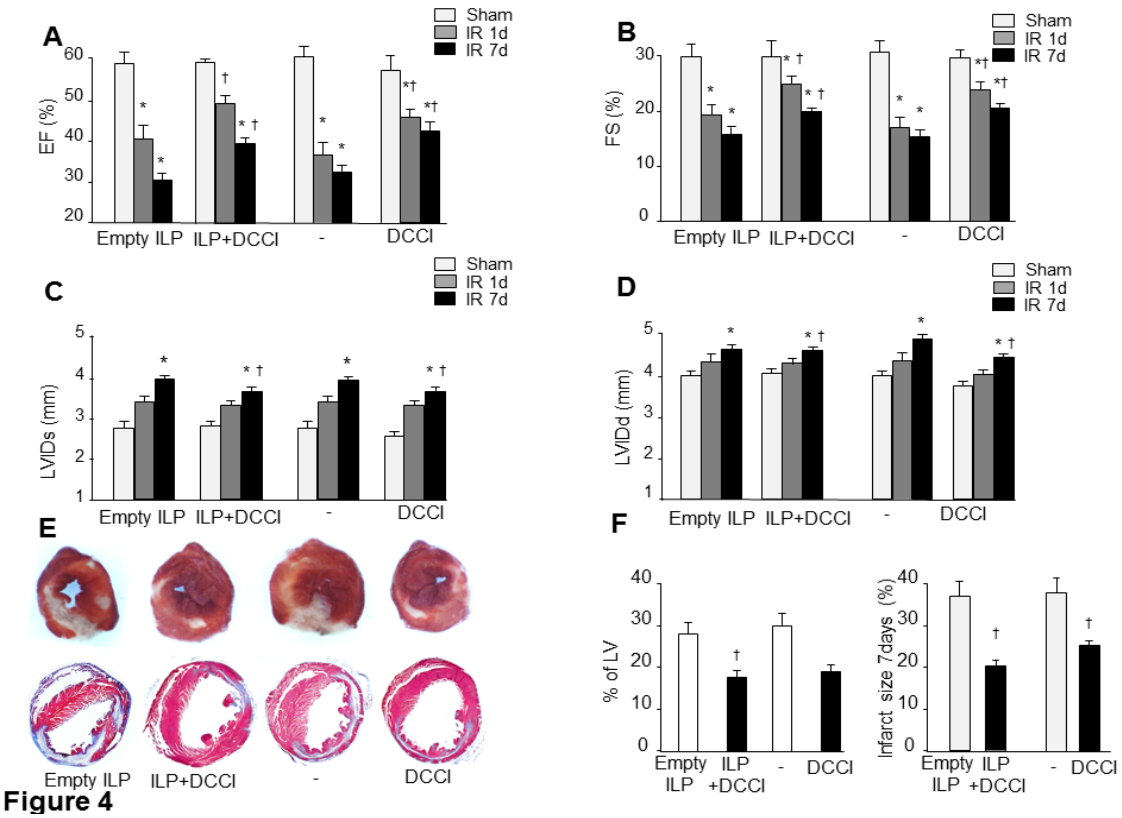

Figure 4

Figure 4-4: DCCI improves cardiac function post-IR. (A-D) Echocardiography measurement of Left ventricular (LV) ejection fraction (EF) (A), fractional shortening (FS) (B) and LV internal diameter (LVID) in systole (C) and diastole (D). (E) Representative images of Tetrazolium staining or Masson's trichrome staining on transverse heart sections at day 1 and 7 days post-IR, respectively. (F) Quantification of the infarcted area at 1 and 7 days post IR (n=5 for each groups). Values are presented as mean ± SEM, *P < 0.05 vs. sham, †P < 0.05 vs. vehicle-treated IR.

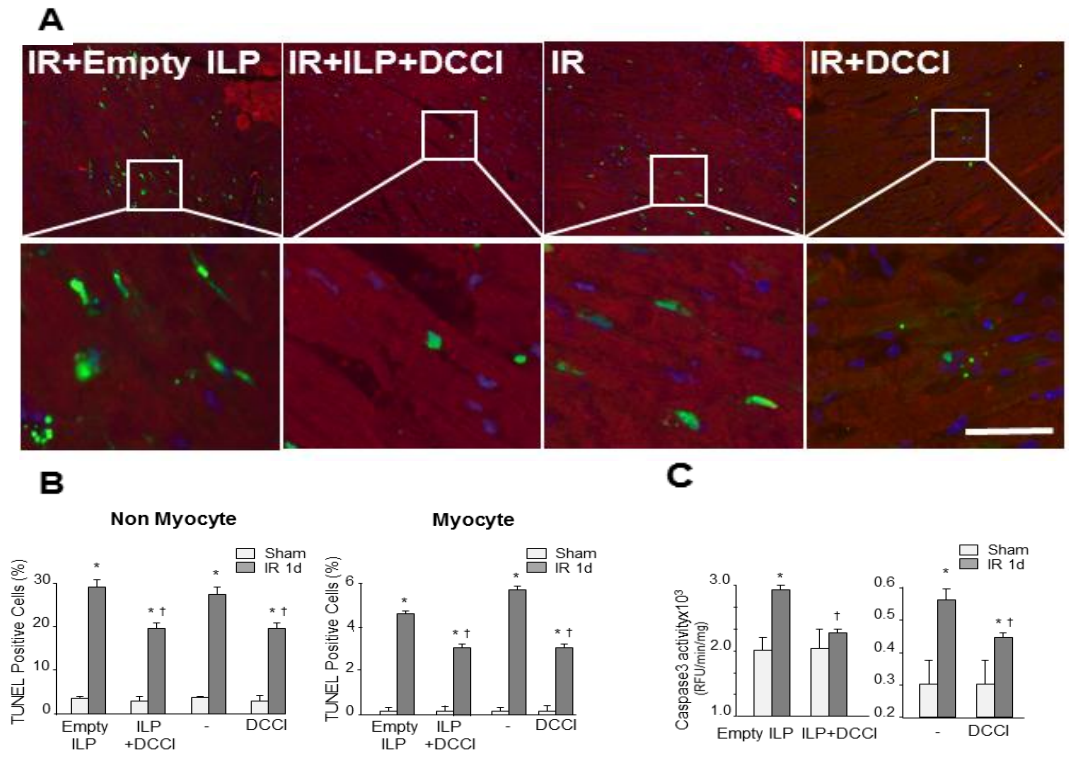

Figure 5

Figure 4-5: Effective doses of DCCI administration offers cardioprotection after acute IR. Ischemia reperfusion (IR) was induced for 24 h. (A) LV tissue sections were assessed for apoptosis using TUNEL assay (green), tropomyosin (red), and DAPI (4′,6-diamidino-2-phenylindole) (blue) staining. Scale bar: 40 μm. (B) The number of TUNEL-positive myocytes (B) and non-myocytes in the reperfused area was expressed as a percentage of total nuclei detected by DAPI staining (n=5 each group). (C) Quantification of caspase-3 activity in the LV using caspase-3 specific fluorogenic substrate (n=6 each group). (D) Immunoblot analysis indicates a decrease in pro-apoptotic signaling in the infarcted region of mice treated with DCCI or empty ILP or vehicle post-IR. Top: Representative immunoblots. Bottom: Quantification of experiments represented as fold change compared to shams (n=6 each group). GAPDH was included as a loading control. Values are presented as mean ± SEM, $^{*}P < 0.05$ vs. shams, $_{\dagger}P < 0.05$ vs. vehicle-treated.

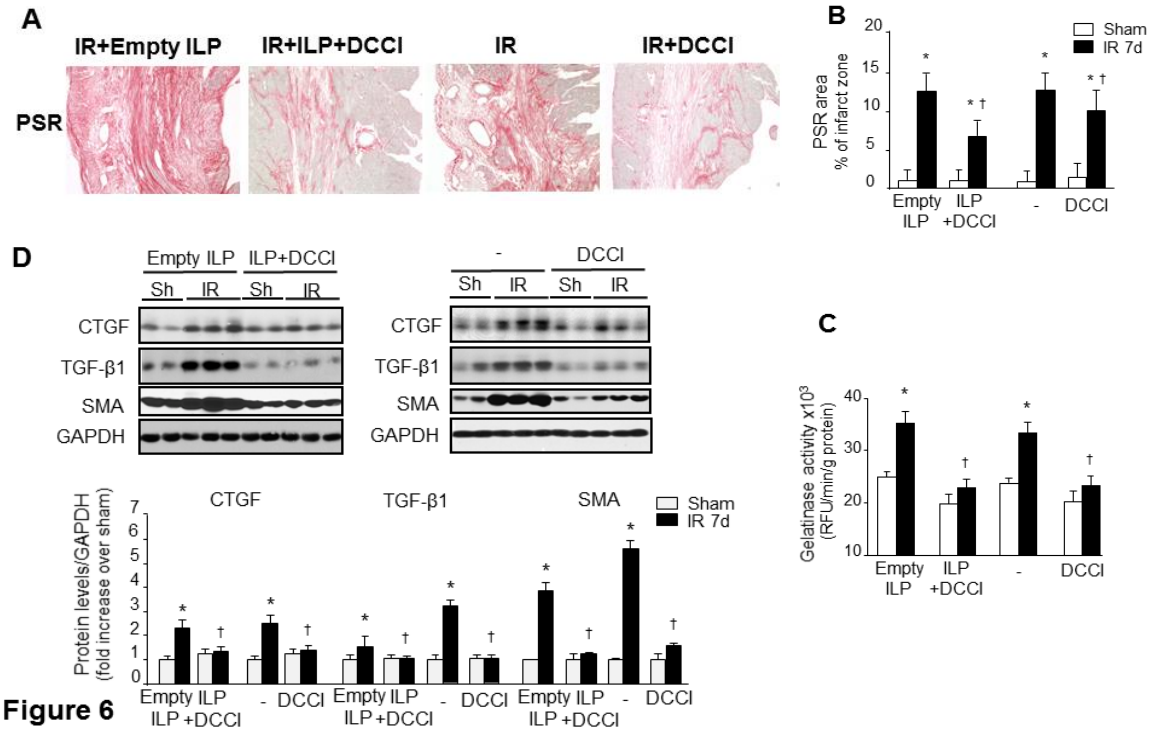

Figure 6

Figure 4-6: Effective doses of DCCI reduces fibrosis differentiation and improves cardiac remodeling after IR. Ischemia reperfusion (IR) was induced for 7 days. (A) Picro-sirus red staining and immunohistochemistry against smooth muscle α-actin (SMA) show reduced collagen and myofibroblast deposition in the injured myocardium of mice treated with DCCI compared to those treated with either empty ILP or vehicle. (C) Gelatinase activity assay in animals subjected to IR and treated with either vehicle or DCCI (n=5 for each groups). (D) Immunoblot analysis indicates a decrease in profibrotic signaling molecules in the infarcted region of mice treated with DCCI vs. the treatment with either empty ILP or vehicle post-IR. Top: Representative immunoblots. Bottom: Quantification of experiments represented as fold change compared to WT animals (n=6 for each groups). GAPDH was included as a loading control. Values are presented as mean ± SEM, $^{*}P < 0.05$ vs. shams, $_{\dagger}P < 0.05$ vs. vehicle-treated IR.

4.7 Supplemental Figures and Tables

Supplemental Table 1: Summary of heart weight, body weight and echocardiographic measurements in 24 h post reperfusion in sham and IR mice treated with either empty or DCCI encapsulated ILP.

	Sham		**1d IR**	
	Empty (n=6)	**DCCI (n=6)**	**Empty (n=8)**	**DCCI (n=8)**
HR (bpm)	456 ±15	486 ±16	471 ±11	490 ±27
HW (mg)	130 ±2	115 ±3	131 ±4	118 ±6
BW (g)	25 ±1	25 ±2	22.6 ±2	24 ±2
HW/BW (mg/g)	7.9 ±0.2	4.7 ±0.3	5.6 ±0.2	5.1 ±0.1
LV Vold (µl)	68 ±8	59 ±4	82 ±6*	72 ±4*†
LV Vols (µl)	30 ±5	28 ±4	50 ±5*	41 ±4*†
LVPWTd (mm)	0.70 ±0.02	0.71 ±0.02	0.64 ±0.03*	0.59 ±0.03*
LVPWTs (mm)	1.00 ±0.04	1.04 ±0.04	0.87 ±0.02*	0.76 ±0.03*

HR indicates heart rate; HW, heart weight; BW, body weight; LV Vold, LV volume during diastole; LV Vols, LV volume during systole; LVPWTd, LV posterior wall thickness diastole; and LVPWTs, LV posterior wall thickness systole. *P<0.05 vs. shams, †P<0.05 vs. non-treated IR.

Supplemental Table 2: Summary of heart weight, body weight and echocardiographic measurements in 7 days post reperfusion in sham and IR mice treated with empty or DCCI encapsulated ILPs.

	Sham		**7d IR**	
	Empty (n=6)	**DCCI (n=6)**	**Empty (n=8)**	**DCCI (n=8)**
HR (bpm)	466 ±14	459 ±24	486 ±22	457 ±14
HW (mg)	128 ±2	130 ±7	200 ±11*	150 ±10*†
BW (g)	25 ±2	25 ±2	25 ±1	25 ±2
HW/BW (mg/g)	4.9 ±0.2	5.3 ±0.3	5.9 ±0.4*	6.1 ±0.3*
LV Vold (µl)	76 ±7	78 ±10	97 ±4*	98 ±3*†
LV Vols (µl)	30 ±3	32 ±6	59 ±3*	56 ±3*†
LVPWTd (mm)	0.60 ±0.01	0.69 ±0.01	0.60 ±0.02*	0.52 ±0.02*
LVPWTs (mm)	0.95 ± 0.06	1.02 ± 0.03	0.71 ± 0.04*	0.71 ±0.03*

HR indicates heart rate; HW, heart weight; BW, body weight; LV Vold, LV volume during diastole; LV Vols, LV volume during systole; LVPWTd, LV posterior wall thickness diastole; and LVPWTs, LV posterior wall thickness systole. *P<0.05 vs. shams, †P<0.05 vs. non-treated IR.

Supplemental Table 3: Summary of heart weight, body weight and echocardiographic measurements in 24 h post reperfusion in sham and IR mice treated or not with 10mg/kg/d of DCCI.

	Sham		**1d IR**	
	-	**DCCI**	**-**	**DCCI**
	(n=6)	**(n=6)**	**(n=8)**	**(n=8)**
HR (bpm)	446 ±15	466 ±16	487 ±11	490 ±27
HW (mg)	115 ±2	115 ±3	118 ±4	118 ±6
BW (g)	23 ±1	25 ±2	23 ±2	24 ±2
HW/BW (mg/g)	5.1 ±0.2	4.7 ±0.3	5.5 ±0.1	5.1 ±0.1
LV Vold (µl)	69 ±8	59 ±4	88 ±6*	72 ±4*†
LV Vols (µl)	29 ±5	28 ±4	57 ±5*	41 ±4*†
LVPWTd (mm)	0.72 ±0.02	0.71 ±0.02	0.61 ±0.03*	0.59 ±0.03*
LVPWTs (mm)	1.05 ±0.04	1.04 ±0.04	0.77 ±0.02*	0.76 ±0.03*

HR indicates heart rate; HW, heart weight; BW, body weight; LV Vold, LV volume during diastole; LV Vols, LV volume during systole; LVPWTd, LV posterior wall thickness diastole; and LVPWTs, LV posterior wall thickness systole. *P<0.05 vs. shams, †P<0.05 vs. non treated IR.

Supplemental Table 4: Summary of heart weight, body weight and echocardiographic measurements in 7 days post reperfusion in sham and IR mice treated or not with 10mg/kg/d of DCCI.

	Sham		**7d IR**	
	-	**DCCI**	**-**	**DCCI**
	(n=6)	**(n=6)**	**(n=8)**	**(n=8)**
HR (bpm)	470 ±14	451 ±24	446 ±22	456 ±14
HW (mg)	124 ±2	126 ±3	132 ±10*	153 ±7*†
BW (g)	25 ±2	26 ±2	24 ±1	26 ±2
HW/BW (mg/g)	5.0 ±0.2	4.8 ±0.3	5.9 ±0.4*	6.1 ±0.3*
LV Vold (µl)	70 ±7	77 ±10	112 ±4*	95 ±3*†
LV Vols (µl)	28 ±3	33 ±6	74 ±3*	59 ±3*†
LVPWTd (mm)	0.63 ±0.01	0.61 ±0.01	0.56 ±0.02*	0.54 ±0.02*
LVPWTs (mm)	0.85 ± 0.06	0.87 ± 0.03	0.69 ± 0.04*	0.66 ±0.03*

HR indicates heart rate; HW, heart weight; BW, body weight; LV Vold, LV volume during diastole; LV VOLs, LV volume during systole; LVPWTd, LV posterior wall thickness diastole; and LVPWTs, LV posterior wall thickness systole. *P<0.05 vs. shams, †P<0.05 vs. non-treated IR.

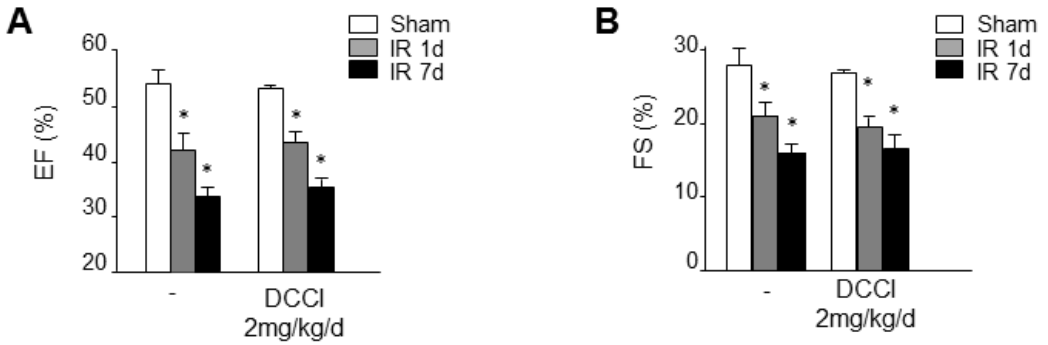

Figure S1: 2mg/kg/d systemic DCCI offers no improvement in cardiac function post-IR. (A, B) Echocardiography measurement of Left ventricular (LV) ejection fraction (EF) (A), fractional shortening (FS) (B). Values are presented as mean ± SEM, $^{*}P < 0.05$ vs. sham, $_{\dagger}P < 0.05$ vs. vehicle-treated IR.

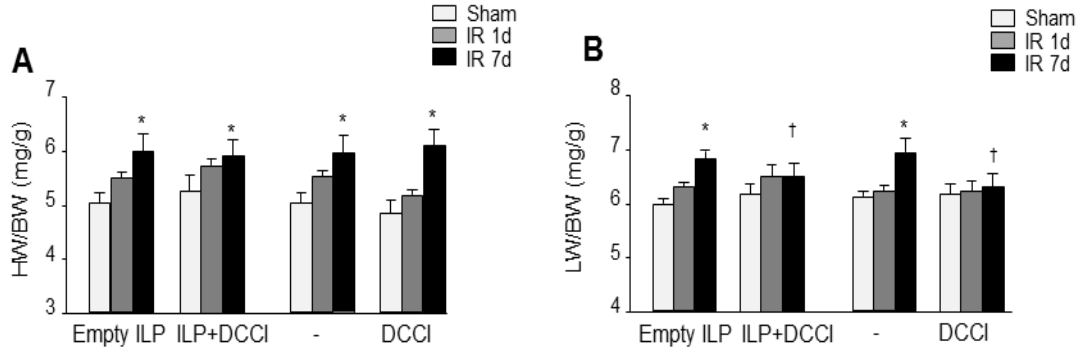

Figure S2: DCCI administration affects remodeling following IR (A, B) Morphometric measurements of heart weight to body weight (HW/BW) (A), Lung weight to body weight (LW/BW) (B). Values are presented as mean ± SEM, $^{*}P < 0.05$ vs. sham, $_{\dagger}P < 0.05$ vs. vehicle-treated IR.

CHAPTER 5

CONCLUDING REMARKS

Inflammatory response is the main mechanism dissipating pathogenic contaminations (312). This hostile function raises the hypothesis that the intense inflammatory response associated with sterile injuries similarly exerts damage to healthy tissue (313). One of the best-known examples of sterile injury associated with intense inflammatory response is myocardial injury. The intense inflammatory response associated with this injury reportedly exerts additional injuries on the delicate structure of the heart (314).

In the late 80s and early 90s, this hypothesis was tested in animal models of ischemia and ischemia reperfusion (315). Several studies demonstrated that treatments with antibodies neutralizing specific mediators including cytokines, chemokines and adhesion molecules showed significant reduction of infarct size and better cardiac function following ischemia and ischemia reperfusion (316). These overwhelmingly positive results pushed for quick transition to clinical trials. Unfortunately, all approaches to use anti-inflammatory pathways (i.e. anti-integrin therapy, anti-leukocyte therapy, anti-TNFα neutralizing antibodies, or anti-steroids) to treat patients with an ischemic episode failed (317).

As the initial interest to target systemic inflammation faded, the question remains whether this field is dead or requires a revised view (318). Over the past 15 years, a better understanding of inflammation biology has altered the simplified views of the past leading to identification of both protective and injurious pathways activated by inflammatory components (319, 320). These discoveries support the idea of the inflammatory response

as a complex and multifaceted phenomenon. Therefore, a paradigm shift is needed in the therapeutic approaches to specifically target the deleterious components of inflammatory response whilst protecting the beneficial ones (321).

A potential scenario explaining failed clinical trials may be associated with complexities related to the effect of anti-inflammatory drugs on other inflammatory cells involved in cardiac repair such as macrophages and hematopoietic stem cells (322). Furthermore, the effect of these drugs may also inhibit the release of some survival factor(s) released by activated inflammatory cells that may play a role in myocyte survival (323, 324). Therefore, strategies to target specific components of inflammation without significantly affecting leukocyte mobilization from the bone marrow and circulation may provide a better understanding about the pleiotropic role played by inflammation during the development of HF.

One of the major components released by activated leukocytes are inflammatory serine proteases (ISP) which are known for their role in killing pathogens (311). However, their role during sterile inflammation such as ischemia and IR has not been studied precisely before. In this project, we have first revealed the effects of cathepsin G and chymase, two major ISPs known to affect cellular function and survival, on cardiomyocytes and fibroblasts and subsequent effects on cardiac function and remodeling following IR.

We have shown that excessive activity of cathepsin G and chymase can result in additional myocyte death and excessive cardiac fibrosis and that effective inhibition of both cathepsin G and chymase using a dual inhibitor of chymase and cathepsin G (DDCI) results in reduced cardiac injury and pathological remodeling and subsequently better cardiac

function post IR. Previous studies had used chymase specific inhibitors in hamster and mice models of IR and showed mixed results which may be due to the fact that other proteases such as cathepsin G may compensate for the inhibited chymase and exert similar effects.

Although cathepsin G and chymase are the major ISPs associated with myocardium injury, inhibition of other ISPs such as elastase showed cardioprotective effects (325). Therefore, a more universal inhibitor of ISPs may offer enhanced cardioprotective effects following IR. Cathepsin C is a lysosomal cysteine protease dipeptidyl peptidase I (DPPI) which is required for the activation of many serine proteases and therefore can be a potential target to inhibit more ISPs following IR. Therefore, inhibition of DPPI activity may offer a potential advantage over inhibiting specific ISPs.

ISPs are known to play a key role on mobilization of inflammatory and hematopoietic stem cells. Therefore, to minimize the potential side effects of systemic inhibition of ISPs, we developed a method to specifically deliver DCCI to injured myocardium. DCCI targeted delivery was achieved by adopting an anti-P-selectin conjugated immunoliposomal delivery platform. Targeted delivery of DCCI was more efficient at inhibiting excessive ISP activity and conferring associated beneficial effects on cardiac function and remodeling at significantly lower doses when compared to systemic delivery.

An additional benefit of utilizing this targeted delivery system, was the slow release characteristic of the immunoliposomal platform, which matched the needs of our study. Though, we have shown that chymase and cathepsin G activities are at their peaks 1 day post IR, chymase activity stayed higher than normal even after 7 days. Therefore, repetitive

systemic administration of high doses of DCCI are required to normalize excessive chymase activity. Repetitive systemic injection of DCCI can further escalate the probability of undesired side effects in remote organs and cells. Targeted delivery offers the opportunity to reduce required injections as administrated DCCI-ILP complex circulates for longer periods of time and DCCI is released at slow rates in a myocardium specific manner.

We have shown that anti-P-selectin conjugated ILPs are effective to deliver DCCI to injured myocardium. However, small modifications can enhance specificity and effectiveness of delivery for future studies. One possible enhancement is to target multiple markers. For example, apoptotic and necrotic cardiomyocytes lose their membrane integrity which exposes their cytoskeletal proteins. Therefore, dual tagging of ILPs with an anti-adhesion molecule antibody and an antibody against cytoskeletal proteins such as myosin may enhance the specificity of delivery. Another modification which may accentuate the beneficial outcomes observed in this study is to utilize active loading methods to encapsulate higher concentrations of DCCI which may offer additional cardio protection following IR.

Although these methods can attenuate inflammatory mediated injury, basal levels of cell loss due to hypoxia and non-inflammatory mediated pathways are inevitable. The loss of functional cardiomyocytes results in reduced cardiac function, thinning of the myocardium, increased wall stress and ultimately, terminal phase of heart failure. Therefore, to minimize the progressive deterioration of cardiac function and integrity, development of regenerative approaches to improve the infarcted area by replacing the damaged cells may be necessary.

Recently, interest has been more inclined toward regeneration therapies with the application of stem cells (326). Although these studies have presented enormous potential, differentiation of seeded cells to functional cardiac cells is extremely sensitive and prone to environmental stimuli, such as growth and differentiation factors (327). Also, inflammation is known to negatively regulate tissue restoration (328, 329). Several studies have shown that inflammation negatively regulates hematopoietic stem cell proliferation (330-332). Most stem cell based regenerative methods are applied at time points when the intensity of inflammation is declined significantly (326). However, the process of seeding cells by itself may initiate an inflammatory response, which in turn can result in limited proliferation and differentiation of seeded stem cells to desired functional cardiac cells (333). Therefore, nanoparticulate delivery platforms such as targeted ILPs offer a promising tool for delivery of these factors and anti-inflammatory agents, simultaneously. This may provide the ideal milieu for stem cells to proliferate and differentiate to desired target cells. Additionally, antibodies can be attached to these nanoparticles to attract and entrap endogenous factors and cells such as pro-angiogenic M2 polarized macrophages to the stem cell seeded segment (334).

On the other hand, no matter how promising the outcomes of any therapeutics in animal models, the final goal is to translate these results to clinical settings. Liposomes are the very first class of nanoparticulate delivery systems that have been successfully translated to clinical applications (335). Doxil®, Ambisome® and DepoDur™ are a few examples of liposomal formulations currently used in clinical setting (336, 337).

To prepare liposomes for clinical applications, industrial large scale preparation approaches have been developed such as spray-drying, freeze-drying, and different

ethanol-injection techniques (338). Although the preparation process is significantly different from those used in lab-scale approaches such as the thin-film hydration method which is used in this project, the final product has similar construct characteristics.

Another important consideration is the need for quality control. In our project, we have set different checkpoints during preparation to warrant the functionality of our liposomal preparation. Industrial approaches introduce several layers of standardization, which can minimize human error. Even so, various levels of quality controls such as size distribution checks are usually put in place to ensure the performance of the liposome preparation (339). Another important consideration for transition to clinical applications is the difference in the biodistribution of liposomes in animal models and in humans. This can be the result of differences in RES and other inflammatory systems between species, which accounts for the removal of foreign bodies (340). Although PEGylation minimizes these complexities, biodistribution in humans should be assessed for any new liposomal preparation prior to clinical investigations (341). Various methods are currently used to investigate biodistribution in humans, such as imaging techniques by incorporating contrast agents in liposomes for use in CT/PET/SPECT imaging methods (342).

Finally, the biggest concern of using ILPs in clinical approaches is the host immunogenic reactions to targeting moieties which can result in increased rate of immunological detection and subsequent clearance (343). Additionally, non-specific interactions between serum proteins and targeting ligands can diminish the targeting ability and effectiveness (344). Besides a few recent studies which used anti-HER2 and anti-EGFR tagged ILPs for cancer therapy, most clinical trials have relied on passive accumulation of plain liposomes due to high permeability in the desired regions (345). Although, this translates well for

myocardial delivery of plain liposomes because ischemic endothelium is highly permeable post-IR, but active targeting can significantly enhance specificity of delivery (256).

Several approaches have developed to counteract the immunological weaknesses of ILPs to enhance their clinical viability. One approach includes using antibody fragments instead of the whole antibody, which decreases immunogenicity and enhances the pharmacokinetic profile of the immunoliposomes (346). Another approach to reduce immunogenic clearance of immunoliposomes is to use humanized antibodies. Humanized antibodies, are antibodies which are raised in non-human species however their protein sequence has been modified to mimic their human variant (347). Incorporation of humanized antibodies, instead of rodent raised non-humanized antibodies as the targeting moiety has resulted in longer circulating times and better clinical applicability (348).

Overall, despite complexities in transition of liposomal delivery approaches to clinical procedures, this method can save those therapeutics which otherwise are ineffective or toxic. However, the gains and the losses of using targeted delivery method instead of conventional systemic should be weighted to select the best choice. In our case avoiding side effects of anti-inflammatory drugs on other organs and cells can significantly outweigh additional considerations needed for clinical usage of immunoliposomal delivery methods and therefore it is suggested for further investigation as a potential therapeutic method following IR.

BIBLIOGRAPHY

1. van Rijt SH, Bein T, Meiners S. Medical nanoparticles for next generation drug delivery to the lungs. The European respiratory journal. 2014;44(3):765-74. Epub 2014/05/06. doi: 10.1183/09031936.00212813. PubMed PMID: 24791828.
2. Bergstrand N. Liposomes for Drug Delivery: From Physico-chemical Studies to Application: Acta Universitatis Upsaliensis; 2003.
3. Hausenloy DJ, Yellon DM. Myocardial ischemia-reperfusion injury: a neglected therapeutic target. J Clin Invest. 2013;123(1):92-100. doi: 10.1172/JCI62874.
4. Neri M, Riezzo I, Pascale N, Pomara C, Turillazzi E. Ischemia/Reperfusion Injury following Acute Myocardial Infarction: A Critical Issue for Clinicians and Forensic Pathologists. Mediators of Inflammation. 2017;2017:14. doi: 10.1155/2017/7018393.
5. Ibanez B, Heusch G, Ovize M, Van de Werf F. Evolving therapies for myocardial ischemia/reperfusion injury. Journal of the American College of Cardiology. 2015;65(14):1454-71. Epub 2015/04/11. doi: 10.1016/j.jacc.2015.02.032. PubMed PMID: 25857912.
6. Gonzalez LM, Moeser AJ, Blikslager AT. Animal models of ischemia-reperfusion-induced intestinal injury: progress and promise for translational research. American journal of physiology Gastrointestinal and liver physiology. 2015;308(2):G63-75. Epub 2014/11/22. doi: 10.1152/ajpgi.00112.2013. PubMed PMID: 25414098; PMCID: Pmc4297854.
7. Granger DN, Kvietys PR. Reperfusion injury and reactive oxygen species: The evolution of a concept. Redox biology. 2015;6:524-51. Epub 2015/10/21. doi: 10.1016/j.redox.2015.08.020. PubMed PMID: 26484802; PMCID: PMC4625011.
8. Eltzschig HK, Eckle T. Ischemia and reperfusion--from mechanism to translation. Nature medicine. 2011;17(11):1391-401. Epub 2011/11/09. doi: 10.1038/nm.2507. PubMed PMID: 22064429; PMCID: Pmc3886192.
9. Schofield ZV, Woodruff TM, Halai R, Wu MC, Cooper MA. Neutrophils--a key component of ischemia-reperfusion injury. Shock (Augusta, Ga). 2013;40(6):463-70. Epub 2013/10/04. doi: 10.1097/shk.0000000000000044. PubMed PMID: 24088997.
10. Sharony R, Yu P-J, Park J, Galloway A, Mignatti P, Pintucci G. Protein targets of inflammatory serine proteases and cardiovascular disease. Journal of Inflammation. 2010;7(1):45. PubMed PMID: doi:10.1186/1476-9255-7-45.
11. Safavi F, Rostami A. Role of serine proteases in inflammation: Bowman-Birk protease inhibitor (BBI) as a potential therapy for autoimmune diseases. Experimental and molecular pathology. 2012;93(3):428-33. Epub 2012/10/02. doi: 10.1016/j.yexmp.2012.09.014. PubMed PMID: 23022357.
12. Wiedow O, Meyer-Hoffert U. Neutrophil serine proteases: potential key regulators of cell signalling during inflammation. Journal of Internal Medicine. 2005;257(4):319-28.
13. Greco MN, Hawkins MJ, Powell ET, Almond HR, Corcoran TW, de Garavilla L, Kauffman JA, Recacha R, Chattopadhyay D, Andrade-Gordon P, Maryanoff BE. Nonpeptide inhibitors of cathepsin G: Optimization of a novel β-ketophosphonic acid lead by structure-based drug design. J Am Chem Soc. 2002;124(15):3810-1. doi: 10.1021/ja017506h.
14. Galagudza M, Korolev D, Postnov V, Naumisheva E, Grigorova Y, Uskov I, Shlyakhto E. Passive targeting of ischemic-reperfused myocardium with adenosine-loaded silica nanoparticles. International Journal of Nanomedicine. 2012;7:1671-8. doi: 10.2147/IJN.S29511. PubMed PMID: PMC3356166.

15. Dalen JE, Alpert JS, Goldberg RJ, Weinstein RS. The epidemic of the 20(th) century: coronary heart disease. The American journal of medicine. 2014;127(9):807-12. Epub 2014/05/09. doi: 10.1016/j.amjmed.2014.04.015. PubMed PMID: 24811552.
16. WHO. Cardiovascular diseases (CVDs) [cited 2017]. Available from: http://www.who.int/mediacentre/factsheets/fs317/en/.
17. Scott MC, Winters ME. Congestive Heart Failure. Emergency medicine clinics of North America. 2015;33(3):553-62. Epub 2015/08/01. doi: 10.1016/j.emc.2015.04.006. PubMed PMID: 26226866.
18. Yellon DM, Hausenloy DJ. Myocardial reperfusion injury. New England Journal of Medicine. 2007;357(11):1121-35.
19. Simonis G, Strasser RH, Ebner B. Reperfusion injury in acute myocardial infarction. Critical Care. 2012;16(Suppl 2):A22-A. doi: 10.1186/cc11280. PubMed PMID: PMC3389482.
20. Frangogiannis NG, Smith CW, Entman ML. The inflammatory response in myocardial infarction. Cardiovascular research. 2002;53(1):31-47. Epub 2001/12/18. PubMed PMID: 11744011.
21. Shen AC, Jennings RB. Myocardial calcium and magnesium in acute ischemic injury. The American journal of pathology. 1972;67(3):417-40. Epub 1972/06/01. PubMed PMID: 5033257; PMCID: Pmc2032743.
22. Travers JG, Kamal FA, Robbins J, Yutzey KE, Blaxall BC. Cardiac fibrosis: The fibroblast awakens. Cir Res. 2016;118(6):1021-40. doi: 10.1161/circresaha.115.306565.
23. Piek A, de Boer RA, Sillje HH. The fibrosis-cell death axis in heart failure. Heart failure reviews. 2016;21(2):199-211. Epub 2016/02/18. doi: 10.1007/s10741-016-9536-9. PubMed PMID: 26883434; PMCID: PMC4762920.
24. Gottlieb RA. Cell death pathways in acute ischemia/reperfusion injury. Journal of cardiovascular pharmacology and therapeutics. 2011;16(3-4):233-8. Epub 2011/08/09. doi: 10.1177/1074248411409581. PubMed PMID: 21821521; PMCID: PMC3337030.
25. Konstantinidis K, Whelan RS, Kitsis RN. Mechanisms of Cell Death in Heart Disease. Arteriosclerosis, thrombosis, and vascular biology. 2012;32(7):10.1161/ATVBAHA.111.224915. doi: 10.1161/ATVBAHA.111.224915. PubMed PMID: PMC3835661.
26. Kerr JF, Wyllie AH, Currie AR. Apoptosis: a basic biological phenomenon with wide-ranging implications in tissue kinetics. British journal of cancer. 1972;26(4):239-57. Epub 1972/08/01. PubMed PMID: 4561027; PMCID: Pmc2008650.
27. Elmore S. Apoptosis: A Review of Programmed Cell Death. Toxicologic pathology. 2007;35(4):495-516. doi: 10.1080/01926230701320337. PubMed PMID: PMC2117903.
28. Elmore S. Apoptosis: a review of programmed cell death. Toxicologic pathology. 2007;35(4):495-516. Epub 2007/06/15. doi: 10.1080/01926230701320337. PubMed PMID: 17562483; PMCID: PMC2117903.
29. Haanen C, Vermes I. Apoptosis and inflammation. Mediators of Inflammation. 1995;4(1):5-15. doi: 10.1155/S0962935195000020. PubMed PMID: PMC2365613.
30. Nicotera P, Leist M, Ferrando-May E. Intracellular ATP, a switch in the decision between apoptosis and necrosis. Toxicology letters. 1998;102-103:139-42. Epub 1999/02/18. PubMed PMID: 10022245.
31. Bradbury DA, Simmons TD, Slater KJ, Crouch SP. Measurement of the ADP:ATP ratio in human leukaemic cell lines can be used as an indicator of cell viability, necrosis and apoptosis. Journal of immunological methods. 2000;240(1-2):79-92. Epub 2000/06/16. PubMed PMID: 10854603.

32. Fink SL, Cookson BT. Apoptosis, pyroptosis, and necrosis: mechanistic description of dead and dying eukaryotic cells. Infection and immunity. 2005;73(4):1907-16. Epub 2005/03/24. doi: 10.1128/iai.73.4.1907-1916.2005. PubMed PMID: 15784530; PMCID: Pmc1087413.
33. Eguchi Y, Shimizu S, Tsujimoto Y. Intracellular ATP levels determine cell death fate by apoptosis or necrosis. Cancer research. 1997;57(10):1835-40. Epub 1997/05/15. PubMed PMID: 9157970.
34. Olivetti G, Quaini F, Sala R, Lagrasta C, Corradi D, Bonacina E, Gambert SR, Cigola E, Anversa P. Acute Myocardial Infarction in Humans is Associated with Activation of Programmed Myocyte Cell Death in the Surviving Portion of the Heart. Journal of Molecular and Cellular Cardiology.28(9):2005-16. doi: 10.1006/jmcc.1996.0193.
35. Ma S, Wang Y, Chen Y, Cao F. The role of the autophagy in myocardial ischemia/reperfusion injury. Biochimica et biophysica acta. 2015;1852(2):271-6. Epub 2014/05/27. doi: 10.1016/j.bbadis.2014.05.010. PubMed PMID: 24859226.
36. Ma S, Wang Y, Chen Y, Cao F. The role of the autophagy in myocardial ischemia/reperfusion injury. Biochimica et Biophysica Acta (BBA) - Molecular Basis of Disease. 2015;1852(2):271-6. doi: http://dx.doi.org/10.1016/j.bbadis.2014.05.010.
37. Czyzyk-Krzeska MF, Meller J, Plas DR. Not all autophagy is equal. Autophagy. 2012;8(7):1155-6. doi: 10.4161/auto.20650. PubMed PMID: PMC3429557.
38. Linkermann A, Green DR. Necroptosis. The New England journal of medicine. 2014;370(5):455-65. doi: 10.1056/NEJMra1310050. PubMed PMID: PMC4035222.
39. Kim CR, Kim JH, Park H-YL, Park CK. Ischemia Reperfusion Injury Triggers TNFα Induced-Necroptosis in Rat Retina. Current Eye Research. 2017;42(5):771-9. doi: 10.1080/02713683.2016.1227449.
40. Koudstaal S, Oerlemans MI, Van der Spoel TI, Janssen AW, Hoefer IE, Doevendans PA, Sluijter JP, Chamuleau SA. Necrostatin-1 alleviates reperfusion injury following acute myocardial infarction in pigs. European journal of clinical investigation. 2015;45(2):150-9. Epub 2014/12/17. doi: 10.1111/eci.12391. PubMed PMID: 25496079.
41. Kalogeris T, Baines CP, Krenz M, Korthuis RJ. Cell Biology of Ischemia/Reperfusion Injury. International review of cell and molecular biology. 2012;298:229-317. doi: 10.1016/B978-0-12-394309-5.00006-7. PubMed PMID: PMC3904795.
42. Monteiro HP, Stern A. Redox modulation of tyrosine phosphorylation-dependent signal transduction pathways. Free Radical Biology and Medicine. 1996;21(3):323-33. doi: http://dx.doi.org/10.1016/0891-5849(96)00051-2.
43. Thannickal VJ, Fanburg BL. Reactive oxygen species in cell signaling. American journal of physiology Lung cellular and molecular physiology. 2000;279(6):L1005-28. Epub 2000/11/15. PubMed PMID: 11076791.
44. Siwik DA, Tzortzis JD, Pimental DR, Chang DL, Pagano PJ, Singh K, Sawyer DB, Colucci WS. Inhibition of copper-zinc superoxide dismutase induces cell growth, hypertrophic phenotype, and apoptosis in neonatal rat cardiac myocytes in vitro. Circulation research. 1999;85(2):147-53. Epub 1999/07/27. PubMed PMID: 10417396.
45. Murphy E, Steenbergen C. Ion transport and energetics during cell death and protection. Physiology (Bethesda, Md). 2008;23:115-23. Epub 2008/04/11. doi: 10.1152/physiol.00044.2007. PubMed PMID: 18400694; PMCID: Pmc2872775.
46. Perricone AJ, Heide RSV. Novel Therapeutic Strategies for Ischemic Heart Disease. Pharmacological research : the official journal of the Italian Pharmacological Society. 2014;0:36-45. doi: 10.1016/j.phrs.2014.08.004. PubMed PMID: PMC4182165.

47. Santulli G, Xie W, Reiken SR, Marks AR. Mitochondrial calcium overload is a key determinant in heart failure. Proceedings of the National Academy of Sciences of the United States of America. 2015;112(36):11389-94. Epub 2015/07/29. doi: 10.1073/pnas.1513047112. PubMed PMID: 26217001; PMCID: PMC4568687.
48. Fill M, Copello JA. Ryanodine receptor calcium release channels. Physiological Reviews. 2002;82(4):893-922. Epub 2002/09/25. doi: 10.1152/physrev.00013.2002. PubMed PMID: 12270947.
49. Orrenius S, Zhivotovsky B, Nicotera P. Regulation of cell death: the calcium-apoptosis link. Nat Rev Mol Cell Biol. 2003;4(7):552-65.
50. Wong R, Steenbergen C, Murphy E. Mitochondrial permeability transition pore and calcium handling. Methods in molecular biology (Clifton, NJ). 2012;810:235-42. Epub 2011/11/08. doi: 10.1007/978-1-61779-382-0_15. PubMed PMID: 22057571; PMCID: PMC3461591.
51. Khorchid A, Ikura M. How calpain is activated by calcium. Nature structural biology. 2002;9(4):239-41. Epub 2002/03/27. doi: 10.1038/nsb0402-239. PubMed PMID: 11914728.
52. Croall DE, Ersfeld K. The calpains: modular designs and functional diversity. Genome biology. 2007;8(6):218. Epub 2007/07/05. doi: 10.1186/gb-2007-8-6-218. PubMed PMID: 17608959; PMCID: Pmc2394746.
53. Rubin H, Sanui H. Complexes of inorganic pyrophosphate, orthophosphate, and calcium as stimulants of 3T3 cell multiplication. Proceedings of the National Academy of Sciences of the United States of America. 1977;74(11):5026-30. Epub 1977/11/01. PubMed PMID: 200943; PMCID: PMC432091.
54. Ott M, Robertson JD, Gogvadze V, Zhivotovsky B, Orrenius S. Cytochrome c release from mitochondria proceeds by a two-step process. Proceedings of the National Academy of Sciences of the United States of America. 2002;99(3):1259-63. Epub 2002/01/31. doi: 10.1073/pnas.241655498. PubMed PMID: 11818574; PMCID: Pmc122177.
55. Gogvadze V, Robertson JD, Zhivotovsky B, Orrenius S. Cytochrome c release occurs via Ca2+-dependent and Ca2+-independent mechanisms that are regulated by Bax. The Journal of biological chemistry. 2001;276(22):19066-71. Epub 2001/03/27. doi: 10.1074/jbc.M100614200. PubMed PMID: 11264286.
56. Von Ahsen O, Waterhouse NJ, Kuwana T, Newmeyer DD, Green DR. The 'harmless' release of cytochrome c. Cell death and differentiation. 2000;7(12):1192-9. Epub 2001/02/15. doi: 10.1038/sj.cdd.4400782. PubMed PMID: 11175256.
57. Gabriel B, Sureau F, Casselyn M, Teissie J, Petit PX. Retroactive pathway involving mitochondria in electroloaded cytochrome c-induced apoptosis. Protective properties of Bcl-2 and Bcl-XL. Experimental cell research. 2003;289(2):195-210. Epub 2003/09/23. PubMed PMID: 14499621.
58. Kutuk O, Basaga H. Bcl-2 protein family: implications in vascular apoptosis and atherosclerosis. Apoptosis : an international journal on programmed cell death. 2006;11(10):1661-75. Epub 2006/09/05. doi: 10.1007/s10495-006-9402-7. PubMed PMID: 16951924.
59. Green DR, Kroemer G. The pathophysiology of mitochondrial cell death. Science (New York, NY). 2004;305(5684):626-9. Epub 2004/08/03. doi: 10.1126/science.1099320. PubMed PMID: 15286356.
60. Martinou JC, Desagher S, Antonsson B. Cytochrome c release from mitochondria: all or nothing. Nature cell biology. 2000;2(3):E41-3. Epub 2000/03/09. doi: 10.1038/35004069. PubMed PMID: 10707095.

61. Hajnoczky G, Csordas G, Das S, Garcia-Perez C, Saotome M, Sinha Roy S, Yi M. Mitochondrial calcium signalling and cell death: approaches for assessing the role of mitochondrial Ca2+ uptake in apoptosis. Cell calcium. 2006;40(5-6):553-60. Epub 2006/11/01. doi: 10.1016/j.ceca.2006.08.016. PubMed PMID: 17074387; PMCID: Pmc2692319.
62. Hockenbery DM, Oltvai ZN, Yin XM, Milliman CL, Korsmeyer SJ. Bcl-2 functions in an antioxidant pathway to prevent apoptosis. Cell. 1993;75(2):241-51. Epub 1993/10/22. PubMed PMID: 7503812.
63. Peters SC, Piper HM. Reoxygenation-induced Ca2+ rise is mediated via Ca2+ influx and Ca2+ release from the endoplasmic reticulum in cardiac endothelial cells. Cardiovasc Res. 2007;73(1):164-71. Epub 2006/11/14. doi: 10.1016/j.cardiores.2006.09.015. PubMed PMID: 17097624.
64. Ramli J, CalderonArtero P, Block RC, Mousa SA. Novel Therapeutic Targets for Preserving a Healthy Endothelium: Strategies for Reducing the Risk of Vascular and Cardiovascular Disease. Cardiology Journal. 2011;18(4):352-63. PubMed PMID: PMC3342824.
65. Davidson SM, Duchen MR. Endothelial mitochondria: contributing to vascular function and disease. Circ Res. 2007;100(8):1128-41. Epub 2007/04/28. doi: 10.1161/01.RES.0000261970.18328.1d. PubMed PMID: 17463328.
66. Bhattacharyya A, Chattopadhyay R, Mitra S, Crowe SE. Oxidative Stress: An Essential Factor in the Pathogenesis of Gastrointestinal Mucosal Diseases. Physiological Reviews. 2014;94(2):329-54. doi: 10.1152/physrev.00040.2012. PubMed PMID: PMC4044300.
67. Zweier JL, Kuppusamy P, Thompson-Gorman S, Klunk D, Lutty GA. Measurement and characterization of free radical generation in reoxygenated human endothelial cells. The American journal of physiology. 1994;266(3 Pt 1):C700-8. Epub 1994/03/01. PubMed PMID: 8166233.
68. Prabhakarpandian B, Goetz DJ, Swerlick RA, Chen X, Kiani MF. Expression and functional significance of adhesion molecules on cultured endothelial cells in response to ionizing radiation. Microcirculation (New York, NY : 1994). 2001;8(5):355-64. Epub 2001/11/01. doi: 10.1038/sj/mn/7800105. PubMed PMID: 11687947.
69. Kerner T, Ahlers O, Reschreiter H, Bührer C, Möckel M, Gerlach H. Adhesion molecules in different treatments of acute myocardial infarction. Critical Care. 2001;5(3):145-50. PubMed PMID: PMC31578.
70. Nishiwaki A, Ueda T, Ugawa S, Shimada S, Ogura Y. Upregulation of P-selectin and intercellular adhesion molecule-1 after retinal ischemia-reperfusion injury. Investigative ophthalmology & visual science. 2003;44(11):4931-5. Epub 2003/10/28. PubMed PMID: 14578419.
71. Kenneth Mallory G, White PD, Salcedo-Salgar J. The speed of healing of myocardial infarction. American Heart Journal. 1939;18(6):647-71. doi: http://dx.doi.org/10.1016/S0002-8703(39)90845-8.
72. Entman ML, Youker K, Shoji T, Kukielka G, Shappell SB, Taylor AA, Smith CW. Neutrophil induced oxidative injury of cardiac myocytes. A compartmented system requiring CD11b/CD18-ICAM-1 adherence. J Clin Invest. 1992;90(4):1335-45. Epub 1992/10/01. doi: 10.1172/jci115999. PubMed PMID: 1357003; PMCID: PMC443178.
73. Libby P, Maroko PR, Bloor CM, Sobel BE, Braunwald E. Reduction of Experimental Myocardial Infarct Size by Corticosteroid Administration. Journal of Clinical Investigation. 1973;52(3):599-607. PubMed PMID: PMC302298.
74. Horstick G, Heimann A, Gotze O, Hafner G, Berg O, Bohmer P, Becker P, Darius H, Rupprecht HJ, Loos M, Bhakdi S, Meyer J, Kempski O. Intracoronary application of C1 esterase

inhibitor improves cardiac function and reduces myocardial necrosis in an experimental model of ischemia and reperfusion. Circulation. 1997;95(3):701-8. Epub 1997/02/04. PubMed PMID: 9024160.
75. Riedemann NC, Ward PA. Complement in Ischemia Reperfusion Injury. The American Journal of Pathology. 2003;162(2):363-7. PubMed PMID: PMC1851148.
76. Maroko PR, Carpenter CB, Chiariello M, Fishbein MC, Radvany P, Knostman JD, Hale SL. Reduction by cobra venom factor of myocardial necrosis after coronary artery occlusion. The Journal of clinical investigation. 1978;61(3):661-70. Epub 1978/03/01. doi: 10.1172/jci108978. PubMed PMID: 641147; PMCID: Pmc372579.
77. Shappell SB, Taylor AA, Hughes H, Mitchell JR, Anderson DC, Smith CW. Comparison of antioxidant and nonantioxidant lipoxygenase inhibitors on neutrophil function. Implications for pathogenesis of myocardial reperfusion injury. The Journal of pharmacology and experimental therapeutics. 1990;252(2):531-8. Epub 1990/02/01. PubMed PMID: 2156049.
78. Mullane KM, Read N, Salmon JA, Moncada S. Role of leukocytes in acute myocardial infarction in anesthetized dogs: relationship to myocardial salvage by anti-inflammatory drugs. The Journal of pharmacology and experimental therapeutics. 1984;228(2):510-22. Epub 1984/02/01. PubMed PMID: 6420544.
79. Tanaka M, Brooks SE, Richard VJ, FitzHarris GP, Stoler RC, Jennings RB, Arfors KE, Reimer KA. Effect of anti-CD18 antibody on myocardial neutrophil accumulation and infarct size after ischemia and reperfusion in dogs. Circulation. 1993;87(2):526-35. Epub 1993/02/01. PubMed PMID: 8093866.
80. Zhang RL, Zhang ZG, Chopp M. Increased therapeutic efficacy with rt-PA and anti-CD18 antibody treatment of stroke in the rat. Neurology. 1999;52(2):273-9. Epub 1999/02/05. PubMed PMID: 9932943.
81. Dove A. CD18 trials disappoint again. Nature biotechnology. 2000;18(8):817-8. Epub 2000/08/10. doi: 10.1038/78412. PubMed PMID: 10932141.
82. Land WG. The Role of Damage-Associated Molecular Patterns (DAMPs) in Human Diseases: Part II: DAMPs as diagnostics, prognostics and therapeutics in clinical medicine. Sultan Qaboos University Medical Journal. 2015;15(2):e157-e70. PubMed PMID: PMC4450777.
83. Frangogiannis NG. The inflammatory response in myocardial injury, repair and remodeling. Nature reviews Cardiology. 2014;11(5):255-65. doi: 10.1038/nrcardio.2014.28. PubMed PMID: PMC4407144.
84. Feng Y, Chao W. Toll-like receptors and myocardial inflammation. International journal of inflammation. 2011;2011:170352. Epub 2011/10/07. doi: 10.4061/2011/170352. PubMed PMID: 21977329; PMCID: PMC3182762.
85. Oyama J, Blais C, Jr., Liu X, Pu M, Kobzik L, Kelly RA, Bourcier T. Reduced myocardial ischemia-reperfusion injury in toll-like receptor 4-deficient mice. Circulation. 2004;109(6):784-9. Epub 2004/02/19. doi: 10.1161/01.cir.0000112575.66565.84. PubMed PMID: 14970116.
86. Timmers L, Sluijter JP, van Keulen JK, Hoefer IE, Nederhoff MG, Goumans MJ, Doevendans PA, van Echteld CJ, Joles JA, Quax PH, Piek JJ, Pasterkamp G, de Kleijn DP. Toll-like receptor 4 mediates maladaptive left ventricular remodeling and impairs cardiac function after myocardial infarction. Circ Res. 2008;102(2):257-64. Epub 2007/11/17. doi: 10.1161/circresaha.107.158220. PubMed PMID: 18007026.
87. Kim SC, Ghanem A, Stapel H, Tiemann K, Knuefermann P, Hoeft A, Meyer R, Grohe C, Knowlton AA, Baumgarten G. Toll-like receptor 4 deficiency: smaller infarcts, but no gain in function. BMC physiology. 2007;7:5. Epub 2007/06/27. doi: 10.1186/1472-6793-7-5. PubMed PMID: 17592640; PMCID: PMC1933437.

88. Kawaguchi M, Takahashi M, Hata T, Kashima Y, Usui F, Morimoto H, Izawa A, Takahashi Y, Masumoto J, Koyama J, Hongo M, Noda T, Nakayama J, Sagara J, Taniguchi S, Ikeda U. Inflammasome activation of cardiac fibroblasts is essential for myocardial ischemia/reperfusion injury. Circulation. 2011;123(6):594-604. Epub 2011/02/02. doi: 10.1161/circulationaha.110.982777. PubMed PMID: 21282498.
89. Takahashi M. NLRP3 inflammasome as a novel player in myocardial infarction. International heart journal. 2014;55(2):101-5. Epub 2014/03/19. PubMed PMID: 24632952.
90. Dinarello CA. A clinical perspective of IL-1beta as the gatekeeper of inflammation. European journal of immunology. 2011;41(5):1203-17. Epub 2011/04/28. doi: 10.1002/eji.201141550. PubMed PMID: 21523780.
91. Mezzaroma E, Toldo S, Farkas D, Seropian IM, Van Tassell BW, Salloum FN, Kannan HR, Menna AC, Voelkel NF, Abbate A. The inflammasome promotes adverse cardiac remodeling following acute myocardial infarction in the mouse. Proceedings of the National Academy of Sciences of the United States of America. 2011;108(49):19725-30. Epub 2011/11/23. doi: 10.1073/pnas.1108586108. PubMed PMID: 22106299; PMCID: PMC3241791.
92. Coley WB. The treatment of malignant tumors by repeated inoculations of erysipelas. With a report of ten original cases. 1893. Clinical orthopaedics and related research. 1991(262):3-11. Epub 1991/01/01. PubMed PMID: 1984929.
93. Marx N, Neumann FJ, Ott I, Gawaz M, Koch W, Pinkau T, Schomig A. Induction of cytokine expression in leukocytes in acute myocardial infarction. J Am Coll Cardiol. 1997;30(1):165-70. Epub 1997/07/01. PubMed PMID: 9207638.
94. Finkel MS, Oddis CV, Jacob TD, Watkins SC, Hattler BG, Simmons RL. Negative inotropic effects of cytokines on the heart mediated by nitric oxide. Science (New York, NY). 1992;257(5068):387-9. Epub 1992/07/17. PubMed PMID: 1631560.
95. Solari R. Identification and distribution of two forms of the interleukin 1 receptor. Cytokine. 1990;2(1):21-8. Epub 1990/01/01. PubMed PMID: 2151761.
96. Evans HG, Lewis MJ, Shah AM. Interleukin-1 beta modulates myocardial contraction via dexamethasone sensitive production of nitric oxide. Cardiovasc Res. 1993;27(8):1486-90. Epub 1993/08/01. PubMed PMID: 8221802.
97. Fantuzzi G, Ku G, Harding MW, Livingston DJ, Sipe JD, Kuida K, Flavell RA, Dinarello CA. Response to local inflammation of IL-1 beta-converting enzyme- deficient mice. J Immunol. 1997;158(4):1818-24. Epub 1997/02/15. PubMed PMID: 9029121.
98. Wang X, Feuerstein GZ, Gu JL, Lysko PG, Yue TL. Interleukin-1 beta induces expression of adhesion molecules in human vascular smooth muscle cells and enhances adhesion of leukocytes to smooth muscle cells. Atherosclerosis. 1995;115(1):89-98. Epub 1995/05/01. PubMed PMID: 7545398.
99. Shen Y, Qin J, Bu P. Pathways Involved in Interleukin-1β–Mediated Murine Cardiomyocyte Apoptosis. Texas Heart Institute Journal. 2015;42(2):109-16. doi: 10.14503/THIJ-14-4254. PubMed PMID: PMC4382874.
100. Gabay C. Interleukin-6 and chronic inflammation. Arthritis Research & Therapy. 2006;8(Suppl 2):S3-S. doi: 10.1186/ar1917. PubMed PMID: PMC3226076.
101. Kukielka GL, Smith CW, LaRosa GJ, Manning AM, Mendoza LH, Daly TJ, Hughes BJ, Youker KA, Hawkins HK, Michael LH, et al. Interleukin-8 gene induction in the myocardium after ischemia and reperfusion in vivo. J Clin Invest. 1995;95(1):89-103. Epub 1995/01/01. doi: 10.1172/jci117680. PubMed PMID: 7814650; PMCID: PMC295378.

102. Luscinskas FW, Kiely JM, Ding H, Obin MS, Hebert CA, Baker JB, Gimbrone MA, Jr. In vitro inhibitory effect of IL-8 and other chemoattractants on neutrophil-endothelial adhesive interactions. J Immunol. 1992;149(6):2163-71. Epub 1992/09/25. PubMed PMID: 1381398.
103. Huber AR, Kunkel SL, Todd RF, 3rd, Weiss SJ. Regulation of transendothelial neutrophil migration by endogenous interleukin-8. Science (New York, NY). 1991;254(5028):99-102. Epub 1991/10/04. PubMed PMID: 1718038.
104. Stangl V, Baumann G, Stangl K, Felix SB. Negative inotropic mediators released from the heart after myocardial ischaemia-reperfusion. Cardiovasc Res. 2002;53(1):12-30. Epub 2001/12/18. PubMed PMID: 11744010.
105. Baggiolini M. Chemokines and leukocyte traffic. Nature. 1998;392(6676):565-8. Epub 1998/04/29. doi: 10.1038/33340. PubMed PMID: 9560152.
106. Frangogiannis NG, Entman ML. Chemokines in Myocardial Ischemia. Trends in Cardiovascular Medicine. 2005;15(5):163-9. doi: http://dx.doi.org/10.1016/j.tcm.2005.06.005.
107. Palomino DC, Marti LC. Chemokines and immunity. Einstein (Sao Paulo, Brazil). 2015;13(3):469-73. Epub 2015/10/16. doi: 10.1590/s1679-45082015rb3438. PubMed PMID: 26466066; PMCID: PMC4943798.
108. Zlotnik A, Yoshie O, Nomiyama H. The chemokine and chemokine receptor superfamilies and their molecular evolution. Genome biology. 2006;7(12):243-. doi: 10.1186/gb-2006-7-12-243. PubMed PMID: PMC1794421.
109. Damås JK, Landrø L, Fevang B, Heggelund L, Tjønnfjord GE, Fløisand Y, Halvorsen B, Frøland SS, Aukrust P. Homeostatic chemokines CCL19 and CCL21 promote inflammation in human immunodeficiency virus-infected patients with ongoing viral replication. Clinical and Experimental Immunology. 2009;157(3):400-7. doi: 10.1111/j.1365-2249.2009.03976.x. PubMed PMID: PMC2745035.
110. White FA, Bhangoo SK, Miller RJ. CHEMOKINES: INTEGRATORS OF PAIN AND INFLAMMATION. Nature Reviews Drug Discovery. 2005;4(10):834-44. doi: 10.1038/nrd1852. PubMed PMID: PMC2792904.
111. Chandrasekar B, Smith JB, Freeman GL. Ischemia-reperfusion of rat myocardium activates nuclear factor-KappaB and induces neutrophil infiltration via lipopolysaccharide-induced CXC chemokine. Circulation. 2001;103(18):2296-302. Epub 2001/05/23. PubMed PMID: 11342480.
112. Tarzami ST, Miao W, Mani K, Lopez L, Factor SM, Berman JW, Kitsis RN. Opposing effects mediated by the chemokine receptor CXCR2 on myocardial ischemia-reperfusion injury: recruitment of potentially damaging neutrophils and direct myocardial protection. Circulation. 2003;108(19):2387-92. Epub 2003/10/22. doi: 10.1161/01.cir.0000093192.72099.9a. PubMed PMID: 14568904.
113. Nagasawa T, Hirota S, Tachibana K, Takakura N, Nishikawa S, Kitamura Y, Yoshida N, Kikutani H, Kishimoto T. Defects of B-cell lymphopoiesis and bone-marrow myelopoiesis in mice lacking the CXC chemokine PBSF/SDF-1. Nature. 1996;382(6592):635-8. Epub 1996/08/15. doi: 10.1038/382635a0. PubMed PMID: 8757135.
114. Orlic D, Kajstura J, Chimenti S, Jakoniuk I, Anderson SM, Li B, Pickel J, McKay R, Nadal-Ginard B, Bodine DM, Leri A, Anversa P. Bone marrow cells regenerate infarcted myocardium. Nature. 2001;410(6829):701-5. Epub 2001/04/05. doi: 10.1038/35070587. PubMed PMID: 11287958.
115. Deshmane SL, Kremlev S, Amini S, Sawaya BE. Monocyte Chemoattractant Protein-1 (MCP-1): An Overview. Journal of Interferon & Cytokine Research. 2009;29(6):313-26. doi: 10.1089/jir.2008.0027. PubMed PMID: PMC2755091.

116. Salcedo R, Ponce ML, Young HA, Wasserman K, Ward JM, Kleinman HK, Oppenheim JJ, Murphy WJ. Human endothelial cells express CCR2 and respond to MCP-1: direct role of MCP-1 in angiogenesis and tumor progression. Blood. 2000;96(1):34-40. Epub 2000/07/13. PubMed PMID: 10891427.
117. Kutlar A, Embury SH. Cellular adhesion and the endothelium: P-selectin. Hematology/oncology clinics of North America. 2014;28(2):323-39. Epub 2014/03/05. doi: 10.1016/j.hoc.2013.11.007. PubMed PMID: 24589269.
118. Uguccioni M, D'Apuzzo M, Loetscher M, Dewald B, Baggiolini M. Actions of the chemotactic cytokines MCP-1, MCP-2, MCP-3, RANTES, MIP-1 alpha and MIP-1 beta on human monocytes. European journal of immunology. 1995;25(1):64-8. Epub 1995/01/01. doi: 10.1002/eji.1830250113. PubMed PMID: 7531149.
119. Engler RL. Free radical and granulocyte-mediated injury during myocardial ischemia and reperfusion. The American journal of cardiology. 1989;63(10):19e-23e. Epub 1989/03/07. PubMed PMID: 2538048.
120. Davis BH, Bronspiegel N, Krause PJ, Clark DA. Chemotactic factor induced neutrophil shape changes in whole blood. A comparison of adults and neonates. Annals of clinical and laboratory science. 1985;15(6):495-503. Epub 1985/11/01. PubMed PMID: 4062230.
121. Hong S, Gronert K, Devchand PR, Moussignac RL, Serhan CN. Novel docosatrienes and 17S-resolvins generated from docosahexaenoic acid in murine brain, human blood, and glial cells. Autacoids in anti-inflammation. J Biol Chem. 2003;278(17):14677-87. Epub 2003/02/19. doi: 10.1074/jbc.M300218200. PubMed PMID: 12590139.
122. Nourshargh S, Alon R. Leukocyte Migration into Inflamed Tissues. Immunity. 2014;41(5):694-707. doi: http://dx.doi.org/10.1016/j.immuni.2014.10.008.
123. Smith CW. Leukocyte-endothelial cell interactions. Seminars in hematology. 1993;30(4 Suppl 4):45-53; discussion 4-5. Epub 1993/10/01. PubMed PMID: 8303310.
124. Schimmel L, Heemskerk N, van Buul JD. Leukocyte transendothelial migration: A local affair. Small GTPases. 2017;8(1):1-15. doi: 10.1080/21541248.2016.1197872. PubMed PMID: PMC5331897.
125. Muller WA. Getting Leukocytes to the Site of Inflammation. Veterinary pathology. 2013;50(1):7-22. doi: 10.1177/0300985812469883. PubMed PMID: PMC3628536.
126. Adams DH, Shaw S. Leucocyte-endothelial interactions and regulation of leucocyte migration. Lancet (London, England). 1994;343(8901):831-6. Epub 1994/04/02. PubMed PMID: 7908081.
127. Telen MJ. Cellular adhesion and the endothelium: E-selectin, L-selectin, and pan-selectin inhibitors. Hematology/oncology clinics of North America. 2014;28(2):341-54. Epub 2014/03/05. doi: 10.1016/j.hoc.2013.11.010. PubMed PMID: 24589270.
128. Hafezi-Moghadam A, Thomas KL, Prorock AJ, Huo Y, Ley K. L-Selectin Shedding Regulates Leukocyte Recruitment. The Journal of Experimental Medicine. 2001;193(7):863-72. PubMed PMID: PMC2193368.
129. Ivetic A, Ridley AJ. The telling tail of L-selectin. Biochemical Society transactions. 2004;32(Pt 6):1118-21. Epub 2004/10/28. doi: 10.1042/bst0321118. PubMed PMID: 15506984.
130. Rzeniewicz K, Newe A, Rey Gallardo A, Davies J, Holt MR, Patel A, Charras GT, Stramer B, Molenaar C, Tedder TF, Parsons M, Ivetic A. L-selectin shedding is activated specifically within transmigrating pseudopods of monocytes to regulate cell polarity in vitro. Proceedings of the National Academy of Sciences of the United States of America. 2015;112(12):E1461-70. Epub 2015/03/17. doi: 10.1073/pnas.1417100112. PubMed PMID: 25775539; PMCID: PMC4378423.

131. Levin JD, Ting-Beall HP, Hochmuth RM. Correlating the kinetics of cytokine-induced E-selectin adhesion and expression on endothelial cells. Biophys J. 2001;80(2):656-67. Epub 2001/02/13. doi: 10.1016/s0006-3495(01)76046-8. PubMed PMID: 11159434; PMCID: PMC1301265.
132. Dole VS, Bergmeier W, Mitchell HA, Eichenberger SC, Wagner DD. Activated platelets induce Weibel-Palade–body secretion and leukocyte rolling in vivo: role of P-selectin. Blood. 2005;106(7):2334-9. doi: 10.1182/blood-2005-04-1530. PubMed PMID: PMC1895274.
133. Nomura S, Okamae F, Abe M, Hosokawa M, Yamaoka M, Ohtani T, Onishi S, Matsuzaki T, Teraoka A, Ishida T, Fukuhara S. Platelets expressing P-selectin and platelet-derived microparticles in stored platelet concentrates bind to PSGL-1 on filtrated leukocytes. Clinical and applied thrombosis/hemostasis : official journal of the International Academy of Clinical and Applied Thrombosis/Hemostasis. 2000;6(4):213-21. Epub 2000/10/13. PubMed PMID: 11030527.
134. Frankhauser P, Baranyai R, Ahrens T, Schloss P, Deuschle M, Lederbogen F. Platelet surface P-selectin expression is highly correlated with serotonin transporter density in human subjects. Thrombosis and haemostasis. 2008;100(6):1201-3. Epub 2009/01/10. PubMed PMID: 19132251.
135. Suzuki J, Hamada E, Shodai T, Kamoshida G, Kudo S, Itoh S, Koike J, Nagata K, Irimura T, Tsuji T. Cytokine secretion from human monocytes potentiated by P-selectin-mediated cell adhesion. International archives of allergy and immunology. 2013;160(2):152-60. Epub 2012/09/29. doi: 10.1159/000339857. PubMed PMID: 23018521.
136. Jutila MA, Rott L, Berg EL, Butcher EC. Function and regulation of the neutrophil MEL-14 antigen in vivo: comparison with LFA-1 and MAC-1. Journal of immunology (Baltimore, Md : 1950). 1989;143(10):3318-24. Epub 1989/11/15. PubMed PMID: 2553811.
137. Arbones ML, Ord DC, Ley K, Ratech H, Maynard-Curry C, Otten G, Capon DJ, Tedder TF. Lymphocyte homing and leukocyte rolling and migration are impaired in L-selectin-deficient mice. Immunity. 1994;1(4):247-60. Epub 1994/07/01. PubMed PMID: 7534203.
138. Mayadas TN, Johnson RC, Rayburn H, Hynes RO, Wagner DD. Leukocyte rolling and extravasation are severely compromised in P selectin-deficient mice. Cell. 1993;74(3):541-54. Epub 1993/08/13. PubMed PMID: 7688665.
139. Labow MA, Norton CR, Rumberger JM, Lombard-Gillooly KM, Shuster DJ, Hubbard J, Bertko R, Knaack PA, Terry RW, Harbison ML, et al. Characterization of E-selectin-deficient mice: demonstration of overlapping function of the endothelial selectins. Immunity. 1994;1(8):709-20. Epub 1994/11/01. PubMed PMID: 7541306.
140. Arai M, Masui Y, Goldschmidt-Clermont P, DiPaula A, Siu C, Kondo T, Becker LC. P-selectin inhibition prevents early neutrophil activation but provides only modest protection against myocardial injury in dogs with ischemia and forty-eight hours reperfusion. J Am Coll Cardiol. 1999;34(1):280-8. Epub 1999/07/10. PubMed PMID: 10400022.
141. Palazzo AJ, Jones SP, Anderson DC, Granger DN, Lefer DJ. Coronary endothelial P-selectin in pathogenesis of myocardial ischemia-reperfusion injury. The American journal of physiology. 1998;275(5 Pt 2):H1865-72. Epub 1998/11/14. PubMed PMID: 9815095.
142. Eniola AO, Willcox PJ, Hammer DA. Interplay between Rolling and Firm Adhesion Elucidated with a Cell-Free System Engineered with Two Distinct Receptor-Ligand Pairs. Biophysical Journal. 2003;85(4):2720-31. PubMed PMID: PMC1303496.
143. Luscinskas FW, Lawler J. Integrins as dynamic regulators of vascular function. FASEB journal : official publication of the Federation of American Societies for Experimental Biology. 1994;8(12):929-38. Epub 1994/09/01. PubMed PMID: 7522194.

144. Arai M, Lefer DJ, So T, DiPaula A, Aversano T, Becker LC. An anti-CD18 antibody limits infarct size and preserves left ventricular function in dogs with ischemia and 48-hour reperfusion. J Am Coll Cardiol. 1996;27(5):1278-85. Epub 1996/04/01. PubMed PMID: 8609356.
145. Baran KW, Nguyen M, McKendall GR, Lambrew CT, Dykstra G, Palmeri ST, Gibbons RJ, Borzak S, Sobel BE, Gourlay SG, Rundle AC, Gibson CM, Barron HV. Double-blind, randomized trial of an anti-CD18 antibody in conjunction with recombinant tissue plasminogen activator for acute myocardial infarction: limitation of myocardial infarction following thrombolysis in acute myocardial infarction (LIMIT AMI) study. Circulation. 2001;104(23):2778-83. Epub 2001/12/06. PubMed PMID: 11733394.
146. Simpson PJ, Todd RF, 3rd, Fantone JC, Mickelson JK, Griffin JD, Lucchesi BR. Reduction of experimental canine myocardial reperfusion injury by a monoclonal antibody (anti-Mo1, anti-CD11b) that inhibits leukocyte adhesion. The Journal of clinical investigation. 1988;81(2):624-9. Epub 1988/02/01. doi: 10.1172/jci113364. PubMed PMID: 3339135; PMCID: Pmc329614.
147. Palazzo AJ, Jones SP, Girod WG, Anderson DC, Granger DN, Lefer DJ. Myocardial ischemia-reperfusion injury in CD18- and ICAM-1-deficient mice. The American journal of physiology. 1998;275(6 Pt 2):H2300-7. Epub 1998/12/09. PubMed PMID: 9843832.
148. Jaeschke H, Smith CW. Mechanisms of neutrophil-induced parenchymal cell injury. Journal of leukocyte biology. 1997;61(6):647-53. Epub 1997/06/01. PubMed PMID: 9201255.
149. Youker K, Smith CW, Anderson DC, Miller D, Michael LH, Rossen RD, Entman ML. Neutrophil adherence to isolated adult cardiac myocytes. Induction by cardiac lymph collected during ischemia and reperfusion. Journal of Clinical Investigation. 1992;89(2):602-9. PubMed PMID: PMC442893.
150. Albelda SM, Smith CW, Ward PA. Adhesion molecules and inflammatory injury. FASEB journal : official publication of the Federation of American Societies for Experimental Biology. 1994;8(8):504-12. Epub 1994/05/01. PubMed PMID: 8181668.
151. Hubbard AK, Rothlein R. Intercellular adhesion molecule-1 (ICAM-1) expression and cell signaling cascades. Free radical biology & medicine. 2000;28(9):1379-86. Epub 2000/08/05. PubMed PMID: 10924857.
152. Davani EY, Boyd JH, Dorscheid DR, Wang Y, Meredith A, Chau E, Singhera GK, Walley KR. Cardiac ICAM-1 mediates leukocyte-dependent decreased ventricular contractility in endotoxemic mice. Cardiovasc Res. 2006;72(1):134-42. Epub 2006/08/29. doi: 10.1016/j.cardiores.2006.06.029. PubMed PMID: 16934241.
153. Entman ML, Youker K, Shappell SB, Siegel C, Rothlein R, Dreyer WJ, Schmalstieg FC, Smith CW. Neutrophil adherence to isolated adult canine myocytes. Evidence for a CD18-dependent mechanism. J Clin Invest. 1990;85(5):1497-506. Epub 1990/05/01. doi: 10.1172/jci114596. PubMed PMID: 1970581; PMCID: PMC296597.
154. Nicolls MR, Gill RG. LFA-1 (CD11a) as a therapeutic target. American journal of transplantation : official journal of the American Society of Transplantation and the American Society of Transplant Surgeons. 2006;6(1):27-36. Epub 2006/01/26. doi: 10.1111/j.1600-6143.2005.01158.x. PubMed PMID: 16433753.
155. Mugge A, Heistad DD, Padgett RC, Waack BJ, Densen P, Lopez JA. Mechanisms of contraction induced by human leukocytes in normal and atherosclerotic arteries. Circulation research. 1991;69(3):871-80. Epub 1991/09/01. PubMed PMID: 1873879.
156. Puente XS, Sanchez LM, Gutierrez-Fernandez A, Velasco G, Lopez-Otin C. A genomic view of the complexity of mammalian proteolytic systems. Biochemical Society transactions. 2005;33(Pt 2):331-4. Epub 2005/03/25. doi: 10.1042/bst0330331. PubMed PMID: 15787599.

157. Puente XS, Lopez-Otin C. A genomic analysis of rat proteases and protease inhibitors. Genome research. 2004;14(4):609-22. Epub 2004/04/03. doi: 10.1101/gr.1946304. PubMed PMID: 15060002; PMCID: Pmc383305.
158. Pham CT. Neutrophil serine proteases fine-tune the inflammatory response. The international journal of biochemistry & cell biology. 2008;40(6-7):1317-33. Epub 2008/01/09. doi: 10.1016/j.biocel.2007.11.008. PubMed PMID: 18180196; PMCID: PMC2440796.
159. Henry CM, Sullivan GP, Clancy DM, Afonina IS, Kulms D, Martin SJ. Neutrophil-Derived Proteases Escalate Inflammation through Activation of IL-36 Family Cytokines. Cell reports. 2016;14(4):708-22. Epub 2016/01/19. doi: 10.1016/j.celrep.2015.12.072. PubMed PMID: 26776523.
160. Afonina IS, Muller C, Martin SJ, Beyaert R. Proteolytic Processing of Interleukin-1 Family Cytokines: Variations on a Common Theme. Immunity. 2015;42(6):991-1004. Epub 2015/06/18. doi: 10.1016/j.immuni.2015.06.003. PubMed PMID: 26084020.
161. Soh UJK, Dores MR, Chen B, Trejo J. Signal transduction by protease-activated receptors. British Journal of Pharmacology. 2010;160(2):191-203. doi: 10.1111/j.1476-5381.2010.00705.x. PubMed PMID: PMC2874842.
162. Leger AJ, Covic L, Kuliopulos A. Protease-activated receptors in cardiovascular diseases. Circulation. 2006;114(10):1070-7. Epub 2006/09/06. doi: 10.1161/circulationaha.105.574830. PubMed PMID: 16952995.
163. Antoniak S, Pawlinski R, Mackman N. Protease-activated Receptors and Myocardial Infarction. IUBMB life. 2011;63(6):383-9. doi: 10.1002/iub.441. PubMed PMID: PMC3121912.
164. Wettschureck N, Offermanns S. Mammalian G proteins and their cell type specific functions. Physiological reviews. 2005;85(4):1159-204. Epub 2005/09/27. doi: 10.1152/physrev.00003.2005. PubMed PMID: 16183910.
165. Minami T, Sugiyama A, Wu SQ, Abid R, Kodama T, Aird WC. Thrombin and phenotypic modulation of the endothelium. Arterioscler Thromb Vasc Biol. 2004;24(1):41-53. Epub 2003/10/11. doi: 10.1161/01.atv.0000099880.09014.7d. PubMed PMID: 14551154.
166. Hansen KK, Oikonomopoulou K, Li Y, Hollenberg MD. Proteinases, proteinase-activated receptors (PARs) and the pathophysiology of cancer and diseases of the cardiovascular, musculoskeletal, nervous and gastrointestinal systems. Naunyn-Schmiedeberg's archives of pharmacology. 2008;377(4-6):377-92. Epub 2007/10/24. doi: 10.1007/s00210-007-0194-2. PubMed PMID: 17952408.
167. Fujie K, Shinguh Y, Inamura N, Yasumitsu R, Okamoto M, Okuhara M. Release of neutrophil elastase and its role in tissue injury in acute inflammation: effect of the elastase inhibitor, FR134043. Eur J Pharmacol. 1999;374(1):117-25. Epub 1999/07/28. PubMed PMID: 10422648.
168. Tissue destruction by neutrophils. New England Journal of Medicine. 1989;321(5):327-9. Epub 1989/08/03. doi: 10.1056/nejm198908033210513. PubMed PMID: 2747775.
169. Carden D, Xiao F, Moak C, Willis BH, Robinson-Jackson S, Alexander S. Neutrophil elastase promotes lung microvascular injury and proteolysis of endothelial cadherins. The American journal of physiology. 1998;275(2 Pt 2):H385-92. Epub 1998/07/31. PubMed PMID: 9683424.
170. Walsh DE, Greene CM, Carroll TP, Taggart CC, Gallagher PM, O'Neill SJ, McElvaney NG. Interleukin-8 up-regulation by neutrophil elastase is mediated by MyD88/IRAK/TRAF-6 in human bronchial epithelium. J Biol Chem. 2001;276(38):35494-9. Epub 2001/07/20. doi: 10.1074/jbc.M103543200. PubMed PMID: 11461907.

171. Benabid R, Wartelle J, Malleret L, Guyot N, Gangloff S, Lebargy F, Belaaouaj A. Neutrophil elastase modulates cytokine expression: contribution to host defense against Pseudomonas aeruginosa-induced pneumonia. J Biol Chem. 2012;287(42):34883-94. Epub 2012/08/29. doi: 10.1074/jbc.M112.361352. PubMed PMID: 22927440; PMCID: PMC3471768.
172. Campbell EJ, Senior RM, McDonald JA, Cox DL. Proteolysis by neutrophils. Relative importance of cell-substrate contact and oxidative inactivation of proteinase inhibitors in vitro. The Journal of clinical investigation. 1982;70(4):845-52. Epub 1982/10/01. PubMed PMID: 6181097; PMCID: Pmc370293.
173. Zimmerman BJ, Granger DN. Reperfusion-induced leukocyte infiltration: role of elastase. The American journal of physiology. 1990;259(2 Pt 2):H390-4. Epub 1990/08/01. PubMed PMID: 2167021.
174. Owen CA, Campbell EJ. The cell biology of leukocyte-mediated proteolysis. Journal of leukocyte biology. 1999;65(2):137-50. Epub 1999/03/24. PubMed PMID: 10088596.
175. Burster T, Macmillan H, Hou T, Boehm BO, Mellins ED. Cathepsin G: roles in antigen presentation and beyond. Molecular immunology. 2010;47(4):658-65. doi: 10.1016/j.molimm.2009.10.003. PubMed PMID: PMC4159238.
176. Chertov O, Ueda H, Xu LL, Tani K, Murphy WJ, Wang JM, Howard OM, Sayers TJ, Oppenheim JJ. Identification of human neutrophil-derived cathepsin G and azurocidin/CAP37 as chemoattractants for mononuclear cells and neutrophils. J Exp Med. 1997;186(5):739-47. Epub 1997/08/29. PubMed PMID: 9271589; PMCID: PMC2199011.
177. Sambrano GR, Huang W, Faruqi T, Mahrus S, Craik C, Coughlin SR. Cathepsin G activates protease-activated receptor-4 in human platelets. The Journal of biological chemistry. 2000;275(10):6819-23. Epub 2000/03/04. PubMed PMID: 10702240.
178. Ortiz-Munoz G, Houard X, Martin-Ventura JL, Ishida BY, Loyau S, Rossignol P, Moreno JA, Kane JP, Chalkley RJ, Burlingame AL, Michel JB, Meilhac O. HDL antielastase activity prevents smooth muscle cell anoikis, a potential new antiatherogenic property. FASEB journal : official publication of the Federation of American Societies for Experimental Biology. 2009;23(9):3129-39. Epub 2009/05/07. doi: 10.1096/fj.08-127928. PubMed PMID: 19417089; PMCID: Pmc2735359.
179. Okada Y, Nakanishi I. Activation of matrix metalloproteinase 3 (stromelysin) and matrix metalloproteinase 2 ('gelatinase') by human neutrophil elastase and cathepsin G. FEBS letters. 1989;249(2):353-6. Epub 1989/06/05. PubMed PMID: 2544455.
180. Rollo EE, Hymowitz M, Schmidt CE, Montana S, Foda H, Zucker S. Neutrophil activator of matrix metalloproteinase-2 (NAM). Clinical & experimental metastasis. 2006;23(5-6):259-68. Epub 2006/11/07. doi: 10.1007/s10585-006-9035-9. PubMed PMID: 17086359.
181. Rafiq K, Hanscom M, Valerie K, Steinberg S, Sabri A. Novel mode for neutrophil protease cathepsin G-mediated signaling: Membrane shedding of epidermal grwoth factor is required for cardiomyocyte anoikis. Circ Res. 2008;102(1):32-41.
182. Omura T, Yoshiyama M, Kim S, Matsumoto R, Nakamura Y, Izumi Y, Ichijo H, Sudo T, Akioka K, Iwao H, Takeuchi K, Yoshikawa J. Involvement of apoptosis signal-regulating kinase-1 on angiotensin II-induced monocyte chemoattractant protein-1 expression. Arterioscler Thromb Vasc Biol. 2004;24(2):270-5. Epub 2003/12/20. doi: 10.1161/01.atv.0000112930.40564.89. PubMed PMID: 14684425.
183. Pintucci G, Iacoviello L, Castelli MP, Amore C, Evangelista V, Cerletti C, Donati MB. Cathepsin G--induced release of PAI-1 in the culture medium of endothelial cells: a new thrombogenic role for polymorphonuclear leukocytes? The Journal of laboratory and clinical medicine. 1993;122(1):69-79. Epub 1993/07/01. PubMed PMID: 8320493.

184. Shimoda N, Fukazawa N, Nonomura K, Fairchild RL. Cathepsin g is required for sustained inflammation and tissue injury after reperfusion of ischemic kidneys. The American journal of pathology. 2007;170(3):930-40. Epub 2007/02/27. doi: 10.2353/ajpath.2007.060486. PubMed PMID: 17322378; PMCID: Pmc1864870.
185. MacIvor DM, Shapiro SD, Pham CT, Belaaouaj A, Abraham SN, Ley TJ. Normal neutrophil function in cathepsin G-deficient mice. Blood. 1999;94(12):4282-93. Epub 1999/12/10. PubMed PMID: 10590073.
186. Abbott RE, Corral CJ, MacIvor DM, Lin X, Ley TJ, Mustoe TA. Augmented inflammatory responses and altered wound healing in cathepsin G-deficient mice. Archives of surgery (Chicago, Ill : 1960). 1998;133(9):1002-6. Epub 1998/09/28. PubMed PMID: 9749856.
187. Shimoda N, Fukazawa N, Nonomura K, Fairchild RL. Cathepsin G Is Required for Sustained Inflammation and Tissue Injury after Reperfusion of Ischemic Kidneys. The American Journal of Pathology. 2007;170(3):930-40. doi: 10.2353/ajpath.2007.060486. PubMed PMID: PMC1864870.
188. Pham CT. Neutrophil serine proteases: specific regulators of inflammation. Nature reviews Immunology. 2006;6(7):541-50. Epub 2006/06/27. doi: 10.1038/nri1841. PubMed PMID: 16799473.
189. Mayet WJ, Csernok E, Szymkowiak C, Gross WL, Meyer zum Buschenfelde KH. Human endothelial cells express proteinase 3, the target antigen of anticytoplasmic antibodies in Wegener's granulomatosis. Blood. 1993;82(4):1221-9. Epub 1993/08/15. PubMed PMID: 8353286.
190. Pendergraft WF, 3rd, Rudolph EH, Falk RJ, Jahn JE, Grimmler M, Hengst L, Jennette JC, Preston GA. Proteinase 3 sidesteps caspases and cleaves p21(Waf1/Cip1/Sdi1) to induce endothelial cell apoptosis. Kidney international. 2004;65(1):75-84. Epub 2003/12/17. doi: 10.1111/j.1523-1755.2004.00364.x. PubMed PMID: 14675038.
191. Coeshott C, Ohnemus C, Pilyavskaya A, Ross S, Wieczorek M, Kroona H, Leimer AH, Cheronis J. Converting enzyme-independent release of tumor necrosis factor alpha and IL-1beta from a stimulated human monocytic cell line in the presence of activated neutrophils or purified proteinase 3. Proceedings of the National Academy of Sciences of the United States of America. 1999;96(11):6261-6. Epub 1999/05/26. PubMed PMID: 10339575; PMCID: PMC26869.
192. Ramaha A, Patston PA. Release and degradation of angiotensin I and angiotensin II from angiotensinogen by neutrophil serine proteinases. Archives of biochemistry and biophysics. 2002;397(1):77-83. Epub 2001/12/19. doi: 10.1006/abbi.2001.2687. PubMed PMID: 11747312.
193. Ng Leong L, Khan Sohail Q, Narayan H, Quinn P, Squire Iain B, Davies Joan E. Proteinase 3 and prognosis of patients with acute myocardial infarction. Clinical Science (London, England : 1979). 2011;120(Pt 6):231-8. doi: 10.1042/CS20100366. PubMed PMID: PMC2999885.
194. da Silva EZM, Jamur MC, Oliver C. Mast Cell Function: A New Vision of an Old Cell. Journal of Histochemistry and Cytochemistry. 2014;62(10):698-738. doi: 10.1369/0022155414545334. PubMed PMID: PMC4230976.
195. Frangogiannis NG, Perrard JL, Mendoza LH, Burns AR, Lindsey ML, Ballantyne CM, Michael LH, Smith CW, Entman ML. Stem cell factor induction is associated with mast cell accumulation after canine myocardial ischemia and reperfusion. Circulation. 1998;98(7):687-98. Epub 1998/08/26. PubMed PMID: 9715862.
196. Urb M, Sheppard DC. The Role of Mast Cells in the Defence against Pathogens. PLoS Pathogens. 2012;8(4):e1002619. doi: 10.1371/journal.ppat.1002619. PubMed PMID: PMC3343118.

197. Metcalfe DD, Baram D, Mekori YA. Mast cells. Physiological reviews. 1997;77(4):1033-79. Epub 1997/11/14. PubMed PMID: 9354811.
198. Fang KC, Wolters PJ, Steinhoff M, Bidgol A, Blount JL, Caughey GH. Mast cell expression of gelatinases A and B is regulated by kit ligand and TGF-beta. Journal of immunology (Baltimore, Md : 1950). 1999;162(9):5528-35. Epub 1999/05/05. PubMed PMID: 10228034.
199. Katunuma N, Kido H. Biological functions of serine proteases in mast cells in allergic inflammation. Journal of cellular biochemistry. 1988;38(4):291-301. Epub 1988/12/01. doi: 10.1002/jcb.240380408. PubMed PMID: 2467915.
200. Pejler G, Ronnberg E, Waern I, Wernersson S. Mast cell proteases: multifaceted regulators of inflammatory disease. Blood. 2010;115(24):4981-90. Epub 2010/03/18. doi: 10.1182/blood-2010-01-257287. PubMed PMID: 20233968.
201. Laine P, Kaartinen M, Penttila A, Panula P, Paavonen T, Kovanen PT. Association between myocardial infarction and the mast cells in the adventitia of the infarct-related coronary artery. Circulation. 1999;99(3):361-9. Epub 1999/01/26. PubMed PMID: 9918522.
202. Steinhoff M, Corvera CU, Thoma MS, Kong W, McAlpine BE, Caughey GH, Ansel JC, Bunnett NW. Proteinase-activated receptor-2 in human skin: tissue distribution and activation of keratinocytes by mast cell tryptase. Experimental dermatology. 1999;8(4):282-94. Epub 1999/08/10. PubMed PMID: 10439226.
203. Berger P, Perng DW, Thabrew H, Compton SJ, Cairns JA, McEuen AR, Marthan R, Tunon De Lara JM, Walls AF. Tryptase and agonists of PAR-2 induce the proliferation of human airway smooth muscle cells. Journal of applied physiology (Bethesda, Md : 1985). 2001;91(3):1372-9. Epub 2001/08/18. PubMed PMID: 11509538.
204. Stack MS, Johnson DA. Human mast cell tryptase activates single-chain urinary-type plasminogen activator (pro-urokinase). The Journal of biological chemistry. 1994;269(13):9416-9. Epub 1994/04/01. PubMed PMID: 8144524.
205. Taipale J, Lohi J, Saarinen J, Kovanen PT, Keski-Oja J. Human mast cell chymase and leukocyte elastase release latent transforming growth factor-beta 1 from the extracellular matrix of cultured human epithelial and endothelial cells. The Journal of biological chemistry. 1995;270(9):4689-96. Epub 1995/03/03. PubMed PMID: 7876240.
206. Dell'Italia LJ, Husain A. Dissecting the role of chymase in angiotensin II formation and heart and blood vessel diseases. Current opinion in cardiology. 2002;17(4):374-9. Epub 2002/08/02. PubMed PMID: 12151872.
207. Tchougounova E, Lundequist A, Fajardo I, Winberg J-O, Åbrink M, Pejler G. A key role for mast cell chymase in the activation of pro-matrix metalloprotease-9 and pro-matrix metalloprotease-2. J Biol Chem. 2005;280(10):9291-6. doi: 10.1074/jbc.M410396200.
208. Zheng J, Wei CC, Hase N, Shi K, Killingsworth CR, Litovsky SH, Powell PC, Kobayashi T, Ferrario CM, Rab A, Aban I, Collawn JF, Dell'Italia LJ. Chymase mediates injury and mitochondrial damage in cardiomyocytes during acute ischemia/reperfusion in the dog. PLoS One. 2014;9(4):e94732. Epub 2014/04/16. doi: 10.1371/journal.pone.0094732. PubMed PMID: 24733352; PMCID: PMC3986229.
209. Hoshino F, Urata H, Inoue Y, Saito Y, Yahiro E, Ideishi M, Arakawa K, Saku K. Chymase inhibitor improves survival in hamsters with myocardial infarction. Journal of cardiovascular pharmacology. 2003;41 Suppl 1:S11-8. Epub 2003/04/12. PubMed PMID: 12688390.
210. Oyamada S, Bianchi C, Takai S, Chu LM, Sellke FW. Chymase Inhibition Reduces Infarction and Matrix Metalloproteinase-9 Activation and Attenuates Inflammation and Fibrosis after Acute Myocardial Ischemia/Reperfusion. J Pharmacol Exp Ther. 2011;339(1):143-51. doi: 10.1124/jpet.111.179697.

211. Jin D, Takai S, Sakaguchi M, Okamoto Y, Muramatsu M, Miyazaki M. An Antiarrhythmic Effect of a Chymase Inhibitor after Myocardial Infarction. Journal of Pharmacology and Experimental Therapeutics. 2004;309(2):490-7. doi: 10.1124/jpet.103.061465.
212. Blancke F, J. Claeys M, Jorens P, Vermeiren G, Bosmans J, L. Wuyts F, J. Vrints C. Systemic Inflammation and Reperfusion Injury in Patients With Acute Myocardial Infarction. Mediators of Inflammation. 2005;2005(6):385-9. doi: 10.1155/MI.2005.385. PubMed PMID: PMC1533902.
213. Frangogiannis NG, Mendoza LH, Ren G, Akrivakis S, Jackson PL, Michael LH, Smith CW, Entman ML. MCSF expression is induced in healing myocardial infarcts and may regulate monocyte and endothelial cell phenotype. American journal of physiology Heart and circulatory physiology. 2003;285(2):H483-92. Epub 2003/04/12. doi: 10.1152/ajpheart.01016.2002. PubMed PMID: 12689859.
214. Savill JS, Wyllie AH, Henson JE, Walport MJ, Henson PM, Haslett C. Macrophage phagocytosis of aging neutrophils in inflammation. Programmed cell death in the neutrophil leads to its recognition by macrophages. J Clin Invest. 1989;83(3):865-75. Epub 1989/03/01. doi: 10.1172/jci113970. PubMed PMID: 2921324; PMCID: PMC303760.
215. Nucera S, Biziato D, De Palma M. The interplay between macrophages and angiogenesis in development, tissue injury and regeneration. The International journal of developmental biology. 2011;55(4-5):495-503. Epub 2011/07/07. doi: 10.1387/ijdb.103227sn. PubMed PMID: 21732273.
216. Qian BZ, Pollard JW. Macrophage diversity enhances tumor progression and metastasis. Cell. 2010;141(1):39-51. Epub 2010/04/08. doi: 10.1016/j.cell.2010.03.014. PubMed PMID: 20371344; PMCID: PMC4994190.
217. Lepidi S, Kenagy RD, Raines EW, Chiu ES, Chait A, Ross R, Clowes AW. MMP9 production by human monocyte-derived macrophages is decreased on polymerized type I collagen. Journal of vascular surgery. 2001;34(6):1111-8. Epub 2001/12/18. doi: 10.1067/mva.2001.119401. PubMed PMID: 11743569.
218. Fox S, Leitch AE, Duffin R, Haslett C, Rossi AG. Neutrophil Apoptosis: Relevance to the Innate Immune Response and Inflammatory Disease. Journal of Innate Immunity. 2010;2(3):216-27. doi: 10.1159/000284367. PubMed PMID: PMC2956014.
219. Walker A, Ward C, Taylor EL, Dransfield I, Hart SP, Haslett C, Rossi AG. Regulation of neutrophil apoptosis and removal of apoptotic cells. Current drug targets Inflammation and allergy. 2005;4(4):447-54. Epub 2005/08/17. PubMed PMID: 16101521.
220. Hawkins LA, Devitt A. Current Understanding of the Mechanisms for Clearance of Apoptotic Cells—A Fine Balance. Journal of Cell Death. 2013;6:57-68. doi: 10.4137/JCD.S11037. PubMed PMID: PMC4147779.
221. Sanjabi S, Zenewicz LA, Kamanaka M, Flavell RA. Anti- and Pro-inflammatory Roles of TGF-β, IL-10, and IL-22 In Immunity and Autoimmunity. Current opinion in pharmacology. 2009;9(4):447-53. doi: 10.1016/j.coph.2009.04.008. PubMed PMID: PMC2755239.
222. Barbay V, Houssari M, Mekki M, Banquet S, Edwards-Levy F, Henry JP, Dumesnil A, Adriouch S, Thuillez C, Richard V, Brakenhielm E. Role of M2-like macrophage recruitment during angiogenic growth factor therapy. Angiogenesis. 2015;18(2):191-200. Epub 2014/12/30. doi: 10.1007/s10456-014-9456-z. PubMed PMID: 25537851.
223. Murphy E, Steenbergen C. Mechanisms underlying acute protection from cardiac ischemia-reperfusion injury. Physiological Reviews. 2008;88(2):581-609.
224. Vander Heide RS, Steenbergen C. Cardioprotection and myocardial reperfusion: Pitfalls to Clinical Application. Circ Res. 2013;113(4):464-77. doi: 10.1161/circresaha.113.300765.

225. Frangogiannis NG. Regulation of the inflammatory response in cardiac repair. Circ Res. 2012;110(1):159-73.
226. Levick SP, Meléndez GC, Plante E, McLarty JL, Brower GL, Janicki JS. Cardiac mast cells: the centrepiece in adverse myocardial remodelling. Cardiovasc Res. 2011;89(1):12-9. doi: 10.1093/cvr/cvq272.
227. Heutinck K, ten Berge I, Hack C, Hamann J, Rowshani A. Serine proteases of the human immune system in health and disease. Mol Immunol. 2010;47(11-12):1943-55.
228. Meyer-Hoffert U, Wiedow O. Neutrophil serine proteases: mediators of innate immune responses. Curr Opin Hematol. 2011;18(1):19-24. doi: 10.1097/MOH.0b013e32834115d1. PubMed PMID: 00062752-201101000-00004.
229. Caughey GH. Mast cell proteases as pharmacological targets. Eur J Pharmacol. 2016;778:44-55. doi: http://dx.doi.org/10.1016/j.ejphar.2015.04.045.
230. Sabri A, Alcott SG, Elouardighi H, Pak E, Derian C, Andrade-Gordon P, Kinnally K, Steinberg SF. Neutrophil cathepsin G promotes detachment-induced cardiomyocyte apoptosis via a protease-activated receptor-independent mechanism. J Biol Chem. 2003;278(26):23944-54.
231. Rafiq K, Kolpakov MA, Abdelfettah M, Streblow DN, Hassid A, Dell'Italia LJ, Sabri A. Role of protein-tyrosine phosphatase SHP2 in focal adhesion kinase down-regulation during neutrophil cathepsin G-induced cardiomyocytes anoikis. J Biol Chem. 2006;281(28):19781-92.
232. Pat B, Chen Y, Killingsworth C, Gladden JD, Shi K, Zheng J, Powell PC, Walcott G, Ahmed MI, Gupta H, Desai R, Wei C-C, Hase N, Kobayashi T, Sabri A, Granzier H, Denney T, Tillson M, Dillon AR, Husain A, Dell'Italia LJ. Chymase inhibition prevents fibronectin and myofibrillar loss and improves cardiomyocyte function and LV torsion angle in dogs with isolated mitral regurgitation. Circulation. 2010;122(15):1488-95. doi: 10.1161/circulationaha.109.921619.
233. Iacoviello L, Kolpakov V, Salvatore L, Amore C, Pintucci G, de Gaetano G, Donati MB. Human endothelial cell damage by neutrophil-derived cathepsin G. Role of cytoskeleton rearrangement and matrix-bound plasminogen activator inhibitor-1. Arterioscler Thromb Vasc Biol. 1995;15(11):2037-46.
234. Hara M, Matsumori A, Ono K, Kido H, Hwang M-W, Miyamoto T, Iwasaki A, Okada M, Nakatani K, Sasayama S. Mast cells cause apoptosis of cardiomyocytes and proliferation of other intramyocardial cells in vitro. Circulation. 1999;100(13):1443-9. doi: 10.1161/01.cir.100.13.1443.
235. Fu L, Wei C-C, Powell PC, Bradley WE, Ahmad S, Ferrario CM, Collawn JF, Dell'Italia LJ. Increased fibroblast chymase production mediates procollagen autophagic digestion in volume overload. J Mol Cell Cardiol.92:1-9. doi: 10.1016/j.yjmcc.2016.01.019.
236. Maryanoff BE, Garavilla Ld, Greco MN, Haertlein BJ, Wells GI, Andrade-Gordon P, Abraham WM. Dual inhibition of cathepsin G and chymase is effective in animal models of pulmonary inflammation. Am J Resp Crit Care Med. 2010;181(3):247-53. doi: 10.1164/rccm.200904-0627OC. PubMed PMID: 19875688.
237. Kukielka GL, Smith CW, Manning AM, Youker KA, Michael LH, Entman ML. Induction of interleukin-6 synthesis in the myocardium: Potential role in postreperfusion inflammatory injury. Circulation. 1995;92(7):1866-75.
238. Hwang M-W, Matsumori A, Furukawa Y, Ono K, Okada M, Iwasaki A, Hara M, Miyamoto T, Touma M, Sasayama S. Neutralization of interleukin-1b in the acute phase of myocardial infarction promotes the progression of left ventricular remodeling. J Am Coll Cardiol. 2001;38(5):1546-53.
239. van den Borne SWM, Diez J, Blankesteijn WM, Verjans J, Hofstra L, Narula J. Myocardial remodeling after infarction: the role of myofibroblasts. Nat Rev Cardiol. 2010;7(1):30-7.

240. Scapini P, Lapinet-Vera JA, Gasperini S, Calzetti F, Bazzoni F, Cassatella MA. The neutrophil as a cellular source of chemokines. Immunol Rev. 2000;177(1):195-203. doi: 10.1034/j.1600-065X.2000.17706.x.
241. Beghdadi W, Madjene LC, Benhamou M, Charles N, Gautier G, Launay P, Blank U. Mast cells as cellular sensors in inflammation and immunity. Front Immunol. 2011;2:37. doi: 10.3389/fimmu.2011.00037. PubMed PMID: PMC3342044.
242. Nicholls SJ, Hazen SL. Myeloperoxidase and cardiovascular disease. Arter Thromb Vasc Biol. 2005;25(6):1102-11. doi: 10.1161/01.ATV.0000163262.83456.6d.
243. Krijnen PAJ, Nijmeijer R, Meijer CJLM, Visser CA, Hack CE, Niessen HWM. Apoptosis in myocardial ischaemia and infarction. J Clin Pathol. 2002;55(11):801-11. PubMed PMID: PMC1769793.
244. Early redistribution of plasma membrane phosphatidylserine is a general feature of apoptosis regardless of the initiating stimulus: inhibition by overexpression of Bcl-2 and Abl. J Exp Med. 1995;182(5):1545-56. PubMed PMID: PMC2192182.
245. Lindstedt KA, Wang Y, Shiota N, Saatinen J, Hyytiainen M, Kokkonen JO, Keski-Oja J, Kovanen PT. Activation of paracrine TGF-β1 signaling upon stimulation and degranulation of rat serosal mast cells: a novel function for chymase. FASEB J. 2001;15(8):1377-88. doi: 10.1096/fj.00-0273com.
246. Wilson TJ, Nannuru KC, Singh RK. Cathepsin G–mediated Activation of pro–matrix metalloproteinase 9 at the tumor-bone interface promotes transforming growth factor-β signaling and bone destruction. Mol Caner Res. 2009;7(8):1224-33. doi: 10.1158/1541-7786.mcr-09-0028.
247. Zhao X-Y, Zhao L-Y, Zheng Q-S, Su J-L, Guan H, Shang F-J, Niu X-L, He Y-P, Lu X-L. Chymase induces profibrotic response via transforming growth factor-β1/Smad activation in rat cardiac fibroblasts. Mol Cell Biochem. 2008;310(1):159-66. doi: 10.1007/s11010-007-9676-2.
248. Mukherjee R, Brinsa TA, Dowdy KB, Scott AA, Baskin JM, Deschamps AM, Lowry AS, Escobar GP, Lucas DG, Yarbrough WM, Zile MR, Spinale FG. Myocardial infarct expansion and matrix metalloproteinase inhibition. Circulation. 2003;107(4):618-25. doi: 10.1161/01.cir.0000046449.36178.00.
249. Ducharme A, Frantz S, Aikawa M, Rabkin E, Lindsey M, Rohde LE, Schoen FJ, Kelly RA, Werb Z, Libby P, Lee RT. Targeted deletion of matrix metalloproteinase-9 attenuates left ventricular enlargement and collagen accumulation after experimental myocardial infarction. J Clin Invest. 2000;106(1):55-62. doi: 10.1172/JCI8768.
250. Owen CA, Campbell EJ. Angiotensin II generation at the cell Surface of activated neutrophils: Novel cathepsin G-mediated catalytic activity that is resistant to inhibition. J Immunol. 1998;160(3):1436-43.
251. Lindberg BF, Gyllstedt E, Andersson K-E. Conversion of angiotensin I to angiotensin II by chymase activity in human pulmonary membranes. Peptides. 1997;18(6):847-53. doi: http://dx.doi.org/10.1016/S0196-9781(97)00011-9.
252. Zheng J, Wei C-C, Hase N, Shi K, Killingsworth CR, Litovsky SH, Powell PC, Kobayashi T, Ferrario CM, Rab A, Aban I, Collawn JF, Dell'Italia LJ. Chymase mediates injury and mitochondrial damage in cardiomyocytes during acute ischemia/reperfusion in the dog. PloS one. 2014;9(4):e94732. doi: 10.1371/journal.pone.0094732.
253. Jin D, Takai S, Yamada M, Sakaguchi M, Kamoshita K, Ishida K, Sukenaga Y, Miyazaki M. Impact of chymase inhibitor on cardiac function and survival after myocardial infarction. Cardiovasc Res. 2003;60(2):413-20. doi: 10.1016/S0008-6363(03)00535-2.

254. Kanemitsu H, Takai S, Tsuneyoshi H, Nishina T, Yoshikawa K, Miyazaki M, Ikeda T, Komeda M. Chymase inhibition prevents cardiac fibrosis and dysfunction after myocardial infarction in rats. Hypertens Res. 2006;29(1):57-64.
255. Hoshino F, Urata H, Inoue Y, Saito Y, Yahiro E, Ideishi M, Arakawa K, Saku K. Chymase inhibitor improves survival in hamsters with myocardial infarction. J Cardiovasc Pharmacol. 2003;41:S11-S8. PubMed PMID: 00005344-200301001-00004.
256. Singh R, Lillard JW. Nanoparticle-based targeted drug delivery. Experimental and molecular pathology. 2009;86(3):215-23. doi: 10.1016/j.yexmp.2008.12.004. PubMed PMID: PMC3249419.
257. Winau F, Westphal O, Winau R. Paul Ehrlich--in search of the magic bullet. Microbes and infection. 2004;6(8):786-9. Epub 2004/06/23. doi: 10.1016/j.micinf.2004.04.003. PubMed PMID: 15207826.
258. Fahmy TM, Fong PM, Goyal A, Saltzman WM. Targeted for drug delivery. Materials Today. 2005;8(8, Supplement):18-26. doi: http://dx.doi.org/10.1016/S1369-7021(05)71033-6.
259. Rowe JM, Löwenberg B. Gemtuzumab ozogamicin in acute myeloid leukemia: a remarkable saga about an active drug. Blood. 2013;121(24):4838-41. doi: 10.1182/blood-2013-03-490482.
260. Takakura Y, Hashida M. Macromolecular Carrier Systems for Targeted Drug Delivery: Pharmacokinetic Considerations on Biodistribution. Pharmaceutical Research. 1996;13(6):820-31. doi: 10.1023/A:1016084508097.
261. Fox ME, Szoka FC, Fréchet JMJ. Soluble Polymer Carriers for the Treatment of Cancer: The Importance of Molecular Architecture. Accounts of chemical research. 2009;42(8):1141-51. doi: 10.1021/ar900035f. PubMed PMID: PMC2759385.
262. Arruebo M, Galán M, Navascués N, Téllez C, Marquina C, Ibarra MR, Santamaría J. Development of Magnetic Nanostructured Silica-Based Materials as Potential Vectors for Drug-Delivery Applications. Chemistry of Materials. 2006;18(7):1911-9. doi: 10.1021/cm051646z.
263. Kortesuo P, Ahola M, Karlsson S, Kangasniemi I, Yli-Urpo A, Kiesvaara J. Silica xerogel as an implantable carrier for controlled drug delivery--evaluation of drug distribution and tissue effects after implantation. Biomaterials. 2000;21(2):193-8. Epub 2000/01/13. PubMed PMID: 10632401.
264. Kingwell BA, Chapman MJ, Kontush A, Miller NE. HDL-targeted therapies: progress, failures and future. Nat Rev Drug Discov. 2014;13(6):445-64. doi: 10.1038/nrd4279.
265. Gao X, Cui Y, Levenson RM, Chung LWK, Nie S. In vivo cancer targeting and imaging with semiconductor quantum dots. Nat Biotech. 2004;22(8):969-76. doi: http://www.nature.com/nbt/journal/v22/n8/suppinfo/nbt994_S1.html.
266. Lombardo D, Kiselev MA, Magaz, #xf9, S, Calandra P. Amphiphiles Self-Assembly: Basic Concepts and Future Perspectives of Supramolecular Approaches. Advances in Condensed Matter Physics. 2015;2015:22. doi: 10.1155/2015/151683.
267. Barman H, Walch M, Latinovic-Golic S, Dumrese C, Dolder M, Groscurth P, Ziegler U. Cholesterol in negatively charged lipid bilayers modulates the effect of the antimicrobial protein granulysin. The Journal of membrane biology. 2006;212(1):29-39. Epub 2007/01/09. doi: 10.1007/s00232-006-0040-3. PubMed PMID: 17206515.
268. Jimenez-Rojo N, Sot J, Viguera AR, Collado MI, Torrecillas A, Gomez-Fernandez JC, Goni FM, Alonso A. Membrane permeabilization induced by sphingosine: effect of negatively charged lipids. Biophys J. 2014;106(12):2577-84. Epub 2014/06/19. doi: 10.1016/j.bpj.2014.04.038. PubMed PMID: 24940775; PMCID: PMC4070072.

269. Konstantinova I, Serebrennikova GA. Positively charged lipids: Structure, synthesis and application1996. 597-8 p.
270. Shalaev EY, Steponkus PL. Glass Transition of a Synthetic Phospholipid in the Lamellar Phase. The Journal of Physical Chemistry B. 2003;107(34):8734-7. doi: 10.1021/jp0303265.
271. Helfrich W. Elastic properties of lipid bilayers: theory and possible experiments. Zeitschrift fur Naturforschung Teil C: Biochemie, Biophysik, Biologie, Virologie. 1973;28(11):693-703. Epub 1973/11/01. PubMed PMID: 4273690.
272. Leroux J, Roux E, Le Garrec D, Hong K, Drummond DC. N-isopropylacrylamide copolymers for the preparation of pH-sensitive liposomes and polymeric micelles. Journal of controlled release : official journal of the Controlled Release Society. 2001;72(1-3):71-84. Epub 2001/06/08. PubMed PMID: 11389986.
273. Kellaway IW. Scientific rationale and clinical implications of sustained-release formulations. British journal of clinical practice Supplement. 1988;60:9-13. Epub 1988/04/01. PubMed PMID: 3151274.
274. Franzen U, Nguyen TT, Vermehren C, Gammelgaard B, Ostergaard J. Characterization of a liposome-based formulation of oxaliplatin using capillary electrophoresis: encapsulation and leakage. Journal of pharmaceutical and biomedical analysis. 2011;55(1):16-22. Epub 2011/02/02. doi: 10.1016/j.jpba.2010.12.037. PubMed PMID: 21282028.
275. Milla P, Dosio F, Cattel L. PEGylation of proteins and liposomes: a powerful and flexible strategy to improve the drug delivery. Current drug metabolism. 2012;13(1):105-19. Epub 2011/09/07. PubMed PMID: 21892917.
276. Woodle MC, Lasic DD. Sterically stabilized liposomes. Biochimica et biophysica acta. 1992;1113(2):171-99. Epub 1992/08/14. PubMed PMID: 1510996.
277. Du H, Chandaroy P, Hui SW. Grafted poly-(ethylene glycol) on lipid surfaces inhibits protein adsorption and cell adhesion. Biochimica et biophysica acta. 1997;1326(2):236-48. Epub 1997/06/12. PubMed PMID: 9218554.
278. Woodle MC. Controlling liposome blood clearance by surface-grafted polymers. Advanced drug delivery reviews. 1998;32(1-2):139-52. Epub 2000/06/06. PubMed PMID: 10837640.
279. Walde P, Namani T, Morigaki K, Hauser H. Formation and Properties of Fatty Acid Vesicles (Liposomes). Liposome Technology, Volume I: Informa Healthcare; 2006. p. 1-19.
280. Gubernator J. Active methods of drug loading into liposomes: recent strategies for stable drug entrapment and increased in vivo activity. Expert opinion on drug delivery. 2011;8(5):565-80. Epub 2011/04/16. doi: 10.1517/17425247.2011.566552. PubMed PMID: 21492058.
281. Fritze A, Hens F, Kimpfler A, Schubert R, Peschka-Süss R. Remote loading of doxorubicin into liposomes driven by a transmembrane phosphate gradient. Biochimica et Biophysica Acta (BBA) - Biomembranes. 2006;1758(10):1633-40. doi: https://doi.org/10.1016/j.bbamem.2006.05.028.
282. Shigehiro T, Kasai T, Murakami M, Sekhar SC, Tominaga Y, Okada M, Kudoh T, Mizutani A, Murakami H, Salomon DS, Mikuni K, Mandai T, Hamada H, Seno M. Efficient Drug Delivery of Paclitaxel Glycoside: A Novel Solubility Gradient Encapsulation into Liposomes Coupled with Immunoliposomes Preparation. PLoS ONE. 2014;9(9):e107976. doi: 10.1371/journal.pone.0107976. PubMed PMID: PMC4180071.
283. Schwendener RA, Schott H. Liposome formulations of hydrophobic drugs. Methods in molecular biology (Clifton, NJ). 2010;605:129-38. Epub 2010/01/15. doi: 10.1007/978-1-60327-360-2_8. PubMed PMID: 20072877.

284. Blume G, Cevc G. Molecular mechanism of the lipid vesicle longevity in vivo. Biochimica et biophysica acta. 1993;1146(2):157-68. Epub 1993/03/14. PubMed PMID: 8452853.
285. Mamot C, Drummond DC, Noble CO, Kallab V, Guo Z, Hong K, Kirpotin DB, Park JW. Epidermal growth factor receptor-targeted immunoliposomes significantly enhance the efficacy of multiple anticancer drugs in vivo. Cancer research. 2005;65(24):11631-8. Epub 2005/12/17. doi: 10.1158/0008-5472.can-05-1093. PubMed PMID: 16357174.
286. Nobs L, Buchegger F, Gurny R, Allemann E. Current methods for attaching targeting ligands to liposomes and nanoparticles. Journal of pharmaceutical sciences. 2004;93(8):1980-92. Epub 2004/07/06. doi: 10.1002/jps.20098. PubMed PMID: 15236448.
287. Maruyama K. PEG-immunoliposome. Bioscience reports. 2002;22(2):251-66. Epub 2002/11/14. PubMed PMID: 12428903.
288. Kirpotin D, Park JW, Hong K, Zalipsky S, Li WL, Carter P, Benz CC, Papahadjopoulos D. Sterically stabilized anti-HER2 immunoliposomes: design and targeting to human breast cancer cells in vitro. Biochemistry. 1997;36(1):66-75. Epub 1997/01/07. doi: 10.1021/bi962148u. PubMed PMID: 8993319.
289. Maruyama K, Takizawa T, Yuda T, Kennel SJ, Huang L, Iwatsuru M. Targetability of novel immunoliposomes modified with amphipathic poly(ethylene glycol)s conjugated at their distal terminals to monoclonal antibodies. Biochimica et biophysica acta. 1995;1234(1):74-80. Epub 1995/03/08. PubMed PMID: 7880861.
290. Scott RC, Wang B, Nallamothu R, Pattillo CB, Perez-Liz G, Issekutz A, Del Valle L, Wood GC, Kiani MF. Targeted delivery of antibody conjugated liposomal drug carriers to rat myocardial infarction. Biotechnology and bioengineering. 2007;96(4):795-802. Epub 2006/10/20. doi: 10.1002/bit.21233. PubMed PMID: 17051598.
291. Lionetti V, Ventura C. Regenerative medicine approach to repair the failing heart. Vascular pharmacology. 2013;58(3):159-63. Epub 2013/01/23. doi: 10.1016/j.vph.2013.01.002. PubMed PMID: 23337493.
292. Takeshita S, Zheng LP, Brogi E, Kearney M, Pu LQ, Bunting S, Ferrara N, Symes JF, Isner JM. Therapeutic angiogenesis. A single intraarterial bolus of vascular endothelial growth factor augments revascularization in a rabbit ischemic hind limb model. Journal of Clinical Investigation. 1994;93(2):662-70. PubMed PMID: PMC293894.
293. Giordano FJ, Ping P, McKirnan MD, Nozaki S, DeMaria AN, Dillmann WH, Mathieu-Costello O, Hammond HK. Intracoronary gene transfer of fibroblast growth factor-5 increases blood flow and contractile function in an ischemic region of the heart. Nature medicine. 1996;2(5):534-9. Epub 1996/05/01. PubMed PMID: 8616711.
294. Losordo DW, Vale PR, Symes JF, Dunnington CH, Esakof DD, Maysky M, Ashare AB, Lathi K, Isner JM. Gene therapy for myocardial angiogenesis: initial clinical results with direct myocardial injection of phVEGF165 as sole therapy for myocardial ischemia. Circulation. 1998;98(25):2800-4. Epub 1998/12/22. PubMed PMID: 9860779.
295. Formiga FR, Pelacho B, Garbayo E, Abizanda G, Gavira JJ, Simon-Yarza T, Mazo M, Tamayo E, Jauquicoa C, Ortiz-de-Solorzano C, Prosper F, Blanco-Prieto MJ. Sustained release of VEGF through PLGA microparticles improves vasculogenesis and tissue remodeling in an acute myocardial ischemia-reperfusion model. Journal of controlled release : official journal of the Controlled Release Society. 2010;147(1):30-7. Epub 2010/07/21. doi: 10.1016/j.jconrel.2010.07.097. PubMed PMID: 20643169.
296. Woo YJ, Panlilio CM, Cheng RK, Liao GP, Suarez EE, Atluri P, Chaudhry HW. Myocardial regeneration therapy for ischemic cardiomyopathy with cyclin A2. The Journal of thoracic and

cardiovascular surgery. 2007;133(4):927-33. Epub 2007/03/27. doi: 10.1016/j.jtcvs.2006.07.057. PubMed PMID: 17382628.
297. Pleger ST, Most P, Boucher M, Soltys S, Chuprun JK, Pleger W, Gao E, Dasgupta A, Rengo G, Remppis A, Katus HA, Eckhart AD, Rabinowitz JE, Koch WJ. Stable myocardial-specific AAV6-S100A1 gene therapy results in chronic functional heart failure rescue. Circulation. 2007;115(19):2506-15. Epub 2007/05/02. doi: 10.1161/circulationaha.106.671701. PubMed PMID: 17470693.
298. Laguens R, Cabeza Meckert P, Vera Janavel G, Del Valle H, Lascano E, Negroni J, Werba P, Cuniberti L, Martinez V, Melo C, Papouchado M, Ojeda R, Criscuolo M, Crottogini A. Entrance in mitosis of adult cardiomyocytes in ischemic pig hearts after plasmid-mediated rhVEGF165 gene transfer. Gene therapy. 2002;9(24):1676-81. Epub 2002/11/29. doi: 10.1038/sj.gt.3301844. PubMed PMID: 12457281.
299. Pitt WG, Husseini GA, Staples BJ. Ultrasonic Drug Delivery – A General Review. Expert opinion on drug delivery. 2004;1(1):37-56. doi: 10.1517/17425247.1.1.37. PubMed PMID: PMC1361256.
300. Zhigang W, Zhiyu L, Haitao R, Hong R, Qunxia Z, Ailong H, Qi L, Chunjing Z, Hailin T, Lin G, Mingli P, Shiyu P. Ultrasound-mediated microbubble destruction enhances VEGF gene delivery to the infarcted myocardium in rats. Clinical imaging. 2004;28(6):395-8. Epub 2004/11/09. doi: 10.1016/j.clinimag.2004.04.003. PubMed PMID: 15531137.
301. Maeda H. Vascular permeability in cancer and infection as related to macromolecular drug delivery, with emphasis on the EPR effect for tumor-selective drug targeting. Proceedings of the Japan Academy Series B, Physical and Biological Sciences. 2012;88(3):53-71. doi: 10.2183/pjab.88.53. PubMed PMID: PMC3365245.
302. Lukyanov AN, Hartner WC, Torchilin VP. Increased accumulation of PEG-PE micelles in the area of experimental myocardial infarction in rabbits. Journal of controlled release : official journal of the Controlled Release Society. 2004;94(1):187-93. Epub 2003/12/20. PubMed PMID: 14684282.
303. Khaw BA, DaSilva J, Hartner WC. Cytoskeletal-antigen specific immunoliposome-targeted in vivo preservation of myocardial viability. Journal of controlled release : official journal of the Controlled Release Society. 2007;120(1-2):35-40. Epub 2007/05/22. doi: 10.1016/j.jconrel.2007.04.013. PubMed PMID: 17512999.
304. Dunehoo AL, Anderson M, Majumdar S, Kobayashi N, Berkland C, Siahaan TJ. Cell adhesion molecules for targeted drug delivery. Journal of pharmaceutical sciences. 2006;95(9):1856-72. Epub 2006/07/20. doi: 10.1002/jps.20676. PubMed PMID: 16850395.
305. Jang Y, Lincoff AM, Plow EF, Topol EJ. Cell adhesion molecules in coronary artery disease. J Am Coll Cardiol. 1994;24(7):1591-601. Epub 1994/12/01. PubMed PMID: 7963103.
306. Rosano JM, Cheheltani R, Wang B, Vora H, Kiani MF, Crabbe DL. Targeted Delivery of VEGF after a Myocardial Infarction Reduces Collagen Deposition and Improves Cardiac Function. Cardiovascular engineering and technology. 2012;3(2):237-47. doi: 10.1007/s13239-012-0089-3. PubMed PMID: PMC3405981.
307. Hooshdaran B, Kolpakov M, Rafiq K, Guo X, Kiani M, Sabri A. Targeting inflammatory serine proteases for cardiac repair after Ischemia Reperfusion injury (1080.10). The FASEB Journal. 2014;28(1 Supplement):1080.10.
308. Wilgus TA, Roy S, McDaniel JC. Neutrophils and Wound Repair: Positive Actions and Negative Reactions. Advances in Wound Care. 2013;2(7):379-88. doi: 10.1089/wound.2012.0383. PubMed PMID: PMC3763227.

309. Takai S, Jin D, Muramatsu M, Okamoto Y, Miyazaki M. Therapeutic applications of chymase inhibitors in cardiovascular diseases and fibrosis. European journal of pharmacology. 2004;501(1-3):1-8. Epub 2004/10/07. doi: 10.1016/j.ejphar.2004.08.040. PubMed PMID: 15464056.
310. Scott RC, Crabbe D, Krynska B, Ansari R, Kiani MF. Aiming for the heart: targeted delivery of drugs to diseased cardiac tissue. Expert opinion on drug delivery. 2008;5(4):459-70. Epub 2008/04/23. doi: 10.1517/17425247.5.4.459. PubMed PMID: 18426386.
311. Rafiq K, Hanscom M, Valerie K, Steinberg SF, Sabri A. Novel mode for neutrophil protease cathepsin G-mediated signaling: membrane shedding of epidermal growth factor is required for cardiomyocyte anoikis. Circulation research. 2008;102(1):32-41. Epub 2007/11/03. doi: 10.1161/circresaha.107.150573. PubMed PMID: 17975113.
312. Zhang L, Wang CC. Inflammatory response of macrophages in infection. Hepatobiliary & pancreatic diseases international : HBPD INT. 2014;13(2):138-52. Epub 2014/04/02. PubMed PMID: 24686541.
313. Smith C, Kruger MJ, Smith RM, Myburgh KH. The inflammatory response to skeletal muscle injury: illuminating complexities. Sports medicine (Auckland, NZ). 2008;38(11):947-69. Epub 2008/10/22. doi: 10.2165/00007256-200838110-00005. PubMed PMID: 18937524.
314. Shen H, Kreisel D, Goldstein DR. Processes of Sterile Inflammation. The Journal of Immunology. 2013;191(6):2857-63. doi: 10.4049/jimmunol.1301539.
315. Liu J, Wang H, Li J. Inflammation and Inflammatory Cells in Myocardial Infarction and Reperfusion Injury: A Double-Edged Sword. Clinical Medicine Insights Cardiology. 2016;10:79-84. doi: 10.4137/CMC.S33164. PubMed PMID: PMC4892199.
316. Deftereos S, Giannopoulos G, Angelidis C, Alexopoulos N, Filippatos G, Papoutsidakis N, Sianos G, Goudevenos J, Alexopoulos D, Pyrgakis V, Cleman MW, Manolis AS, Tousoulis D, Lekakis J. Anti-Inflammatory Treatment With Colchicine in Acute Myocardial Infarction: A Pilot Study. Circulation. 2015. doi: 10.1161/circulationaha.115.017611.
317. Heymans S, Hirsch E, Anker SD, Aukrust P, Balligand J-L, Cohen-Tervaert JW, Drexler H, Filippatos G, Felix SB, Gullestad L, Hilfiker-Kleiner D, Janssens S, Latini R, Neubauer G, Paulus WJ, Pieske B, Ponikowski P, Schroen B, Schultheiss H-P, Tschöpe C, Van Bilsen M, Zannad F, McMurray J, Shah AM. Inflammation as a therapeutic target in heart failure? A scientific statement from the Translational Research Committee of the Heart Failure Association of the European Society of Cardiology. European Journal of Heart Failure. 2009;11(2):119-29. doi: 10.1093/eurjhf/hfn043. PubMed PMID: PMC2639409.
318. Vinten-Johansen J. Involvement of neutrophils in the pathogenesis of lethal myocardial reperfusion injury. Cardiovascular research. 2004;61(3):481-97. Epub 2004/02/14. doi: 10.1016/j.cardiores.2003.10.011. PubMed PMID: 14962479.
319. Christia P, Frangogiannis NG. Targeting inflammatory pathways in myocardial infarction. European journal of clinical investigation. 2013;43(9):986-95. doi: 10.1111/eci.12118. PubMed PMID: PMC3745791.
320. Smith JA. Neutrophils, host defense, and inflammation: a double-edged sword. Journal of leukocyte biology. 1994;56(6):672-86. Epub 1994/12/01. PubMed PMID: 7996043.
321. Saxena A, Russo I, Frangogiannis NG. Inflammation as a therapeutic target in myocardial infarction: learning from past failures to meet future challenges. Translational research : the journal of laboratory and clinical medicine. 2016;167(1):152-66. doi: 10.1016/j.trsl.2015.07.002. PubMed PMID: PMC4684426.
322. Jans DM, Martinet W, Fillet M, Kockx MM, Merville MP, Bult H, Herman AG, De Meyer GR. Effect of non-steroidal anti-inflammatory drugs on amyloid-beta formation and macrophage

activation after platelet phagocytosis. Journal of cardiovascular pharmacology. 2004;43(3):462-70. Epub 2004/04/13. PubMed PMID: 15076232.
323. Muller M, Raabe O, Addicks K, Wenisch S, Arnhold S. Effects of non-steroidal anti-inflammatory drugs on proliferation, differentiation and migration in equine mesenchymal stem cells. Cell biology international. 2011;35(3):235-48. Epub 2010/11/20. doi: 10.1042/cbi20090211. PubMed PMID: 21087205.
324. Coussens LM, Werb Z. Inflammation and cancer. Nature. 2002;420(6917):860-7. doi: 10.1038/nature01322. PubMed PMID: PMC2803035.
325. Bidouard JP, Duval N, Kapui Z, Herbert JM, O'Connor SE, Janiak P. SSR69071, an elastase inhibitor, reduces myocardial infarct size following ischemia-reperfusion injury. European journal of pharmacology. 2003;461(1):49-52. Epub 2003/02/06. PubMed PMID: 12568915.
326. Krishna KA, Krishna KS, Berrocal R, Rao KS, Sambasiva Rao KRS. Myocardial infarction and stem cells. Journal of Pharmacy and Bioallied Sciences. 2011;3(2):182-8. doi: 10.4103/0975-7406.80761. PubMed PMID: PMC3103911.
327. Drummond-Barbosa D. Stem cells, their niches and the systemic environment: an aging network. Genetics. 2008;180(4):1787-97. Epub 2008/12/18. doi: 10.1534/genetics.108.098244. PubMed PMID: 19087970; PMCID: PMC2600921.
328. Ennis WJ, Sui A, Bartholomew A. Stem Cells and Healing: Impact on Inflammation. Advances in Wound Care. 2013;2(7):369-78. doi: 10.1089/wound.2013.0449. PubMed PMID: PMC3842880.
329. Kizil C, Kyritsis N, Brand M. Effects of inflammation on stem cells: together they strive? EMBO reports. 2015;16(4):416-26. Epub 2015/03/06. doi: 10.15252/embr.201439702. PubMed PMID: 25739812; PMCID: PMC4388609.
330. Ekdahl CT, Claasen JH, Bonde S, Kokaia Z, Lindvall O. Inflammation is detrimental for neurogenesis in adult brain. Proceedings of the National Academy of Sciences of the United States of America. 2003;100(23):13632-7. Epub 2003/10/29. doi: 10.1073/pnas.2234031100. PubMed PMID: 14581618; PMCID: PMC263865.
331. Iosif RE, Ekdahl CT, Ahlenius H, Pronk CJ, Bonde S, Kokaia Z, Jacobsen SE, Lindvall O. Tumor necrosis factor receptor 1 is a negative regulator of progenitor proliferation in adult hippocampal neurogenesis. The Journal of neuroscience : the official journal of the Society for Neuroscience. 2006;26(38):9703-12. Epub 2006/09/22. doi: 10.1523/jneurosci.2723-06.2006. PubMed PMID: 16988041.
332. Monje ML, Toda H, Palmer TD. Inflammatory blockade restores adult hippocampal neurogenesis. Science (New York, NY). 2003;302(5651):1760-5. Epub 2003/11/15. doi: 10.1126/science.1088417. PubMed PMID: 14615545.
333. Zhang J. Engineered Tissue Patch for Cardiac Cell Therapy. Current treatment options in cardiovascular medicine. 2015;17(8):399-. doi: 10.1007/s11936-015-0399-5. PubMed PMID: PMC4676725.
334. Okubo M, Kioi M, Nakashima H, Sugiura K, Mitsudo K, Aoki I, Taniguchi H, Tohnai I. M2-polarized macrophages contribute to neovasculogenesis, leading to relapse of oral cancer following radiation. Scientific reports. 2016;6:27548. Epub 2016/06/09. doi: 10.1038/srep27548. PubMed PMID: 27271009; PMCID: PMC4897643.
335. Chang H-I, Yeh M-K. Clinical development of liposome-based drugs: formulation, characterization, and therapeutic efficacy. International Journal of Nanomedicine. 2012;7:49-60. doi: 10.2147/IJN.S26766. PubMed PMID: PMC3260950.

336. Bulbake U, Doppalapudi S, Kommineni N, Khan W. Liposomal Formulations in Clinical Use: An Updated Review. Pharmaceutics. 2017;9(2):12. doi: 10.3390/pharmaceutics9020012. PubMed PMID: PMC5489929.
337. Barenholz Y. Doxil(R)--the first FDA-approved nano-drug: lessons learned. Journal of controlled release : official journal of the Controlled Release Society. 2012;160(2):117-34. Epub 2012/04/10. doi: 10.1016/j.jconrel.2012.03.020. PubMed PMID: 22484195.
338. Daraee H, Etemadi A, Kouhi M, Alimirzalu S, Akbarzadeh A. Application of liposomes in medicine and drug delivery. Artificial Cells, Nanomedicine, and Biotechnology. 2016;44(1):381-91. doi: 10.3109/21691401.2014.953633.
339. Moon MH, Giddings JC. Size distribution of liposomes by flow field-flow fractionation. Journal of pharmaceutical and biomedical analysis. 1993;11(10):911-20. Epub 1993/10/01. PubMed PMID: 8305595.
340. Holsapple MP, West LJ, Landreth KS. Species comparison of anatomical and functional immune system development. Birth defects research Part B, Developmental and reproductive toxicology. 2003;68(4):321-34. Epub 2003/12/12. doi: 10.1002/bdrb.10035. PubMed PMID: 14666995.
341. Vllasaliu D, Fowler R, Stolnik S. PEGylated nanomedicines: recent progress and remaining concerns. Expert opinion on drug delivery. 2014;11(1):139-54. Epub 2013/12/04. doi: 10.1517/17425247.2014.866651. PubMed PMID: 24295065.
342. Bacic G, Niesman MR, Bennett HF, Magin RL, Swartz HM. Modulation of water proton relaxation rates by liposomes containing paramagnetic materials. Magnetic resonance in medicine. 1988;6(4):445-58. Epub 1988/04/01. PubMed PMID: 3380005.
343. Cheng Z, Al Zaki A, Hui JZ, Muzykantov VR, Tsourkas A. Multifunctional nanoparticles: cost versus benefit of adding targeting and imaging capabilities. Science (New York, NY). 2012;338(6109):903-10. Epub 2012/11/20. doi: 10.1126/science.1226338. PubMed PMID: 23161990; PMCID: PMC3660151.
344. !!! INVALID CITATION !!! {}.
345. Dawidczyk CM, Kim C, Park JH, Russell LM, Lee KH, Pomper MG, Searson PC. State-of-the-art in design rules for drug delivery platforms: lessons learned from FDA-approved nanomedicines. Journal of controlled release : official journal of the Controlled Release Society. 2014;187:133-44. Epub 2014/05/31. doi: 10.1016/j.jconrel.2014.05.036. PubMed PMID: 24874289; PMCID: PMC4132889.
346. Sawant RR, Torchilin VP. Challenges in development of targeted liposomal therapeutics. The AAPS journal. 2012;14(2):303-15. Epub 2012/03/15. doi: 10.1208/s12248-012-9330-0. PubMed PMID: 22415612; PMCID: PMC3326155.
347. Laffleur B, Pascal V, Sirac C, Cogne M. Production of human or humanized antibodies in mice. Methods in molecular biology (Clifton, NJ). 2012;901:149-59. Epub 2012/06/23. doi: 10.1007/978-1-61779-931-0_9. PubMed PMID: 22723099.
348. Park YS. Tumor-Directed Targeting of Liposomes. Bioscience reports. 2002;22(2):267-81. doi: 10.1023/A:1020190606757.

LIST OF PUBLICATIONS

Peer Reviewed Papers:

-**Hooshdaran B**, Kolpakov MA, Guo X,Miller AS, Wang T, Tilley D, Sabri A. *"Dual inhibitor of chymase and cathepsin G augments caridoprotection after IR injury"* accepted, minor revision, journal of basic cardiology.

-**Hooshdaran B**, Kolpakov MA1, Rafiq K, Guo X, Wang T, Tang Y, Rafiq K, Tilley D, Kiani MF, Sabri A *"Targeted delivery of Chymase and cathepsin G inhibitor augments cardioprotection after IR injury"* under preparation.

-Kolpakov MA, Rafiq K, Guo X, **Hooshdaran B**, Wang T, Vlasenko L, Bashkirova YV, Zhang X, Chen X, Iftikhar S, Libonati JR, Kunapuli SP, Sabri A. *"Protease-activated receptor 4 deficiency offers cardioprotection after acute ischemia reperfusion injury",* J Mol Cell Cardiol. 2016 Jan;90:21-9. doi: 10.1016/j.yjmcc.2015.11.030. Epub 2015 Nov 28.

-Kolpakov MA, Rafiq K, Guo X, **Hooshdaran B**, Wang T, Vlasenko L, Bashkirova YV, Zhang X, Chen X, Iftikhar S, Libonati JR, Kunapuli SP, Sabri A. *"Loss of protease-activated receptor 4 prevents inflammation resolution and predisposes the heart to cardiac rupture after myocardial infarction"* Circulation, accepted, under revision.

-Guo X, Kolpakov MA, Wang T, **Hooshdaran B**,Vlasenko L, Bashkirova YV, Zhang X, Chen X, Iftikhar S, Libonati JR, Kunapuli SP, Sabri A. *"Local Expression of Factor X is Increased in Response to Pressure Overload and Mediates Cardiac Hypertrophy and Fibrosis"* Circulation, Submitted.

Conference Proceedings:

-**Hooshdaran B**, Kolpakov M, Guo X, Bashkirova Y, Wang T, Schappel W, Tang Y, Kiani MF, Sabri A. Targeted Delivery of a Dual Cathepsin G and Chymase Inhibitor by Immunoliposomes Augments Cardioprotection in Mice. Circulation. 2016;134(Suppl 1):A16159-A.

-**Hooshdaran B**, Kolpakov M, Rafiq K, Guo X, Kiani M, Sabri A. Targeting inflammatory serine proteases for cardiac repair after Ischemia Reperfusion injury (1080.10). The FASEB Journal. 2014;28(1 Supplement):1080.10.

-Guo X, Kolpakov M, **Hooshdaran B**, Vlasenko L, Schappell W, Wang T, Liu S, Crandall D, Andrade-Gordon P, Houser SR. Local Expression of Coagulation Factor X (FXa) is Increased in Response to Pressure Overload and Mediates Cardiac Hypertrophy and Fibrosis. Circulation. 2016;134(Suppl 1):A18832-A.

-Guo X, **Hooshdaran B**, Rafiq K, Xi H, Kolpakov M, Houser S, Koch W, Liggett S, Sabri A. Death-associated protein kinase mediates myofibril degeneration and myocyte apoptosis induced by beta-adrenergic receptors (404.3). The FASEB Journal. 2014;28(1 Supplement):404.3.

-Guo X, **Hooshdaran B**, Rafiq K, Xi H, Kolpakov M, Liu S, Zhang X, Chen X, Houser SR, Koch WJ. Death Associated Protein Kinase Mediates Myofibril Degeneration and Myocyte Apoptosis Induced by Beta-adrenergic Receptors. Circulation. 2016;134(Suppl 1):A16144-A.

-Kolpakov MA, Guo X, **Hooshdaran B**, Rafiq K, Bashkirova YV, Vlasenko L, Wang T, Seqqat R, Kunapuli SP, Houser SR. Protease-Activated Receptor 4 Deficiency Impairs Resolution of Inflammation and Predisposes the Heart to Cardiac Rupture After Myocardial Infarction. Circulation. 2016;134(Suppl 1):A14611-A.

-Kolpakov MA, Guo X, **Hooshdaran B**, Scalia R, Houser SR, Sabri A, Rafiq K. Inflammatory Serine Proteases Regulate Insulin Signaling and Myocyte Death During the Development of Diabetic Cardiomyopathy. Circulation. 2013;128(Suppl 22):A14321-A.

-Kolpakov MA, **Hooshdaran B**, Guo X, Rafiq K, Vlasenko L, Bashkirova YV, Wang T, Qi Z, Garikipati VN, Kishore R. Cardiac Angiogenesis and Arteriogenesis Suppression After Myocardial Infarction Through Activation of Dipeptidyl Peptidase I. Circulation. 2016;134(Suppl 1):A14409-A.

-Kolpakov MA, **Hooshdaran B**, Guo X, Wang T, Rafiq K, Vlasenko L, Qi Z, Garikipati VN, Kishore R, Houser SR. DPPI Deficiency Enhances Both Angiogenesis and Arteriogenesis and Improves Cardiac Function after Myocardial Infarction. The FASEB Journal. 2016;30(1 Supplement):1211.2-.2.
-Kolpakov MA, **Hooshdaran B**, Rafiq K, Vlasenko L, Seqqat R, Houser SR, Kunapuli SP, Sabri A, editors. Inhibition of PAR-4 Prevents Myocyte Apoptosis but Impairs Cardiac Healing and Function after Myocardial Ischemia. CIRCULATION RESEARCH; 2012: LIPPINCOTT WILLIAMS & WILKINS 530 WALNUT ST, PHILADELPHIA, PA 19106-3621 USA.
-Qi Z, Kolpakov M, **Hooshdaran B**, Rafiq K, Guo X, Wang T, Pham C, Sabri A. Gene Deletion of Dipeptidyl Peptidase I Reduces Myocyte Loss and Preserves Cardiac Function After Myocardial Ischemia-Reperfusion Injury. Circulation Research. 2012;111(Suppl 1):A126-A.
-Rafiq K, Kolpakov M, Guo X, **Hooshdaran B**, Sabri A. Activation of the E3 ligase Cbl by Neutrophil Cathepsin G Impairs Insulin Receptor Signaling in Cardiomyocyte Degeneration. Circulation. 2013;128(Suppl 22):A15057-A.